

**CIRCULAR INTERACTIVE MATERIAL: Making Ubiquitous Computing More
Scalable and Sustainable**

A Dissertation
Presented to
The Academic Faculty

By

Tingyu Cheng

In Partial Fulfillment
of the Requirements for the Degree
Doctor of Philosophy in the
School of Interactive Computing
College of Computing

Georgia Institute of Technology

August 2024

© Tingyu Cheng 2024

CIRCULAR INTERACTIVE MATERIAL: Making Ubiquitous Computing More Scalable and Sustainable

Thesis committee:

Dr. Gregory Abowd, Co-advisor
College of Engineering
Northeastern University

Dr. HyunJoo Oh, Co-advisor
School of Industrial Design & School of
Interactive Computing
Georgia Institute of Technology

Dr. Thad Starner
School of Interactive Computing
Georgia Institute of Technology

Dr. Carmel Majidi
Department of Mechanical Engineering
Carnegie Mellon University

Dr. Josiah Hester
School of Interactive Computing
Georgia Institute of Technology

Dr. Sean Follmer
Department of Mechanical Engineering
Stanford University

Date approved: June 05, 2024

To my parents, my friends, my lovely Yangyi and Booboo

ACKNOWLEDGMENTS

I am profoundly grateful to Hyunjoo Oh and Gregory Abowd, my lovely, esteemed co-advisors and mentors, for their unwavering support, trust and understand throughout my PhD journey. It has been an immense honor to have them guide me. Their keen attention to my concerns and ideas, along with their invaluable guidance on research, leadership, and teamwork, have been pivotal in my development. They have taught me not only how to publish papers but also how to engage in meaningful and long-lasting impact research. Their inspiration has been a driving force in my academic endeavors. I must also acknowledge Josiah Hester, my third "unofficial" advisor, who has been like an elder brother to me, steering my research towards genuine sustainable computing. He guides me move from topics like sustainable interactive materials to life cycle assessment and intermittent/low-power computing and etc.

Special thanks go to my thesis committee members. Besides Josiah, Thad Starner, a long-standing mentor, has consistently provided insightful feedback and constructive advice, always ready to explore new ideas with me. Carmal Majidi, my advisor before joining Georgia Tech, offered thoughtful feedback and encouragement that significantly bolstered my confidence and vision in my research. Sean Follmer's relentless support and probing questions have prompted me to think more critically and quantitatively about evaluating the sustainability of the edge devices I developed.

I am also indebted to the brilliant researchers and friends I have collaborated with throughout this journey. Youngwook Do, my best friend and comrade, has consistently inspired me with his creativity and diligence. Dingtian Zhang and Jungwook Park, both senior PhD mentors when I entered the program, were instrumental to me in how translating theoretical ideas into practical outcomes. Yuhui Zhao and Charles Ramey, who started the program around the same time as I did, have been my partners in navigating and overcoming numerous research challenges. My experience at Georgia Tech was greatly en-

hanced by the GT Ubicomp, CodeCraft, and Ka Moamoa labmates and friends, including but not limited to Yang Zhang, Dong Whi Yoo, Vedant Das Swain, Mehrab Bin Morshed, Jiawei Zhou, Hyeokhyen Kwon, Harish Haresamudram, Shruthi Hiremath, Jin Yu, Hao-Ping (Hank) Lee, Ceara Byrne, Abu Bakar, Rishabh Goel, Eric Greenlee, Saad Ahmed, John Mamish, Yaman Sangar, Chris Kraemer, Diana Wang, Yingting Gao, Haiqing Xu and Tejonidhi Deshpande whose support and feedback were invaluable.

I was also privileged to mentor many talented students, from undergraduates to graduates. I want to highlight four exceptional students—Bu Li, Yunzhi Li, Zhihan Zhang, and Jiachen Li—who have grown from collaborators to friends and continue to impress me with their creativity and intellect.

My three internship experiences at Chatham Labs, Meta Reality Labs, and Accenture Technologies Lab were unforgettable, thanks to colleagues and mentors like Marcello Giordano, Carolina Brum Medeiros, Tovi Grossman, Daniel Wigdor, Taylor Tabb, Eric M. Gallo, Aditi Maheshwari, and Andreea Danielescu.

Lastly, my prior lab experiences before joining Georgia Tech have shaped my skills, research interests, and broader academic perspectives. I am especially thankful to all my mentors, including Lining Yao and Carmal Majidi at Carnegie Mellon University, Teng Zhang at Syracuse University, Katia Bertoldi at Harvard, Yoshihiro Kawahara at Tokyo University and Tiefeng Li at Zhejiang University.

SUMMARY

Weiser has predicted the third generation of computing would result in individuals interacting with many computing devices and ultimately can “weave themselves into the fabric of everyday life until they are indistinguishable from it” [1]. However, how to achieve this seamlessness and what associated interaction should be developed are still under investigation. On the other hand, for achieving a fully immersive intelligent environment, we might produce trillions of smart devices, but their current configuration (*e.g.*, plastic housing, PCB-board) will inevitably increase environment burden. In my research, I work on creating computational materials with different encoded material properties such as conductivity, transparency or water-solubility that can be seamlessly integrated into our living environment to enrich different modalities of information communication. Meanwhile, this material intelligence will also affect devices’ usefulness and life expectancy from a sustainability perspective.

This thesis contains five works to scope the future pervasiveness of IoT devices, and meanwhile paying attention to their entire device life cycle. They emphasize different aspects that are crucial to construct the circular interactive material embedded environment by balancing the tension between **scalability** and **sustainability**. Silver Tape is a simple fabrication technique leveraging the inkjet printing circuits to transfer silver traces onto everyday surfaces without any post-treatment [2]. This method allows users to quickly fabricate versatile sensors by leveraging the intrinsic material property (*e.g.*, heat-resistive) and meanwhile the transferred sensors can be **repaired** when damaged. Duco is the second project that negates the need for any human intervention by leveraging a hanging robotic system that automatically sketches large-scale circuitry. We have explored not only how to incorporate these computational abilities into our living structures such as walls, but also created erasable ink that allows users to **erase** the circuitry and embed the surface with new capabilities to make the walls reusable. PITAS is a thin-sheet robotic material com-

posed of a reversible phase transition actuating layer and a heating/sensing layer to create shape-changing devices that can locally or remotely convey physical information such as shape, color, texture and temperature changes. This project achieved a distinctive **renewal** process by immersing the material-actuator in ethanol, allowing the devices with new life. Then, the next project Functional Destruction aims to further promote sustainability by designing devices that **self-destruct** once they have fulfilled their purpose. The last project, called Recy-ctronics, is to extend the idea from Functional Destruction by developing **fully recyclable** circuits, by not only treating the physical disintegration as the end of a device's life but the beginning point of a device's new lifespan. This work also extends beyond traditional thin-sheet electronics, introducing three distinct form factors: sheets, foam, and tubes.

TABLE OF CONTENTS

Acknowledgments	iv
Summary	vi
List of Tables	xiv
List of Figures	xv
Chapter 1: Introduction	1
1.1 Thesis Statement and Research Questions	4
1.2 Document Structure	6
1.3 Contributions	7
Chapter 2: Background and Related Work	9
2.1 Conventional Ambient Computing Interfaces	9
2.2 Interactive Materials Enabled Interfaces in Everyday Life	10
2.3 Fabrication Methods/tools to Augment Living Environment	10
2.4 Versatile Form factor, Scale, Sensing and Actuation Modalities	11
2.4.1 Sustainable Making and Unmaking	12
Chapter 3: Inkjet Printing and Transferring Repairable Electronics to Every- day Surfaces	14

3.1	FABRICATION PROCESS	15
3.1.1	Printing	16
3.1.2	Transferring	17
3.1.3	Assembling	17
3.1.4	Re-transferability	18
3.2	ELECTRICAL & MECHANICAL ANALYSES	18
3.2.1	Transfer Resolution	19
3.2.2	Resistance Change Using Different Substrates	20
3.2.3	Resistance Change Using Different Adhesives	20
3.2.4	Transfer to Everyday Surfaces	21
3.2.5	Transfer to Different Geometries	22
3.2.6	Bending Tests	22
3.3	APPLICATIONS	23
3.3.1	LED Decorations	23
3.3.2	Bending Sensors for Soft-bodied Robots	24
3.3.3	Circuitry for High-Temperature Applications	25
3.3.4	Touch Panel Extensions for Mobile Devices	25
3.3.5	Water Leakage Sensor	26
3.3.6	Wirelessly Powered Resonator by Multi-layer Circuit	26
3.4	DISCUSSION AND LIMITATIONS	26
3.4.1	Stretchabilities	26
3.4.2	On Skin Transfer	27
3.4.3	Robustness	27

3.4.4 Hysteresis of Silver Nanoparticles 27

Chapter 4: Duco, A Fully Autonomous Erasable Circuits Fabrication Robot to Enable Interactivity On Large Surfaces 29

4.1 DUCO WORKFLOW OVERVIEW 31

4.1.1 Creating the Digital Design 31

4.1.2 Initial System Setup 31

4.1.3 Drawing Tools and Substrate Selection 32

4.1.4 Preliminary System Testings and Drawing 32

4.1.5 Connection and Post-process 32

4.2 DUCO FABRICATION SYSTEM 33

4.2.1 Design Principles 33

4.2.2 Hardware Design 34

4.3 DRAWING TOOLS EVALUATION 37

4.3.1 Resolution, Accuracy and Speed Testings 38

4.3.2 Drawing Tool Testings 40

4.3.3 Substrate Testing 42

4.4 APPLICATIONS 43

4.4.1 Interactive Piano 44

4.4.2 Interactive Coffee Maker Control 45

4.4.3 Capacitive Sensing Wall 46

4.4.4 FM Energy Harvester 47

4.4.5 3D Interactive Lamp 49

4.5 DISCUSSION 49

Chapter 5: PITAS: Renewable Sensing and Actuating Embedded Robotic Sheet for Physical Information Communication	53
5.1 System Overview	54
5.2 Fabrication Pipeline	55
5.2.1 Phase Transition Actuator	55
5.2.2 Sensor & Heater	58
5.2.3 Instant Conductive Glue & Electrode	59
5.2.4 Fabrication Methods	61
5.3 System Characterization	64
5.3.1 Electrical Properties For the Conductive Silicone	64
5.3.2 Mechanical Properties For the Phase Transition Actuator	66
5.4 Communication & Control Methods	67
5.5 Application	69
5.5.1 Home decor artifact for emotional communication: 3D artificial rose	69
5.5.2 Office accessory for information delivery: Actuatable sticky notes	70
5.6 Limitation & Future Work	71
Chapter 6: Functional Destruction: utilizing sustainable materials' physical transiency for electronics applications	74
6.1 Introduction	74
6.2 Functional Destruction: Design Space and Overview	77
6.2.1 Design considerations for destruction	77
6.2.2 Sustainable Material Considerations	80
6.2.3 Using Highly Accessible Materials & Tools	81

6.2.4	Application Domains	81
6.2.5	Design Space in Practice	82
6.3	Beeswax based heat-melttable electronics	87
6.4	Chocolate-based Edible Electronics	89
6.5	Fully Passive, Chipless RFID Implementation	96
6.5.1	Principles of Chipless RFID	96
6.5.2	Experimental Setup	97
6.5.3	Results	98
Chapter 7: Recy-ctronics: Designing Fully Recyclable Electronics With Varied Form Factors		100
7.1	Introduction	100
7.2	General Recy-ctronics Design Rules	102
7.2.1	Recycling approach for Recy-ctronics	103
7.2.2	Versatile electronics from simple materials	105
7.3	Sheet	106
7.3.1	Application 1: Recyclable Sheet Electronics— from multiple components to minimal components	108
7.4	Foam	110
7.4.1	Foam-based Electronics Primitives	112
7.4.2	Application 2: Recyclable Interactive Pen Tip	114
7.5	Tube	114
7.6	Recycling Process	118
7.7	Life Cycle Assessment	122

Chapter 8: Discussion	125
8.1 Life Cycle Assessment	125
8.2 Power	126
8.3 Towards Sustainable And Complex Systems	127
Chapter 9: Conclusion	130
References	132

LIST OF TABLES

- 1.1 A position table to highlight the contribution for each of my completed work. 7
- 3.1 Resistance variance before and after transfer for different printing substrates. 20
- 3.2 Resistance variance before and after transfer for different transfer materials. 21

LIST OF FIGURES

1.1	(a) Sustainable Physical intelligence for versatile interaction with sustainability in mind. (b) A shape changing artificial rose's blossom can indicate happiness emotion while is bio-degradable. (c) Swelled sensible surface texture can augment everyday surface with tactile information and is completely recyclable. (d) Chocolate-based RFID can encode identifiable information and consumable to destroy the data.	3
3.1	Overview of Silver Tape. (a, b) Fabrication process. Conductive patterns are printed on transfer paper (a), and then peeled off and transferred (b) by hand. (c-e) Schematics of the transfer process of silver nanoparticles from transfer paper to a sticky substrate.	16
3.2	Silver traces transferred to different substrates. (a) Transfer process. (b) Successfully transferred conductive patterns on various substrates: (1) Scotch tape (3M Scotch 810), (2) polyimide electrical tape (3M 1205), (3) vinyl insulation tape (3M Super 33+), (4) water soluble wave soldering tape (3M 5414), (5) Scotch removable tape (3M Scotch 811), (6) masking tape (3M Scotch 234).	18
3.3	Connection methods. (a) Pasting two sticky substrates using their own adhesive force. (b) Conductive paste/epoxy. (c) Pierce punch to make a stable, solderable connection. (d) Temporary liquid metal connection mainly for measurement.	19
3.4	(a) Silver trace is transferred onto PDMS and connected with LED. (b) Part of the trace is removed. (c) Recovering the damaged portion with a new silver trace. (d) The silver trace is recovered.	19
3.5	Silver traces transferred onto different materials and geometries.	22
3.6	(a) Transfer resolution. (b) Resistance under outward bending. (c) Resistance under inward bending.	23

3.7	Applications: (a1) Pasting the patterns sequentially onto the window. (a2,a3) In the daytime, it does not interfere with the field of vision, while at night working as a decoration. (b1) The resistance sensor pattern is transferred onto the soft robot. (b2, b3) The resistance reading changes accordingly when the robot is resting and moving accordingly. (c1) Closeup of the connection between the transferred silver traces and temperature sensor. (c2) Add-on temperature sensor on a frying pan. (c3) Reading of the temperature sensor (can tolerate up to 250°C). (d1) The touch panel is folded to the back of the mobile device when not in use. (d2,d3) Flip the touch panel back to its working mode and perform the zoom-in function. (e1) Water leakage occurs and dissolves the Spiral pattern which is wrapped outside the black pipe. (e2,e3) Our sensor detects when there is no water leakage and when water leakage occurs. (f1) LED circuit fabricated by two layers of transferred silver nanoparticle traces. (f2,f3) LED device powered up wirelessly.	24
4.1	Demonstration of the hardware design: Top-left: Overview of the system. Middle: The explosion view of the drawing platform. Top-right: Two highlighted functions designed for circuit fabrication. Bottom: Highlighting drawing tools and cutting tool with associated applications.	33
4.2	(a) Resistance evaluation for the conductive ink on different substrates. (b) Resolution and accuracy testings. (c) Characterization of the dielectric ink. (d) Drawing speed testing.	38
4.3	Drawing quality evaluation on various surfaces with different roughness and topology.	40
4.4	laser cutting head testing: (a) Speed and power testing. (b) Resolution testing. (c) Substrates that laser cutting head can cut.	43
4.5	Interactive Piano: (a) Overview of the system. (b) The control board, the battery and the portable speaker connections. (c) The drawing process overview. (d) Playing the capacitive keys. (e) Tuning the volume. (f) The schematics of two layers and their functions.	44
4.6	Interactive Coffee Maker Control: (a) Demonstration the drawing and schematics of two layers and their functions. (b) The overview look of the coffee maker controller. (c) Brewing coffee remotely by using the controller. . . .	46
4.7	Capacitive Sensing Wall: (a) Zoom-in look of the surface texture of wall. (b) Zoom-in look of UV curing and dielectric ink brushing. (c) Overview of the sensing wall. (d) Human touch is detected by the capacitive sensing wall. (e) Detailed schematic for each drawing layer.	47

4.8	Printed FM Energy Harvester on glass: (a) The front view of the printed FM energy harvester with components mounted. (b) The fabrication process for the energy harvester. (c) When the energy harvester is capturing energy and powering up a blue-tooth module with embedded temperature and location sensor. (d) The design for the energy harvester. (e) The simulation result of the FM energy harvester (f) A closer view of the electrical components: the rectifier, the power management board and the blue-tooth module. . . .	48
4.9	3D Interactive Lamp: (a) An overview when the system is drawing the circuits. (b) A zoom-in look of the drawing and laser cutting areas. (c) When the lamp is turned on via capacitive sensor. (d) The overview of the fabrication setup. (e) Detailed decomposition of the assembly.	50
5.1	Overview of the PITAS system.	54
5.2	(a) Material preparation step for phase transition actuator and conductive silicone; (b) The material composition; (c) The two main fabrication options: 2D cutting & 3D printing; (d) The fundamental working mechanism for the system; (e) Detailed fabrication process.	56
5.3	Four categories of PITAS design primitives.	58
5.4	(a) Vinyl cutting process for the sensing samples; (b) Two example resistive sensing modalities: stretching and bending; (c) Three example capacitive sensing modalities: touching, pressing and sliding; (d) schematics for both sensing approaches; (e) Raw sensing data for resistive (stretch) sensing and capacitive (touch, press) sensing.	60
5.5	(a) Two parts of the instant conductive adhesive; (b) Conductive hook & loop connection method; (c) Conductive fabrics connection method; (d) Conductive thread connection method.	61
5.6	Four different fabrication approaches: (a) manual crafting; (b) vinyl cutting; (c) laser cutting; (d) optional 3D printing.	64
5.7	(a) Conductivity test results; (b) Heating speed test for five sample with different sizes; (c) Temperature curve for different input power; (d) Cooling speed test for five sample with different sizes	68
5.8	(a) Five phase transition actuator sample with different thickness; (b) Different bending curvatures achieved by the phase transition actuators; (c) The force testing setup and the results for the 3mm phase transition actuator sample.	69

5.9	(a) Configuration of hardware system; (b) A mobile application to visualize the sensing data; (c) An actual device that participants used in the workshops.	70
5.10	Overview of the actuation and sensing modules for PITAS	70
5.11	(a) Overview of the artificial rose and leaves fabricated by PITAS; (b) Delivering color change (colorless to pink) and flower blossom to partners remotely when missing each other; (c) Delivering the depression by enabling the color change (green to yellow) and leaf hanging down remotely.	71
5.12	(a) Different actuation modalities; (b) Remotely synchronize the task progress by tapping or bending the Post-in note with PITAS attached on the back. . .	71
6.1	The overview for functional destruction, including fabrication methods, destruction types, sustainable cycles, and potential application domain.	75
6.2	Overview of the design space for functional destruction, including detailed destruction types, sustainable electronic materials selections, available fabrication methods, and the potential application spaces.	77
6.3	The overview for inkjet printing water-soluble electronics, where conductive patterns are (a) printed on hydrographic films, (b) peeled off from the PET backing, and (c) directly dissolved in water.	80
6.4	(a) Printing resolution. (b) Resistance change over time for printing once and twice. (c) Printed devices.	83
6.5	(a) PVA-hydrogel combined printed water leakage sensor. (b) Resistance changes when there is a water leakage. (c) The sensor before and after swelling from the water leakage.	84
6.6	(a) PVA sheets with different layer thicknesses. (b) 3D printed different PVA composites. (c) Demonstration of the computational dissolvability within the same sheet.	86
6.7	(a) Detailed print-transferring fabrication method for highly conductive circuitry on beeswax. (b) Resistance change for straight and serpentine patterns respectively. (c) Demonstration of when the patterns are melted on a hot plate.	86

6.8	(a) Mixing steps for making the beeswax-graphite composite and the post-mixing shaping methods. (b) Conductivity testing results for different ratios of graphite powder. (c) Testing results for the resistance change under different heating temperatures. (d) Testing results of the resistance change over time for different graphite powder ratios.	89
6.9	Demonstration of creating a self-destroying circuit from Beeswax: (a) The front LED circuitry side; (b) backside to show the Beeswax-graphite composite is sealed inside; (c) The LEDs are on; (d) The circuits are damaged and the LEDs turn off. (e) The Beeswax-graphite heater reaches 50°C under thermal camera.	90
6.10	Demonstration of the devices made out of the beeswax-graphite composite and the re-configuring process including (1) an LED, (2) a capacitive touch sensor, (3) a resistive bending sensor with digital output displayed in background, Row 4: re-configuring process for the conductive beeswax sensors, and Row 5: the capacitive touch and bending test results.	91
6.11	Overview of the chocolate-based edible electronics: (a) 3D printing chocolate. (b) Assembling the 3D printed parts with the edible gold leaf that creates the electrode. (c) Optional chocolate mold-casting method. (d, e) Basic resistance and resolution testing for applying edible gold leaf onto different chocolates. (f, g) Demonstration of versatile 3D printed chocolate geometries and laser-cut edible gold leaf.	92
6.12	Detailed fabrication pipeline: 1) Sheet preparation, 2) Laser cutting/etching, 3) sugar paper transferal, and 4) final chocolate transfer steps.	92
6.13	(a) The circular pattern can be read to provide the calories contained in the chocolate. (b) The mesh pattern can be read to provide the chocolate flavor. (c) The wavy pattern can be read to confirm the presence or consumption of the chocolate.	93
6.14	(a) Four code primitives designed by Vena et al. [150], where we demonstrated Code '01'. (b) Our experimental setup.	95
6.15	(a) "C" shape resonator design on PVA, beeswax, and chocolate substrates. (b-d) RCS measurements results.	97
7.1	General design strategy. (a) Load versus strain curve under uniaxial deformation for different types of PVA and Cyclic loading to increasing strains as a function of strain. (b) Demonstration of PVA's mechanical flexibility (rigid, highly flexible, stretchable) for versatile types of devices (sheet, foam, tube).	103

7.2	Sheet fabrication and basic characterization. (a) Fabrication process for making recyclable electronics with thin-sheet form factor. (b) Contact angle between LM and different substrates. (c) Resolution testing for trace width and gap width. (d,e) Different device and pattern design primitives.	104
7.3	Sheet application. (1) Recyclable Sheet-based proximity sensor that responds to finger position. (2) Recyclable RFID tag used in two different application scenarios, including recyclable RFID clothing price tags and marathon RFID tracker. Both the proximity sensor and RFID tags are collected and recycled.	107
7.4	Foam fabrication and basic characterization. (a) Fabrication process for making recyclable foam electronics. (b) The pore diameter for the 1:2:4 foam recipe. (c) The conductivity testing for the interactive foam. (d,e) Different types and dimensions of recyclable interactive foams through mold casting or laser cutting.	111
7.5	Foam sensing primitives. (a, b) Capacitive sensing based pressure sensor and controller and (c, d) Resistive sensing based mechanical contact switch and bending sensor.	113
7.6	Recyclable interactive pen tip application. (a) From 1-4, we showcase recyclable interactive pen tips with different hardness and tactile feelings, from hard, medium, soft to brush feelings. (b) The disassembly look of the interactive pen for mobile devices with replaceable pen tips. (c) Young's modules for the foams with different material composition.	115
7.7	Tube fabrication and basic characterization. (a) Fabrication process for making recyclable tube electronics. (b-d) Recyclable tube with different diameters, wall thickness and length. (e) Three types of tube-based devices, including LED, sensor and actuator. (f) Basic electrical and mechanical testing results for tubes.	117
7.8	Two tube-based applications. (1) A fully recyclable sensor embedded haptic ring, and (2) An hand-weaved interactive LED.	118
7.9	Recycling process. (a) All three form factors-sheet, foam and tube will undergo immersion in the water until complete dissolution. Then the LM and PVA will be separately collected to conclude the recycling process. (b) Lab-scale recycling experiment over two months.	119
7.10	Comparative environmental impact analysis of Recy-ctronics sheet and conventional FR4 PCB.	121

CHAPTER 1

INTRODUCTION

Mark Weiser envisioned the computer for the 21st century should be a truly integral and invisible part of people's lives [1]. We have all witnessed the remarkable development along with this vision, where more and more computational devices are distributed in our living environment to serve users within the same space or looped in the internet to even bring remote users closer. However, the current networked environment or living space is still enabled by the limited numbers of IoT (internet of things) devices, where the average number of connected devices per U.S household in 2022 is 22. We are still far away from providing fully immersive interaction experience to users and the interaction modalities from the existing smart devices are limited. Taking cameras, the most powerful imaging sensing system as an example, besides the privacy concern, it can only capture images for a limited areas per device, where each device requires substantial efforts for maintenance (*e.g.*, change battery, repairment) and the usefulness often outlasts its lifetime by becoming E-waste that piled around our living spaces. Can we envision a future where intelligence seamlessly integrates into everyday physical world, providing users with a more natural and diverse interaction experience, while also considering their eventual destination and well-being? Instead of relying on cameras, can we use capacitive sensing matrix embedded in our room walls to capture indoor activity? Also, can these systems be self-powered without raising environmental concerns such as the use of batteries?

To enable this off the desktop world of ubiquitous computing in a sustainable manner, throughout my PhD journey, I was greatly influenced by the way how nature can effortlessly detect activity, exchange information, and provide responses. All living beings possess a degree of "physical intelligence" that determines their behavior (*e.g.*, encoded sensing, actuation). For example, *Mimosa pudica*, is a plant that can sense human's touch and

quickly respond to close its leaves. This is caused by the anisotropic structure located at the base of its root, allowing change of pressure only in length direction, which causes the overall movement. Can we borrow this anisotropic mechanism in designing our everyday surfaces (*e.g.*, tabletop), so it can sense our touch and deliver haptic feedback? Additionally, another important characteristic of living organisms is that after they fulfill their purposes, they begin to break down and prepare for the next life cycle. However, the lifespan of current smart devices often exceeds their usefulness and results in accumulation in the environment or becoming electronic waste. When we design these devices, we never have destruction in our mind. My PhD research aims to integrate sustainability with physical intelligence by bringing "sustainable physical intelligence" into our environment. This entails devices to sense surrounding activities, deliver information, or communicate locally or remotely. Moreover, it could involve considering how the built-in materials intelligence can facilitate self-destruct or recycling, mirroring the processes found in nature.

What is sustainable physical intelligence and why is it important? First, physical intelligence is referred as physically encoded sensing, actuation, control, memory, logic, computation and etc [3], which is leveraging the physical property with computational intelligence from a material perspective. For example, PVA (polyvinyl alcohol) as a typical water soluble material can be computationally designed with different levels of water-solubility (*e.g.*, by alternating thickness, porosity, hydrolyzed level) within the same sheet that can respond to different levels of water existence (*e.g.*, moisture, flood). One can further leverage this material-based intelligence to make smart water-leakage sensor by embedding conductive materials inside as the sensing electrodes or communication antenna and loop it in our ubiquitous computing world. I see the opportunities to utilize novel manufacturing approaches and materials to redesign our living environment by encoding physical intelligence to it, but what is still missing is where will these devices go after they fulfill the intended functions. So, I propose the concept of "sustainable physical intelligence" which will not only influences the performance or user interaction of devices but determines their

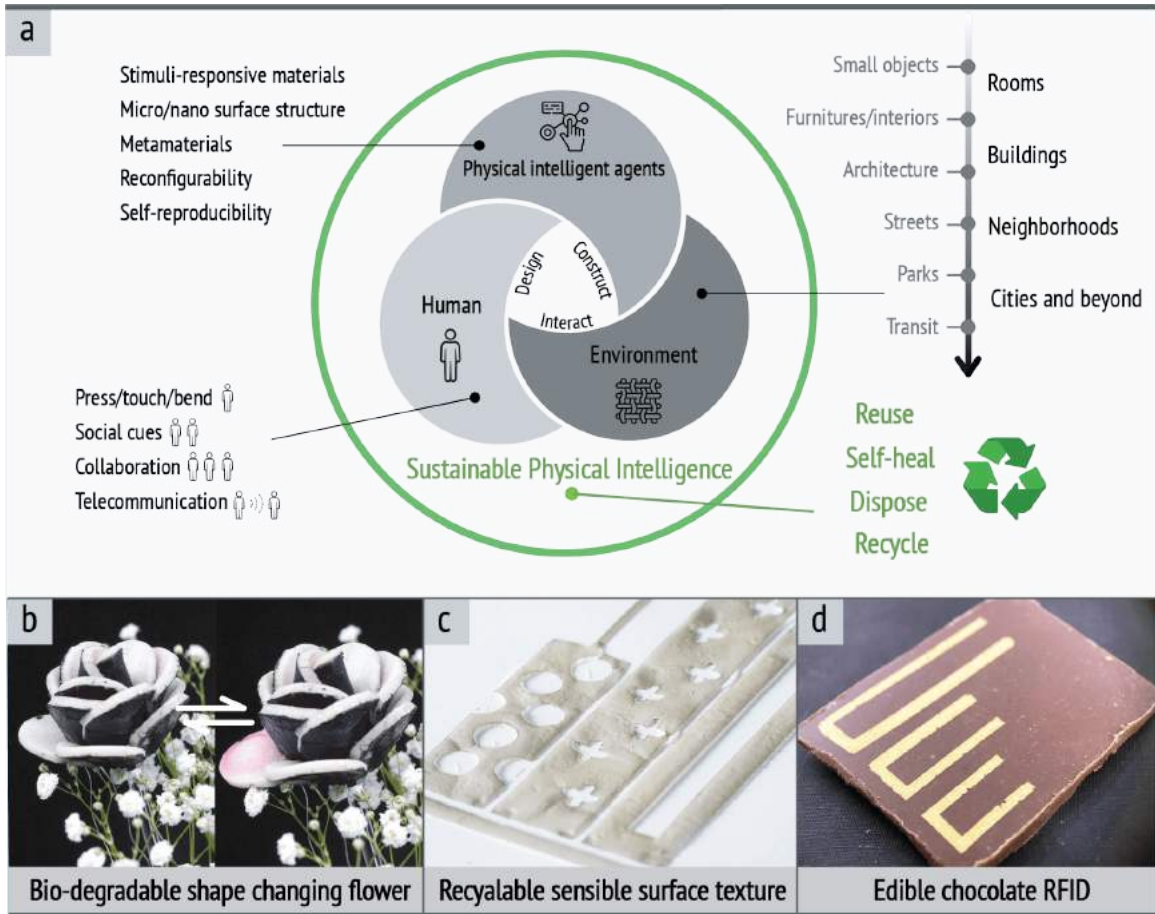


Figure 1.1: (a) Sustainable Physical intelligence for versatile interaction with sustainability in mind. (b) A shape changing artificial rose’s blossom can indicate happiness emotion while is bio-degradable. (c) Swelled sensible surface texture can augment everyday surface with tactile information and is completely recyclable. (d) Chocolate-based RFID can encode identifiable information and consumable to destroy the data.

life expectancy and alleviate environmental burdens. For example, a sustainable version of the PVA-based water-leakage sensor could be the device that starts as a water-leakage sensor for your home. As it senses the existence of water, it is also self-powered by water’s potential energy. Later, it degrades and breaks down naturally, reconfiguring itself into a soil moisture sensor that flows into your garden. Over time, it breaks down into compost without adding any environmental burden. Moving beyond the water-leakage sensor example, I further envision that one day 3D printing chocolates may encode Wi-Fi access passwords and be securely disposed by simply eating (Figure 1.1 d); a vivid artificial

flower made of completely bio-degradable shape changing materials can deliver emotional interactions (Figure 1.1 b); and a surface filled with expandable particles can convey sensible tactile information and meanwhile can be entirely recycled for making new devices. (Figure 1.1 c).

1.1 Thesis Statement and Research Questions

The natural world is abundant with living beings capable of perceiving, reacting, and communicating. What makes this even more amazing is their remarkable adaptability, allowing them to self-repair, revitalize, or even decompose and begin a new life cycle. Throughout my PhD, I started with a project called Silver Tape, which is a simple fabrication technique leveraging the inkjet printing circuits to transfer silver traces onto everyday surfaces without any post-treatment [2]. This method allows users to quickly fabricate versatile sensors by leveraging the material property such as transfer to heat-resistive kapton tapes to make heat-endurant sensor, or to 3M water-soluble sheets to make water-leakage sensor. More importantly, we also paid attention to how the transferred sensors can be **repaired** when damaged. Moving beyond the size limitation of inkjet printer that was used in Silver Tape, we try to further augment the large open spaces in our living environment like walls, facades, glass windows, etc. The second project I completed is Duco which negates the need for any human intervention by leveraging a hanging robotic system that automatically sketches multi-layered circuitry (*e.g.*, FM energy harvester, sensing arrays, interactive graphics) by loading various functional inks. We have explored not only how to incorporate these computational abilities into our living structures, but also created erasable ink that allows users to **erase** the circuitry and embed the surface with new capabilities. Besides sensors, in my thesis direction, I believe output is another unique element that the physical intelligence can enable. PITAS is a thin-sheet robotic material composed of a reversible phase transition actuating layer and a heating/sensing layer. The synthetic sheet material enables non-expert makers to create shape-changing devices that can locally or remotely

convey physical information such as shape, color, texture and temperature changes. The functional material that causes the transformation is the small particles embedded within the layer which will naturally escape from the matrix during prolonged actuation, thus compromising their performance. However, a distinctive **renewal** process can be accomplished by immersing the material-actuator in ethanol, which allows for its diffusion into the silicone-based material. Functional Destruction [4] is my next project, aiming to promote sustainability by designing devices that **self-destruct** once they have fulfilled their purposes. Specifically, we create these electronics through three different methods: 1) by inkjet printing conductive silver traces on poly(vinyl alcohol) (PVA) substrates to create water-soluble sensors; 2) by mixing a conductive beeswax material configured as a meltable sensor; and 3) by fabricating edible electronics with 3D printed chocolate and culinary gold leaf. To enable practical applications of these devices, we implement a fully transient and sustainable chipless RF detection system. Continuing the development of transient electronics, my most recent work Recy-ctronics aims not only to make transient electronics that can disintegrate but to ensure that they can be **fully recycled** for new device life.

Throughout my PhD studies, I have searched for ways to construct a future computational material-based environment of "robotic materials." These materials could sense the surroundings, exchange information, produce shape outputs, and adapt to environmental changes. They would also have the capability to self-destruct or be recyclable for new device lives, considering not only their usage but also their final destination. This approach seeks to incorporate computation on a large scale while also considering the entire lifespan of the devices.

Research Statement: I aim to leverage material properties to add versatile **sensing, actuation, or communication** capabilities into everyday materials such as glass and concrete, as novel human-computer-environment interfaces. Achieving this seamless integration re-

quires innovative **fabrication tools, materials and techniques** to construct interactive devices within our built environment. Moreover, I prioritize not only the design and usage of these devices, but also their **end-of-life sustainability**.

My thesis aims to address the following three research questions:

(1) What fabrication tools and approaches do we need in order to augment our environment with novel interactions?

(2) What sensing, actuation, or communication mechanisms should we develop to provide more natural interaction?

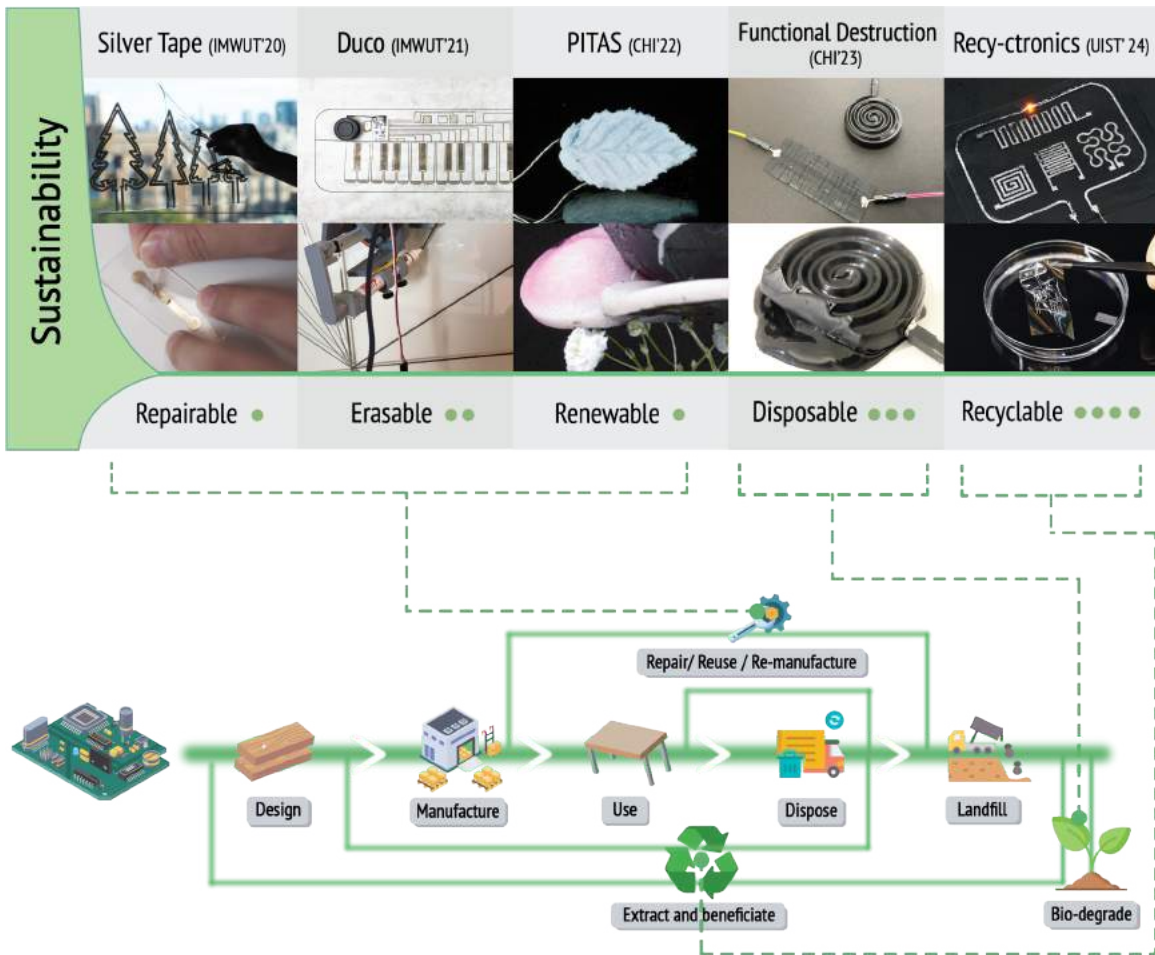
(3) How can we re-evaluate the ubiquitously embedded interactive devices through a more sustainable lens?

1.2 Document Structure

To answer the above questions and effectively design sustainable physical intelligence to enable natural human-computer-environment interaction, we need to build computation into everyday physical objects, creating a new type of ambient interface. Also, we must carefully consider the end-of-life cycle of these objects and their environmental impact. In section 2, I provide related background literature on conventional ambient computing, physical intelligence enabled interface, the fabrication methods to augment everyday surface with interaction and versatile sensing and actuation mechanisms and sustainable making in HCI. In section 3, I present a highly accessible, repairable, inkjet printing based approach to make different types of sensors with small scale. In Chapter 4, I introduce Duco, which is a circuit drawing robot that can directly draw and erase different types of circuit on every surfaces with meter-scale. In section 5, besides sensors span across different scales, I develop a shape transformable robotic sheet to deliver different types of physical information and its functionality can rejuvenate. In section 6, I discuss a method to design circuits with destruction and disposal in mind, enabling the controlled breakdown

of the devices, while also providing the opportunity for functional interactions. In Chapter 7, I further extend the disintegration of transient electronics for making fully recyclable electronics to further enhance electronics' sustainability. In Chapter 8, I discuss several key takeaways and future directions in terms of designing, using and disposing these novel sustainable devices. In Chapter 9, I conclude my dissertation.

Table 1.1: A position table to highlight the contribution for each of my completed work.



1.3 Contributions

1. I introduce different sets of highly accessible materials (*e.g.*, beeswax, PVA) with digital fabrication approaches (*e.g.*, 3D printing, mold-casting, inkjet printing) for making sustainable electronics. (RQ1)

2. I design and investigate novel sensing (*e.g.*, self/mutual capacitance, resistive), actuation (*e.g.*, phase transformation) and energy harvesting (*e.g.*, FM energy harvesting) for embedding versatile interactive modalities in our living environment. (RQ2)
3. I not only aim to add a wide range of interactive devices to our built environment, but also re-evaluate them with a more sustainable perspective, enabling devices that can be repairable, erasable, degradable, or completely recyclable to extend their lifespan. (RQ3)
4. I further discuss several observations and future directions for promoting the development of such sustainable interactive devices, including devices' life cycle assessment, their democratization for practical use and other technical challenges I encountered. (RQ1-3)

CHAPTER 2

BACKGROUND AND RELATED WORK

In this section, I start with presenting a brief background on the development of commodity IoT devices and different types of ambient interfaces and how they can contribute to construct the networked built environment that we can living in. Second, I review the emerging trends for novel material property enabled interfaces. Thirdly, I explore the possible fabrication approaches that can be utilised for integrating sensing and actuating capabilities in our everyday materials. Then, I introduce different types of sensing and actuation devices/systems span across different scales and form factors. Lastly, discuss what are the existing guidelines and practices for sustainable making.

2.1 Conventional Ambient Computing Interfaces

The invention of the first generation of IoT devices can be traced back to around 1999, a computer scientist Kevin Ashton, proposed putting radio-frequency identification (RFID) chips on products to track their status. As we are entering 21st century, billions of networked ‘smart’ physical objects are distributed around the world, from our living homes (*e.g.*, smart speaker, appliances), buildings (*e.g.*, package locker), to larger city scale (*e.g.*, toll road system). They are communicating all the time to receive and send out information to increase the intelligence and autonomy level of our living environment. Moving forward, along with a vision to further gracefully integrate the IoT devices into everyday things, ambient computing has drawn increasing attention. For example, embedding the display capability into clothing [5] and nails [6], and even wood [7]. Besides displays, people have also developed capacitance based sensors can be embedded with the sofa to control the function of home appliance [8], or cover the entire wall to enable more passive sensing for human gestures [9] or indoor locations [10].

2.2 Interactive Materials Enabled Interfaces in Everyday Life

There is also a recent trend that push the boundary of ambient computing to the material level. How we can computationally design materials and weave the functionalities into everyday life. Most of the work focuses on utilizing novel material as a new type of physical interface. People have weaved shape memory alloys (SMA) [11] , pneumatic tubes [12, 13] and other new composites (*e.g.*, nylon thread and silicone) [14] into textile wearables. Others have constructed stand-alone interactive devices using 3D printed shape memory polymers [15, 16], expandable particles [17] or phase transition materials [18]. There are also works on embedding novel materials into our living building materials, such as the integration of conductive materials as energy harvester on room windows [9], and the use of optical fibers as both input sensors and visual outputs in building walls [19]. Among this work, PneUI introduces silicone based pneumatic actuators as an elastic interface with performance that most motor based tangible interfaces do not have [20]. Self-healing UI is work from the same research group talking about how to use polymer polyborosiloxane (PBS) and a conductive filler to make interfaces that can physically self-heal [21]. These two examples show how encoded computational capability plays a irreplaceable role in constructing interfaces. The material property will determine how we interact with them.

2.3 Fabrication Methods/tools to Augment Living Environment

Over the past few decades, HCI researchers have made extensive efforts for developing fabrication techniques for novel sensors and actuators. Some approaches demonstrate utilizing 3D printing [22, 16, 23], vinyl/laser cutting [24, 25, 26, 27, 28], or inkjet printing [29, 2, 30, 31]. Others bridge fabrication techniques including chemical etching [32], screen printing [33, 34, 35, 36, 37], silicon mold casting [38, 39, 40], spraying [8, 41], and free hand drawing [42, 43]. There are also various fabrication techniques have been proposed to support the creation of soft material-based devices including soft lithography [44], mold-casting

[20], laser cutting and stacking, and 3D printing [45, 46], by using hobbyist digital fabrication equipment such as vinyl cutters [47], personal laser cutters [48] and dispensing-based 3D printers [49].

2.4 Versatile Form factor, Scale, Sensing and Actuation Modalities

Among different sensing and actuating devices that are distributed in our life, they usually span over a wide range of form factors, from completely flat [30], to 2.5D [50] to even 3D [20], or different scales. For example, most of the ink-jet printed sensors are limited within the printing substrate size [30] (*e.g.*, US letter, A4), which Duco team tried to build a drawing robot which can drawing sensors or energy harvesters beyond meter size [9]. Besides different outlook differences, different sensing, communication and actuation mechanisms are introduced for mapping versatile purposes.

Soft material-based shape-changing interfaces which can dynamically change their orientation, form, volume, texture, or stiffness, has been an emerging area within HCI [51, 52, 53]. Researchers have made tremendous developments [20, 54, 55, 56, 57], mainly due to their ability to serve a wide range of users [20, 16], adaptability to various form factors [58, 11, 59], and diverse functionality [60]. Researchers have also demonstrated how their versatile sensing abilities can be combined with different types of actuation mechanisms, including sensing for pneumatic actuators [20], shape memory polymers [16], shape memory alloys [61]. There are also other works that are presented as tool kits or parametric design interfaces for more general purposes [62, 63, 64, 65]. Although there have been advancements in the sensing and actuation mechanisms of soft material shape-changing interfaces, current methods are still in their infancy and are limited. Electroactive polymers, for example, are capable of providing high-frequency locomotion but usually require pre-processing of the materials (*e.g.*, uniform pre-stretch of the material) and high voltages to trigger the actuation [66, 67]. Pneumatic-based shape-changing interfaces, which utilize commodity materials and electronic components to provide large strains or forces

with rapid response time, require external compressors and pressure-regulating components, limiting their miniaturization and practicality for untethered applications [68, 69, 20].

These sensors and actuators can also be combined to delivery a wide range of information across different fields, including VR/AR [70], mobile devices [71] or wearables [72]. Many of these haptic devices have different form factors. For example, researchers have presented a jacket embedded with an array of pneumatically-actuated airbags and force sensors that can provide precisely directed forces and high-frequency vibration effects for virtual reality applications [73]. Similarly, *PneuHaptic* is a pneumatic-based bracelet that can trigger a range of tactile sensations on the arm by alternately pressurizing and depressurizing pneumatic chambers [72]. Researchers have also explored different types of materials that can be used to convey haptic information such as thin and flexible shape memory alloys (SMA) [74], self-contained retractable wire systems [70] and piezo-based interfaces for electro-tactile output on users' fingers [37].

2.4.1 Sustainable Making and Unmaking

Calls for sustainable guidelines and practices within HCI have existed for a long time. Under Sustainable HCI (SHCI), there is a growing focus on more environmentally-conscious fabrication and design [75, 76, 77, 78, 79]. For example, Lazaro Vasquez et al. proposed the Life Cycle Analysis as a guideline to evaluate the sustainability of a design practice, which urges researchers to consider using the materials with the lowest “embodied energy” and carbon dioxide emissions [76]. However, implementing these materials in practice is challenging. Even with such guidelines for choosing materials, fabrication methods, and means for disposal, a recent review has shown that one-third of prototyping or digital fabrication research still relies on plastics [80]. Even when researchers desire to choose eco-friendly materials like PLA, the effort to source from a responsible manufacturer and find proper disposal (i.e., industrial composting facility or proper recycling centers) often dissuades

their use. It is not surprising that when researchers consider materials for prototyping interactive systems, price and performance are most often prioritized over sustainability.

Compared to making or constructing with sustainable materials, much less work has focused on sustainable unmaking. Song et al. recently propose a method to embed expandable particles into 3D prints for “unmaking” [81]. Another work proposed a method of making wireless heating interfaces that are backyard decomposable within 60 days [82]. There are other parallel “un” practices, including uncrafting [83] and unfabricating [84]. Combined, these practices lead the discourse in HCI on novel experimentation with physical objects and materiality for destruction. Our work is inspired by the sustainable unmaking vision and introduces functional destruction – leveraging the destruction process for functional purposes.

CHAPTER 3

INKJET PRINTING AND TRANSFERRING REPAIRABLE ELECTRONICS TO EVERYDAY SURFACES

In the past decade, digital fabrication tools such as laser cutter and 3D printer have benefited not only manufacturers and suppliers but also researchers, makers, artists, and even children to embody their own design. Such tools allow users to play with a wide range of materials (e.g., paper, metal sheet, plastic, rubber-like material, etc) in easy, fast, low-cost, and compact processes. Our motivation is to further extend this idea to the digital fabrication of electric/electronic circuits beyond a significant body of prior work to realize the both accessible processes and diverse material selections at the same time, where inkjet printing conductive circuits has shown promising potentials [30].

The conductive ink for inkjet printing normally requires either heat sintering or chemical sintering (known as sintering-free) process in order to dry out or dissolve the polymer shell outside the conductive particles, which prohibits the agglomeration of the ink. For heat sintering, it requires additional equipment such as heat guns or ovens to heat up the printed pattern, which is relatively costly and time-consuming. Moreover, if not handled professionally, such procedures can damage the printing substrates [30]. In this regard, chemical sintering shows brighter advantage, since it offers relatively precise and highly conductive traces, without requiring expensive machines or non-reusable stencil sheets that are inevitable in other methods like 3D printing or screen printing. However, conventional inkjet printing of silver traces with a sintering-free process has been limited to the specially-coated paper that ensures the formation of bulk silver and good adhesion of traces to the substrate. This limitation has heavily restricted people's design choices with this fabrication technique, which prevents it from being adopted in a broader spectrum of applications.

Here we propose Silver Tape, an extension of sintering-free inkjet printed circuit, which

allows us to explore many types of materials as substrates of conductive traces, without losing the benefits of its easy, rapid, low-cost, and compact nature. With our technique, users simply inkjet print the target pattern onto Kodak photo paper (Kodak AZERTY5149), Fujifilm Paper Kassai Pro or Epson premium photo paper GLOSSY which are commercially available; customized Mitsubishi PET film, which is not yet commercially available, apply substrates (e.g., Scotch tape, PDMS elastomer, 3D printed soft structure, etc.) on top of the printed traces, and peel the pattern off for practical use. The applied substrates enable printed traces with corresponding properties, many of which cannot be previously achieved by conventional paper substrates.

The biggest yet simplest finding in this project was that we can transfer inkjet printed silver traces only when we use less sticky papers as printing media, whose property has been regarded bad for a medium of inkjet printed circuit – because less adhesive surface cannot maintain the silver traces against mechanical scratches. However, we turned this undesired disadvantage of low adhesiveness of a substrate into the advantage by using less-adhesive surfaces as temporary transfer medium.

3.1 FABRICATION PROCESS

The fabrication process of Silver Tapes consists of three simple steps: **printing** (Figure Figure 3.1a), **transferring** (Figure Figure 3.1b) and **assembling**. Instead of relying on additional heat sintering, our Inkjet-printed pattern becomes conductive due to the chemical sintering reaction on the surface of the chosen temporary transfer paper. Additionally, our method can be achieved with a standard desktop inkjet printer loaded, silver ink, and a wide selection of sticky tapes, which is easy, fast, compact, and low-cost as we will describe in greater details later.

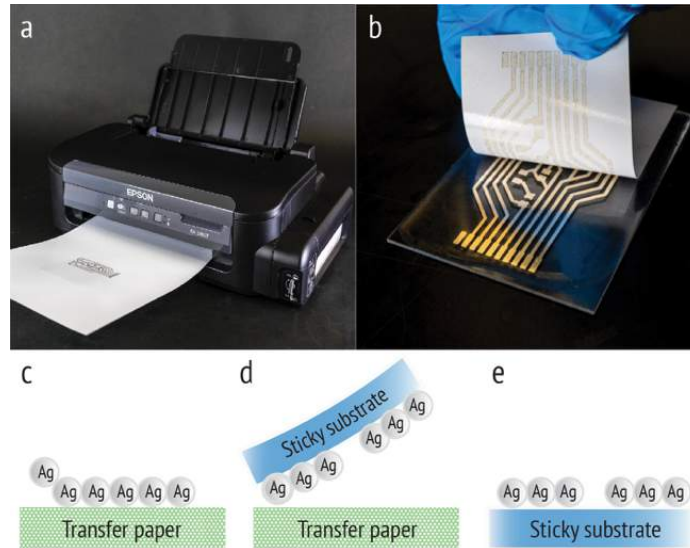


Figure 3.1: Overview of Silver Tape. (a, b) Fabrication process. Conductive patterns are printed on transfer paper (a), and then peeled off and transferred (b) by hand. (c-e) Schematics of the transfer process of silver nanoparticles from transfer paper to a sticky substrate.

3.1.1 Printing

For printing silver ink, we used a desktop inkjet printer (Epson PX-S160T) and silver nanoparticle ink (Mitsubishi Paper Mills NBSIJ-MU01) in order to carry out all the testings and applications. We adopted the printing method based on the literature [30].

For the printing paper selection, we investigated four different papers: commercialized glossy photo paper (Kodak AZERTY5149), Fujifilm Paper Kassai Pro, Epson premium photo paper GLOSSY, and customized Mitsubishi PET film, all of which are commercially available except the PET film. All four papers can cause chemical sintering process on the surface [30], and support the transfer process.

N.b., The customized Mitsubishi PET film was made by Mitsubishi Paper Mills, by replacing the surfacial “sticky layer” on the conventional Mitsubishi PET film for silver ink printing (NB-TP-3GU100) into the “release layer” composed of non-sticky particles. This release layer helps us peel the sticky substrate off the transfer paper surface; in case of using commercially available transfer paper, silver traces is relatively easy to peel, but it is

hard to peel the sticky substrate off the “white” surface without any silver traces on it, due to the high stickiness of the paper surface. Thus, the special PET film is superior in terms of easy transfer compared to the other candidate paper substrates. The sample of customized Mitsubishi PET film is available as “Transfer sheet” at E-mail: agnano@mpm.co.jp.

3.1.2 Transferring

We applied the adhesive side of a sticky substrate such as a tape onto a transfer paper. To facilitate a successful peeling/transferring process, we rub the tape gently to ensure a seamless contact between the adhesive and the printed pattern, and then slowly peeled off the adhesive.

Our method is compatible of a wide range of tapes, several of which we selected as examples for demonstration and evaluation next, including Scotch tape (3M Scotch 810), polyimide electrical tape (3M 1205), vinyl insulation tape (3M Super 33+), Scotch transparent tape, water soluble tape (3M 5414), Scotch removable tape (3M Scotch 811), and masking tape (3M Scotch 234) (Figure 3b) . We evaluated the above example substrates and proved their compatibility with our method. We also observed that the low adhesion and rough surface of Scotch removable tape and masking tape cause nanoparticle residuals left on the printing paper after transfer. We reported the procedure and several key results of comprehensive performance evaluation in the electrical and mechanical analyses section.

3.1.3 Assembling

After we transfer the patterns onto target substrates, we connect the conductive traces with other electronic components. Silver Tape allows four commonly used connection methods: (a) adhesive force inherent to the sticky substrate for extension of wiring, (b) conductive paste (Bare Paint) /epoxy (CW2400) to make permanent connection, (c) fixing a stable, solderable connection with metal pierce punch SK11 pierce punch, and (d) liquid metal eutectic gallium indium (EGaIn) for temporary connection to connect with, for example,

the probes to measure electric properties of testing circuit (Figure 4d).

3.1.4 Re-transferability

On top of printing, transferring, and assembling. Sometimes the transferred pattern might get damaged, for example when over-bended, accidentally scratched, which are likely to happen in reality but rarely considered in previous literatures. Our technique allows users to quickly fix the damaged portion by re-transferring a new trace onto the damaged part to recover the conductivity of the trace, or even using commercially-available circuit eraser to erase the unwanted part of the silver traces and retransfer with a desired one. In Figure 5, we show that we partially remove the transferred pattern and replace with a new one.

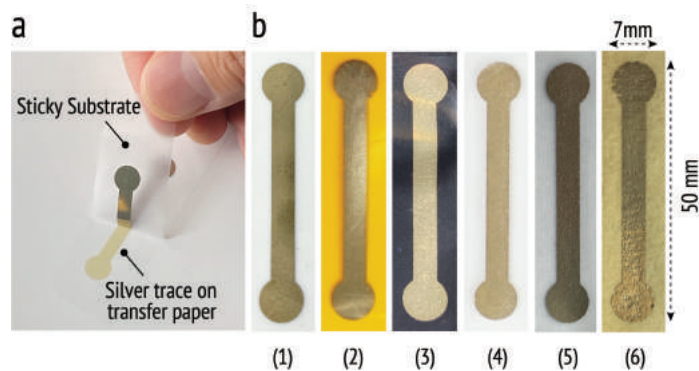


Figure 3.2: Silver traces transferred to different substrates. (a) Transfer process. (b) Successfully transferred conductive patterns on various substrates: (1) Scotch tape (3M Scotch 810), (2) polyimide electrical tape (3M 1205), (3) vinyl insulation tape (3M Super 33+), (4) water soluble wave soldering tape (3M 5414), (5) Scotch removable tape (3M Scotch 811), (6) masking tape (3M Scotch 234).

3.2 ELECTRICAL & MECHANICAL ANALYSES

To better understand the transferring process and evaluate the electrical and mechanical performance of our technique, we carried out several tests. We also summarized our key findings in this section to help predict and guide the design procedures for researchers, makers, and hobbyists to adopt our method in their applications.

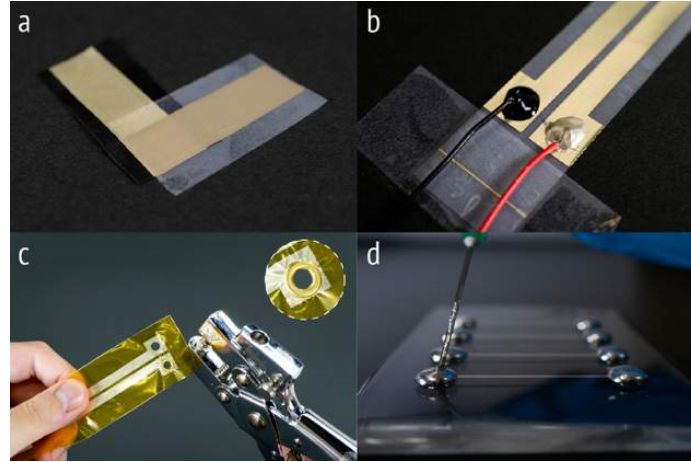


Figure 3.3: Connection methods. (a) Pasting two sticky substrates using their own adhesive force. (b) Conductive paste/epoxy. (c) Pierce punch to make a stable, solderable connection. (d) Temporary liquid metal connection mainly for measurement.



Figure 3.4: (a) Silver trace is transferred onto PDMS and connected with LED. (b) Part of the trace is removed. (c) Recovering the damaged portion with a new silver trace. (d) The silver trace is recovered.









3.2.1 Transfer Resolution

We first tested the transfer resolution, which decides the widths of printed traces. An ideal circuit fabrication approach should be in high resolution, able to provide thin traces to support fine-grained circuitry patterns. Figure 7a shows the transferred silver patterns with seven different widths we tested. In this test, we printed the the pattern in different widths on Mitsubishi PET film and transferred onto PDMS sheet. We took multiple trials and measurements and found the thinnest pattern we could achieve was 0.1 mm. Traces less than 0.1 mm caused breakage. Note that the resolution 0.1 mm is better than the value reported in [30], which is the resolution of traces inkjet printed on paper. We speculated this difference mainly came from the high resolution of the printer we used.

3.2.2 Resistance Change Using Different Substrates

We investigated the resistance variance before and after transfer, where we used the same tape (Scotch transparent tape) to transfer 7 mm thick traces (with a 50 mm length) from different printing substrates, including Kodak photo paper, Fujifilm Paper Kassai Pro, Epson premium photo paper GLOSSY and customized Mitsubishi PET film (Table 3.1). For each substrate, the pattern is printed and transferred 20 times, where we measured the resistance of the traces before and after the transfer. Table 3.1 summarizes our results. We found that all the printing substrates show promising conductivity after transfer, while Fujifilm Paper Kassai Pro, Epson premium photo paper GLOSSY and customized Mitsubishi PET film show much smaller resistance variance before and after transfer than the Kodak photo paper. We selected the customized Mitsubishi PET film as the printing substrate for most of the rest testings and applications.

Table 3.1: Resistance variance before and after transfer for different printing substrates.




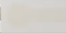









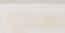

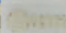

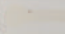










Substrates	Printing Patterns		Resistance (ohm/sq)	
	On Tapes	On Sustrates	Before	After
Kodak Premium Photo Paper			0.53±0.02	1.44±0.61
Epson Premium Photo Paper			0.16±0.03	0.27±0.04
Fujifilm Paper Kassai Pro			0.14±0.01	0.30±0.06
Mitubishi PET Film			0.15±0.01	0.28±0.05

3.2.3 Resistance Change Using Different Adhesives

We also investigated the electrical performance with different adhesive materials when we used customized Mitsubishi PET film as the printing substrate for all these tests. To facilitate others' access to our technique, we used only off-the-shelf tapes. We did an extensive search and purchased 14 different tapes we found on the market. We used these tapes together with PDMS sheets, soft 3D printing material Tango Black plus to transfer the designed pattern printed on the customized Mitsubishi PET film (Table 3.2). Same as the test before, we measured the variance of the resistance before and after the transfer. The

pattern is printed 20 times and transferred 20 times. Table 3.2 summarizes our results. As we can see, all transfer materials consistently show successful transfer, whereas the highlighted transfer materials on the right side of the table are showing relatively higher resistance variances mainly due to the stickiness difference or the surface roughness level of the transfer materials. Additionally, we looked into the datasheet of these tapes and found that in order to achieve a relatively smaller resistance variance, adhesion between 0.4N/cm to 6N/cm would be a good selection range. Adhesion lower than 0.4N/cm could also show successful transfer but might with bigger resistance variance, while too big adhesion might make transfer material not able to be peeled off from the printing substrate.

Table 3.2: Resistance variance before and after transfer for different transfer materials.

Peeling F.	Substrate	Printing Patterns		Resistance (ohm/sq)		Peeling F.	Substrate	Printing Patterns		Resistance (ohm/sq)	
		On Tapes	On Sustrates	Before	After			On Tapes	On Sustrates	Before	After
Unclear	Scotch Double Sided			0.14±0.01	0.27±0.05	2.5N/cm	Scotch Magic Tape			0.14±0.01	0.20±0.03
Unclear	PDMS			0.14±0.01	0.20±0.02	Unclear	Tango Black +			0.15±0.01	0.31±0.08
6N/cm	Scotch Heavy Duty			0.14±0.01	0.21±0.03	Unclear	Scotch 2080			0.14±0.01	0.32±0.11
0.4N/cm	3M Water Soluble Tape			0.15±0.01	0.21±0.05	1.5N/cm	Scotch 2093			0.15±0.01	0.40±0.13
2.4N/cm	Polymide Tape			0.14±0.01	0.23±0.05	3.5N/cm	Scotch 234			0.14±0.01	0.30±0.09
1.55N/cm	Scotch Transparent			0.15±0.01	0.28±0.05	3.5N/cm	Scotch General Purpose			0.14±0.01	0.36±0.09
2.8N/cm	Scotch Super 33+			0.14±0.01	0.24±0.05	0.3N/cm	Scotch Removable			0.14±0.01	0.32±0.09

3.2.4 Transfer to Everyday Surfaces

With the adhesive nature of the tapes, we can transfer and directly paste the conductive pattern onto different everyday surfaces for real-world uses. In Figure 6, we show a conductive pattern (i.e., 7 mm width, 50 mm length) transferred onto different materials including aluminum, glass, granite, wood, foam, fabrics, and acrylic. From the microscopic images, we also visualized the connection of the silver nanoparticle when they are on the tapes, and perceived some minor cracks which might cause the increase of the resistance.

3.2.5 Transfer to Different Geometries

Besides different materials, we also tested how the resistance will vary when we transfer the conductive patterns onto different geometries. We drew three basic geometries – flex, corner, twist, which exemplify most of the everyday objects. We measured the resistance before and after the substrate is coated onto the geometry. In general, we found the resistance increases after transfer, due to the local stretching of the substrates. The flex geometry caused the resistance to increase from 0.37 to 1.22 Ω/sq , corner from 0.37 to 4.04 Ω/sq , and twist from 0.37 to 6.54 Ω/sq . As we can see, the twisty shape shows a much bigger resistance change than the other two. We speculate when under twisting, the transferred silver traces got multiple local stretches along with the twist, which could loosen the density of silver nanoparticles and increase the resistance.



Figure 3.5: Silver traces transferred onto different materials and geometries.

3.2.6 Bending Tests

From the geometry test, we found mechanical status especially bending is a strong factor on the resistance variance of the transferred traces using our method. Here we investigated bending – both inward and outward bending. We measured resistance at different bending angles and Figure 7 (b,c) summarize our results. In the case of outward bending, the sheet resistance decreases as the bending radius is increasing, since along with the increase of

the bending radius, the less propagation of cracks will happen with silver traces. For the inward bending tests, the sheet resistance gets higher as we increase the bending radius. This is because the density of silver decreases at the bent region. Based on this result, we recommend inward bending for more consistent and reliable electrical connections.

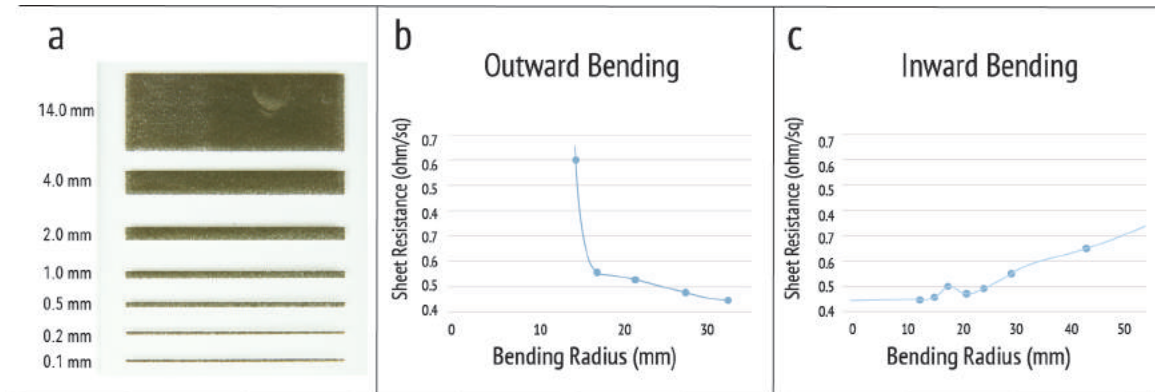


Figure 3.6: (a) Transfer resolution. (b) Resistance under outward bending. (c) Resistance under inward bending.

3.3 APPLICATIONS

Based on the results from previous evaluations, we developed six application examples applying our technique. These applications present different key features of prototyping processes, including sensing and actuating, single- and multi-layer circuitry, domain-specific use and daily usage in varied scales.

3.3.1 LED Decorations

We built a large LED display (100 cm by 30 cm) to demonstrate how Silver Tape can provide a fast and easy routine of fabricating a large conductive pattern (Figure 9a). We inkjet printed seven Christmas tree patterns on different A4-sized Mitsubishi PET films and transferred them onto one big PDMS sheet, where the PDMS sheet is cured on top of an acrylic board backing in a ratio of base to cure 20:1 (Dow Corning Sylgard 184) under room temperature. Note that the size of this demo is beyond what a standard desktop printer can

print. However, The modularity nature of this technique allows us to print and transfer part by part, eliminating the need for large printers. Specifically, seven Christmas tree patterns are printed and transferred separately. LEDs are mounted later on with conductive paste Cemedine SXECA48. Daytime and nighttime views of the LED circuit are shown in Figure 9 a2 and a3.

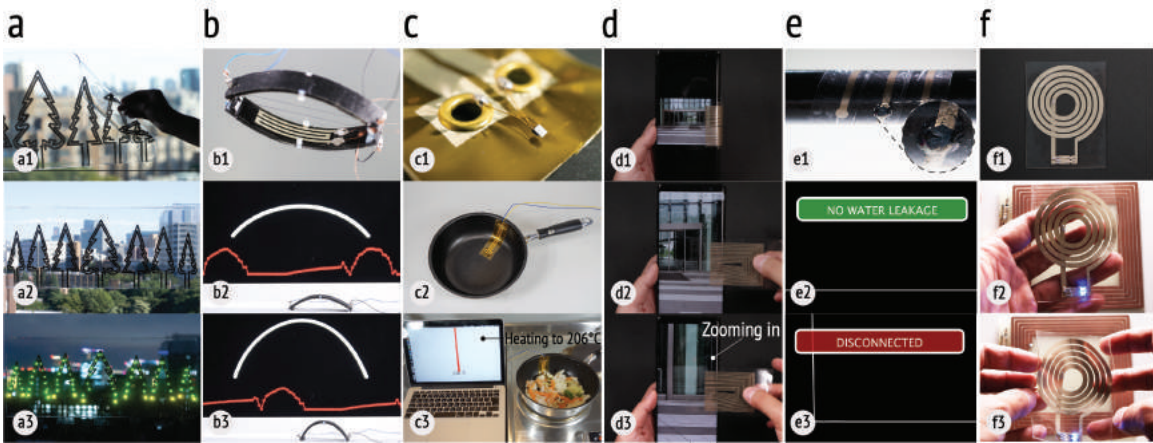


Figure 3.7: Applications: (a1) Pasting the patterns sequentially onto the window. (a2,a3) In the daytime, it does not interfere with the field of vision, while at night working as a decoration. (b1) The resistance sensor pattern is transferred onto the soft robot. (b2, b3) The resistance reading changes accordingly when the robot is resting and moving accordingly. (c1) Closeup of the connection between the transferred silver traces and temperature sensor. (c2) Add-on temperature sensor on a frying pan. (c3) Reading of the temperature sensor (can tolerate up to 250°C). (d1) The touch panel is folded to the back of the mobile device when not in use. (d2,d3) Flip the touch panel back to its working mode and perform the zoom-in function. (e1) Water leakage occurs and dissolves the Spiral pattern which is wrapped outside the black pipe. (e2,e3) Our sensor detects when there is no water leakage and when water leakage occurs. (f1) LED circuit fabricated by two layers of transferred silver nanoparticle traces. (f2,f3) LED device powered up wirelessly.

3.3.2 Bending Sensors for Soft-bodied Robots

Attaching sensors to close the loop in controlling soft-bodied robots is challenging due to the non-compatibility of traditional sensors with soft-bodied materials. This application shows that Silver Tape can be a promising application as it easily enables loading soft-bodied robots with sensors without any additional layers. Our soft robot application is

3D printed by Objet260 Connex3 with soft 3D printing material TangoBlack +, which is quite sticky and made it a good substrate for Silver Tape (Figure 9b). We transferred a resistance-based bending sensor to a 3D printed inching worm robot and actuated the robot with a shape memory alloy (SMA). The bending motion of the robot changes the resistance of the bending sensor. We read the resistance change using a voltage divider circuit with an Arduino board. This bending sensor can also be applied to on-body locations for posture sensing. Specifically, resistance change can be calibrated using Kinovea motion analyzer to map the corresponding bending angle.

3.3.3 Circuitry for High-Temperature Applications

Conventional inkjet printed paper circuit could not endure heat over 120°C. This example application shows the attachable temperature sensor to a frying pan (Figure 9c). We printed the conductive pattern on Mitsubishi PET film and transferred to Kapton tape (Lifework Concierge LCA110, heat tolerant up to 250°C) to wire up a tiny platinum resistance thermometer (RS Pro PT100) on both ends of the two silver traces. Resistance change of the sensor by heat was measured by an Arduino.

3.3.4 Touch Panel Extensions for Mobile Devices

We made a striped pattern based touch panel extension, which was printed on Mitsubishi PET film and transferred to Scotch heavy-duty tape. The touch input will be generated when fingers are in contact with the printed conductive lines. The whole panel extension patch can be fully folded and attached to the back of the phone when not in use. A user can use this extended touch panel for quick commands without blocking the phone screens. For example, Figure 9 d2 and d3 demonstrate a zoom-in gesture.

3.3.5 Water Leakage Sensor

Figure 9e shows a water leakage sensor, which we made by printing and transferring a spiral pattern onto the 3M 5414 water soluble tape. Leaked water dissolves the substrate and conductive patterns, which we can detect by measuring resistance with an Arduino. We threshold the resistance measurement for detection. Figure 9e1 is showing the moment when water leaks out from a hole and dissolves the spiral pattern which gets detected in 9e3.

3.3.6 Wirelessly Powered Resonator by Multi-layer Circuit

We demonstrate a design of multi-layer circuit by transferring a silver coil pattern on the top/bottom of the PDMS substrates and connecting with silver conductive epoxy via holes. Figure 9f demonstrates wireless power transfers to the fabricated coil. AC power (i.e., 6.78 MHz) was emitted from an external power source via a transmitter coil. The emitted energy was then inductively coupled to the fabricated coil and transferred to an LED via this inductive link.

3.4 DISCUSSION AND LIMITATIONS

3.4.1 Stretchabilities

As mentioned previously, due to the limitation from the material itself, silver nanoparticle traces are barely stretchable. However, stretchability is playing an irreplaceable role in many applications such as wearable devices. We expect that prestretching the PDMS substrate before transfer can be a way to increase the stretchability of Silver Tape, without losing the benefits (i.e., simplicity) of our method.

3.4.2 On Skin Transfer

As for the silver transfer on skin, only short length 1 cm of the conductive trace was successful so far in our pilot test, due to the wrinkles on the skin surface, which might cause the cracks on the transferred traces. However, we regard directly transferring silver onto our skin as a possible future application, like tattoo paper-based methods described in [24, 35]

3.4.3 Robustness

There are two aspects to consider: the robustness of the transfer step and longevity of the transferred traces. For the first one, similar to what have been discussed in the transfer quality section, the transferred pattern quality has been barely affected when different participants were conducting the transfer step in terms of different peeling direction, force, speed, or even geometries. However, the transferred pattern could be fragile. Two participants also raised a concern about the fragility in the questionnaire. This is mainly due to the brittle nature of the silver nanoparticles. Any accidental scratches or over bending would cause the permanent breakage of the transferred pattern. Laminating a cover layer like [30] or simply applying another tape layer on top of the transferred circuitry could potentially prevent the circuit breakage.

3.4.4 Hysteresis of Silver Nanoparticles

We observed the hysteresis of the transferred silver nanoparticles traces when conducting experiments, where the resistance will take sometime to recover or settle to a stable value. Inspired by the work [85] of rubbing liquid metal particles (EGaIn) into the printed silver nanoparticles, we might be able to minimize the hysteresis effect of the silver nanoparticles.

For the future research directions, fabricating large scale electronics with multi-functionalities is in high priority. This work provided a solution for large scale electronic fabrication, but still many manual steps are involved. We would like to explore more automated systems

which could provide an end-to-end solution for userd by not only designing and printing the conductive traces, but also auto-mounting the electronics. For example, the robotic arm or remote-controlled robots equipped with conductive dipping machine might worth investigating. Another research direction would be how to apply the conductive patterns and electronics onto conformal surfaces robustly without losing the rapid and easy nature. We believe transfer technique has a promising potential to solve this. Instead of transferring non-stretchable silver nanoparticle, one could transfer stretchable conductive material such as carbon grease, PEDOT:PSS, with the help of a deformable transfer media like foam. We believe both directions are worth for further investigation in order to reach the goal of digital fabrication of electronics.

CHAPTER 4

DUCO, A FULLY AUTONOMOUS ERASABLE CIRCUITS FABRICATION ROBOT TO ENABLE INTERACTIVITY ON LARGE SURFACES

To date, advances in fabrication methods for electronics have emphasized packing the most functionality into the smallest form factors. Such optimizations have paved the way for the fabrication of devices with increasing complexity and diversity of form factors (*e.g.*, mobile phones, activity trackers, etc.). However, little has been done to enable the digital fabrication of electronics with large surface areas. On the other hand, large vertical surfaces are ubiquitous and abundant in our daily lives (*e.g.*, walls, windows, fences), functioning mainly as space dividers or infrastructure coverage. They exist everywhere and take up substantial spaces, yet are used mostly for structural purposes without interactivity. Many interactive art installations and research projects [41, 8, 19] have recently attracted great attention by demonstrating practical uses for adding additional functional layers with arbitrary designs by taking advantage of these existing large and vertical surfaces.

Existing circuit fabrication methodologies, such as printed electronics (*e.g.*, inkjet printing, 3D printing, etc.), have demonstrated the advantages of providing low cost, highly accessible digital electronic fabrication methods. We have seen advances that increase the level of customization in the printed electronic process [86], serve a broader spectrum of users [2], and extend the number of everyday surfaces and objects to which printed electronics can be applied [87]. Notably, *Inkjet-printed circuits* pioneered an easy, fast, and cheap digital fabrication method for prototyping functional electronic devices [30]. In addition, many other inkjet-based advances have resulted in a wider variety of sensors [88], displays [89] and other interactive objects [31].

However, there are no such digital fabrication tools to prototype large-scale circuits. Among the current systems for fabricating large-scale circuits, the challenge lies in the

need for human efforts (*e.g.*, preparing and aligning stencils, manually painting or spraying the functional materials, removing the stencils), making it laborious and extremely difficult for large-scale fabrication (*e.g.*, large amount of human efforts and time, material waste left on stencils, non-reusable stencils for different designs, poor manual consistency and repeatability of circuits) [41, 8]. It is also noteworthy that even to prepare the stencils, most of the existing machines are still taking up much of the plane space (*e.g.*, CNC routers used in [19], laser cutters used in [8]). The vertical spaces have not made the best use as direct fabrication workspaces so far.

To advance the field of recasting large-scale everyday vertical surfaces as smart surfaces which can be highly beneficial to the three previously identified circuit fabrication domains relying on large surface areas (*e.g.*, human-scale sensing, energy harvesting, 3D interactive artifact), a digital fabrication system that can meet the following four criteria is needed: 1) to greatly reduce the amount of human intervention required during the fabrication process without requiring any stencils, 2) exhibit superior circuit fabrication performance by paying attention to resolution, accuracy, repeatability, 3) support circuit fabrication with a diverse selection of tools on versatile vertical everyday surfaces and 4) take advantage of utilizing vertical spaces as main fabrication sites.

With these considerations, we propose Duco, a direct circuit writing (DCW) system for creating high-fidelity large-scale electronics. Duco supports three types of tools: a drawing pen/brush equipped with conductive, dielectric, and cleaning inks to additively draw circuits on top of the vertical surfaces, a laser cutting head for subtractively making 2D cutouts on large surfaces, and a UV LED head to automatically cure inks that are printed. Duco is able to effortlessly switch between different inks using a custom rotary tool changing mechanism.

To validate the proposed system for circuit fabrication on versatile substrates with a wide range of visual and surface features (*e.g.*, surface roughness, topology), we demonstrate applying Duco to six vertical everyday surfaces (wall paint, wall paper, wood, glass,

acrylic, and ceramic). Duco enables the DCW method to fabricate circuits directly onto target vertical surfaces, eliminating the need for manual transfer or pasting steps.

4.1 DUCO WORKFLOW OVERVIEW

Our system for large-scale circuit drawing involves five steps: (1) sketching a circuit pattern, (2) setting up the system, (3) selecting tools and substrates, (4) drawing the pattern by operating the system, and (5) wiring up the circuits.

4.1.1 Creating the Digital Design

The first step for drawing a functional circuit is to develop the circuit graphic design. Any 2D vector graphic design software, such as Adobe Illustrator or Sketch can be utilized for this step. We can also use professional circuit design software (*e.g.*, KiCad), which allows users to export each circuit design layer as separate SVG files. Once the circuit design is completed, users can upload it to our interface. Our user interface can also automatically identify a solid pattern (*e.g.*, square, rectangular pattern), where users can self-define the drawing tool width in our interface, so the solid pattern will get filled up automatically. To prepare design files for multi-layer circuit fabrication, a user can export each layer as a separate SVG file while keep the same drawing location on canvas.

4.1.2 Initial System Setup

After exporting the graphic patterns, the next step is to set up the system. The anchors with stepper motors are supposed to be fixed onto the drawing substrate. Then, dimensional parameters need to be collected, labeled as a, b and c in ?? step 2, given that they are required by the interface. For the next step, selected tools will need to be mounted on the central platform.

4.1.3 Drawing Tools and Substrate Selection

Our system provides three options for tools: (1) a drawing pen/brush, loaded with conductive, dielectric, or cleaning inks, (2) a laser cutting head as the cutting tool that can make 2D cutouts, and (3) a UV LED head to automatically cure the inks. For the substrate selection, users are allowed to select one substrate from our library. Each substrate is tested and encoded with its optimal operating parameters.

4.1.4 Preliminary System Testings and Drawing

Once the tools and the target substrate are selected, a series of preliminary tests should be conducted to ensure the system performs correctly. First, a drawing position test will be executed, where users are requested to move the drawing tool to a specific location on canvas. Second, a tool pressure test is recommended to achieve the optimal pressure for the drawing tools. Additionally, if a multi-layer task is specified, tool switching mechanisms will also be tested after which the drawing is ready to start and will finish with no labor involved.

4.1.5 Connection and Post-process

Finally, after the drawing task is completed, we need to cure the inks before connecting the electronic components. The sintering process for the Dycotec DM-SIJ-3200 [90] silver nanoparticle ink requires a temperature as low as 100°C, and the curing process for the NEA 121 [91] dielectric ink takes only 30s under ultraviolet light. Users can also implement one of the three connection methods for mounting electronic components: conductive paste (Bare Paint [92]) and conductive epoxy adhesive (MG Chemicals 8331 [93]) for permanent and robust connections and liquid metal (EGaIn) for temporary connections.

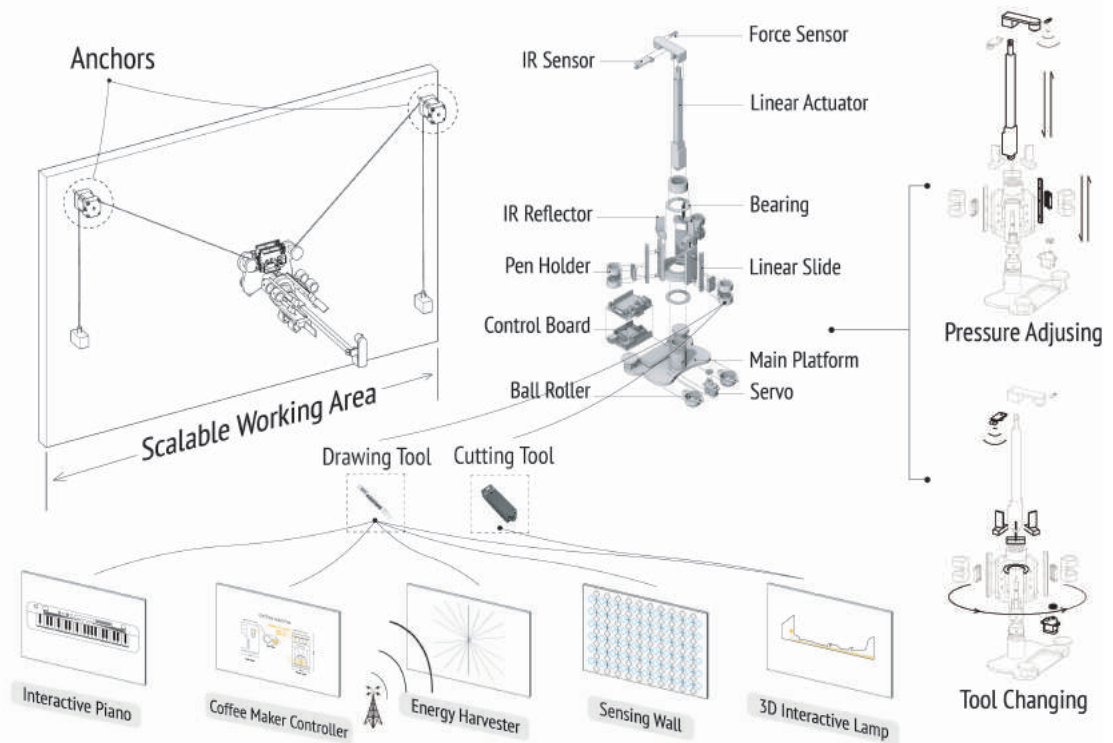


Figure 4.1: Demonstration of the hardware design: Top-left: Overview of the system. Middle: The explosion view of the drawing platform. Top-right: Two highlighted functions designed for circuit fabrication. Bottom: Highlighting drawing tools and cutting tool with associated applications.

4.2 DUCO FABRICATION SYSTEM

4.2.1 Design Principles

Similar to most of the existing digital fabrication systems (*e.g.*, 3D printer, CNC router or inkjet printer), which do not require users' attention after the jobs have been uploaded to the system, for prototyping large-scale circuits, we take the negation of human efforts as the key feature to not only save the user's time, but also enable fabrication with much higher precision than manual labor while assuring user's safety for circuit deployment at vantage points that are difficult to reach (*e.g.*, bridge, building). Overall, in order to ensure our system for large-scale circuit fabrication with a high level of drawing performance on

everyday surfaces, we set five criteria for hardware design.

1. *A compact, autonomous system:* To enable large-scale circuit drawing with minimum human intervention, our system should be an autonomous platform that can support large and adjustable moving areas as well as maintain compactness to be easily set up.
2. *Low-cost and easy to use:* To support a broad spectrum of users, we expect our system to be low-cost, made from off-the-shelf parts, and easy to use.
3. *High-precision performance:* Drawing functional circuits requires precision. To prevent defects (*e.g.*, open circuits or shorts), we require the system movement to be smooth and precise.
4. *Versatility of connecting tools and inks:* Drawing functional circuits also requires applying more than one ink (*e.g.*, *conductive and dielectric*). Our system should be able to carry multiple tools and switch from one to another accurately to support multi-material deposition.
5. *Robustness to support everyday surfaces:* To facilitate drawing circuits on a wide range of everyday surfaces, our system should be able to adjust itself to a variety of surface conditions including geometries and textures. This involves keeping the tool in proper contact with the substrate, and yields the need for constant contact control which requires a mechanism that is responsible for pressing the tools gently against rough surfaces or surfaces with complex geometries.

4.2.2 Hardware Design

As shown in [Figure 4.1](#), our drawing platform is comprised of several mounting slots and a functional arm. Two anchors along with the stepper motors are together set on the target vertical drawing surface and connected to the central drawing platform. The

system enables high motion resolution through the help of stepper motors which drive the GT2 timing belts to move the drawing platform. Weights are added to tighten the belts, but can also be replaced by a winder mechanism for a more compact system design. For the control board, an Arduino Uno is used to receive commands via the serial port from the user's PC.

We have also tested different moving modes for the system. By driving the system at a high speed (*e.g.*, higher than 20 cm/s), we can more rapidly prototype circuits. To achieve optimal resolution and quality for the circuits, we can enable microstepping mode, but this mode inevitably sacrifices operating time.

Tightened belts driven by stepper motors are enabling a stable and robust system design but are essentially constrained to move on a relatively fixed 2D plane because of the tension in the ropes, which makes it impractical and challenging to handle concave or convex textures. To facilitate the fabrication of circuits on versatile surfaces, we employ a combination of pressure sensor and linear actuator to actively adapt to surface changes on the target surface material. To further reduce the amount of human intervention, we also added a tool switching module to enable the possibility of using more than one ink or tool within a task.

It is also noteworthy that Duco is highly maker friendly: all components are either directly purchased or 3D printed by an FDM 3D printer. All the details are collected and further discussed in our online repository.

Inks and Tools:

With the goal of fabricating circuits directly on target substrates, we have identified several existing tools that are suitable for our purposes: Inkjet-printing head, extruding nozzle, and commodity pens. After our investigation and also inspired by many existing circuitry drawing works [94, 43, 95], we selected our main drawing tool to be the commodity pen. We selected commodity pens based on the following five aspects: (1) The drawing tool

needs to be low-cost. The heavily used pen in this work is a 4mm MOLOTOW painting marker [96] which is only \$4.8 each. (2) These pens can be easily loaded with different functional inks. Also thanks to the low-cost manner of the empty marker, we can simply have a set of markers loaded with conductive, dielectric, erasing or even other functional inks. (3) Pens are light-weight. For our hanging system, adding too much weight onto the drawing platform can cause the platform to tilt or lean to one side. (4) It is easy to draw traces with different widths by utilizing different pen diameters. (5) It is simple to mount, replace, and control pens. Both inkjet printing head, and nozzle extruder require extra wiring and more complex control logic. Drawing pens only require a linear actuator to push the pen along a linear slide, and use a rubber band to constantly retract the pen back. Due to the above advantages, we chose pens as our tool of choice for fabricating large-scale circuits. We identified Dycotec DM-SIJ-3200 and NEA 121 as our conductive and dielectric inks. We also investigated several solvents that can be used as cleaning inks to correct or erase the circuits.

Tool Switch Mechanism:

We build an automatic tool switching mechanism to further lower the need for human intervention. The stepper motors are locked to their positions during the tool switching. Both of these designs improve our drawing quality and accuracy.

Our automatic switching tool module design is highlighted in Figure 4.1. We fabricated a central carriage composed of three slots. Each slot is equipped with a linear slide and pen holder. This configuration can hold three different tools concurrently. If the number of concurrent tools required increases, it is possible to simply add more slots. The tool slots rotate in and out of the primary drawing position on command. To achieve this, the carriage rotates by using a continuous servo. The IR sensor will receive the reflected signal from the reflector that we mounted on the top of each slot and send the command to the controller to stop the platform at current position. We have also tested other low-cost sensor options,

(e.g., encoder, RGB sensor) and eventually chose IR sensor which allows the pen to rotate from an arbitrary angle, but we agree other sensors might also work.

Contact Force Sensing:

Smooth circuit drawing on surfaces with different geometries and textures can be challenging. Adapting to these changes is necessary for drawing on a broad range of daily objects. We expect our system to be able to fulfill tasks smoothly and automatically even on surfaces with some roughness or various topology. Also, in order to ensure the drawing tool is held against the drawing surface with consistent force, a contact pressure control system is developed. The pressure control system is tuned to push the drawing pen against the target surface with proper amount of force which creates consistent trace drawings with precise width while preventing the tool from scratching or catching on the drawing surface.

Our implementation of the pressure control loop involves two simple components, a force sensitive resistor (FSR), and a linear actuator. The FSR detects the pressure of the pen applied against the drawing surface and transmits this data to the control board. The control board then commands the linear actuator to retract back or push forward the pen according to the detected pressure data.

In practice, deadlock may occur when a pressure range is not reachable. This situation implies the surface roughness or topology level is outside of the acceptable range. The platform performs reliable and quick contact feedback control when being operated on surfaces that fall within our calibrated range.

4.3 DRAWING TOOLS EVALUATION

In order to better understand the performance of our circuit drawing robotic system, we carried out a series of tests. These tests included general resolution and accuracy tests as well as electrical and mechanical tests for the drawing tools and substrates. Each test is corresponding to one key criteria of Duco. We believe these test results validate the

circuit drawing capabilities of the system. Additionally, these tests establish a procedure for evaluating new drawing tools and substrates.

4.3.1 Resolution, Accuracy and Speed Testings

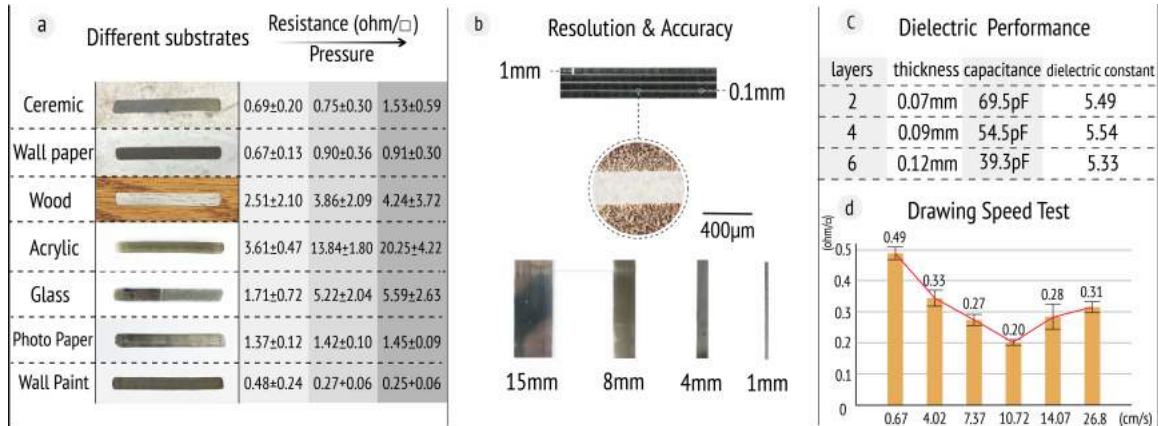


Figure 4.2: (a) Resistance evaluation for the conductive ink on different substrates. (b) Resolution and accuracy testings. (c) Characterization of the dielectric ink. (d) Drawing speed testing.

Resolution Testing

To test the drawing resolution of our system, we examine the thinnest line width that Duco can achieve as well as the smallest gap achievable between two lines. Figure 4.2b shows that the smallest line gap that we can achieve is 0.1mm. We have carried out a series of tests by drawing four lines in a group with line to line gap of 10mm, 5mm, 1mm, 0.5mm, 0.4mm, 0.3mm, 0.2mm till 0.1mm which is the minimal gap that we were still able to observe consistent drawing results without any line intersections. The tests are done on acrylic sheet with a trace length of 5cm, and has been repeated for 5 groups with 4 lines in a group. At the bottom of Figure 4.2b, we show the thinnest line width that we achieve is 1mm. It is clear for this drawing system that line width will be directly determined by the pen tip width. We have also tested 15mm, 8mm, and 4mm lines to demonstrate the possibility of directly drawing conductive traces in different widths. It is important to

note that wider drawing tips can dramatically reduce the drawing time for solid patterns compared to using thinner tips to draw multiple paths.

Accuracy Testing

Additionally, we demonstrated the system's accuracy tests for drawing both single layer and multi-layer circuits on acrylic sheet. For single layer accuracy testing, we first used a 4mm pen to draw a ground truth pattern with a length of 5cm and repeated the pattern for 10 times with a 2cm center-to-center deviation in our graphic design. We then measured the real center-to-center differences and compare with 2cm, which we achieved 2.05cm real deviation in average, which represents 2.5% error. We also repeated this test 3 times, and achieved similar results of 2.04cm and 2.02cm deviations on average. For the multi-layer accuracy testing, we tried to determine how well two layers can be aligned after the system automatically switches the pen. We mounted two pens with different colors, conducted a task which involved switching the tool and drawing a dot. Over 15 trials we achieved an average of 1.2 ± 0.7 mm distance between the centers of two consecutive dots.

Drawing Speed Testing

Duco platform is similar to 3D printer that the speed can have both pros (*e.g.*, save fabrication time) and cons (*e.g.*, lower the quality of the print) to the system. The printing speed for Duco will also play an essential role in evaluating its performance. As indicated in Figure 4.2 d, we have carried out the speed testing with an attention to how different drawing speeds can cause the variations of resistance. Among the tests, We used a single line pattern as our testing pattern, with a dimension of 7cm long and 2mm wide. This pattern has been repeated 10 times for each speed, and we have tested multiple speeds ranging from 0.67 cm/s to 26.8 cm/s. According to the results, all the traces have reliably shown conductivity within an acceptable range, where 10.72 cm/s is the optimal drawing speed that exhibits the best electrical performance. Also, the testing results have shown that the

slower drawing speed of 0.67 cm/s exhibits relatively poor electrical performance which we speculate when the system moves too slow, the pen tip also scratches the pattern.

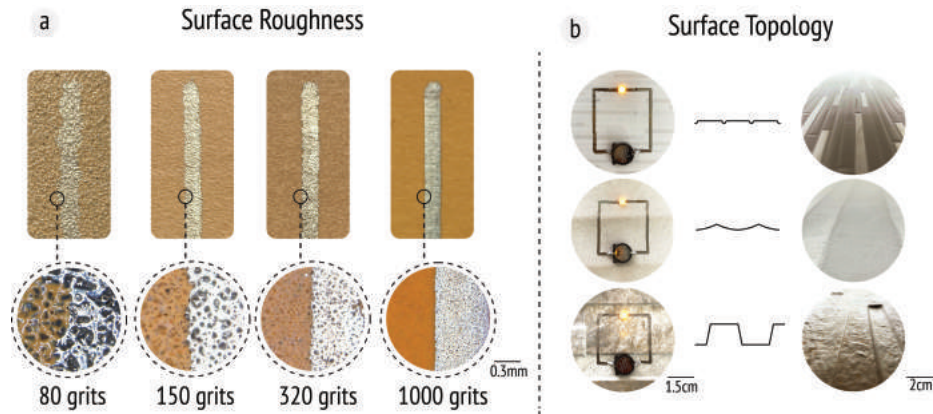


Figure 4.3: Drawing quality evaluation on various surfaces with different roughness and topology.

4.3.2 Drawing Tool Testings

Along with the machine’s drawing resolution, the electrical properties of the circuits are also a determining factor for the quality of large-scale electronics fabrication. We have evaluated three different conductive inks (SunChemical EMD 5730, Mitsubishi Paper Mills NBSIJ-MU0 and Dycotec DM-SIJ-3200), two dielectric inks (Dycotec DM-INI-7003 and NEA 121) as well as two different cleaning solvents (ethylglycol and ethanol) [97, 29]. Most of these inks have a viscosity from 1-200 cPs, which can be easily loaded into the commodity markers. We have also considered and tested *Circuit Scribe* and *Bare Paint*, which are micro-particle based materials and have a viscosity around 15000 cPs. Since the micro-particle based materials are not extrudable from the refillable markers and require pneumatic dispensing, we chose to omit these materials from our officially supported materials library for the sake of maintaining overall design simplicity.

Conductive Silver Pen

In order to support the drawing of circuits on a wide range of substrates as well as to minimize the post-treatment efforts, we selected Dycotec DM-SIJ-3200 as our conductive ink which can be cured at low temperature. We have mainly tested out resultant circuit conductivity on seven different substrates (ceramic, wall paper, wall paint, wood, acrylic, glass and photo paper), which exemplify most vertical surface materials encountered in our daily lives. We summarized the results in Figure 4.2 a. The 4mm by 40mm rectangular pattern was tested 15 times at a constant contact pressure. We reported the mean value and the standard deviation of the circuit's resistance measured by a four-probe setup. We observed very consistent values from each substrate, with relatively large variances for wood and glass substrates. These variances were likely caused by the uneven surface topology of wood and the poor surface adhesion of glass. For the pen contact pressure, we tested three different pressure settings. Surprisingly, we found that as pen contact pressure increases, circuit conductivity decreases for all the tested substrates. We speculate that after passing a certain amount of contact pressure, the pen tip begins to scratch away the patterns as it is drawing. In order to standardize the testing, all the samples are heat-sintered in an oven for 15 mins at 120°C. We failed to observe any conductivity for the wall paint substrates until we heat treated the wall paint again under 200°C for another 3 minutes.

Dielectric Pen

When choosing the dielectric ink for the system, the performance of the two inks we evaluated were very similar. Both inks can be quickly cured by a 3.3 V ultraviolet LED within 15 to 20 seconds. We ultimately chose the NEA 121 ink because of its more accessible price. In order to characterize the performance of our dielectric ink, we first drew a 10mm by 10mm silver square at the bottom and then 2, 4, and 6 layers of dielectric ink were drawn on top. We then connect the most top dielectric layer with a copper tape to measure the capacitance by using a LCR meter (Agilent, U1733C), and the results are presented in

Figure 4.2 c.

Cleaning Pen

Drawing mistakes or accidental ink spreading can occur during the fabrication tasks. In order to allow the redrawing of circuits in the same area or the modification of existing designs, erasing will be necessary. Inspired by [29, 97], we have investigated 2 different solvents (ethylglycol and ethanol) as our cleaning inks. Unlike [29, 97], which utilized cleaning inks mainly dispensed onto photo paper, our work has introduced 7 materials as drawing substrates. However, not all substrates require special cleaning solvents to erase drawn traces. For example, due to low surface adhesion, the conductive traces on glass substrates are fairly easy to be erased even by using water. Conversely, the ink bonding on acrylic sheets is extremely strong and can not be removed by any of the solvents we investigated.

4.3.3 Substrate Testing

Surface Roughness

The majority of everyday vertical surfaces are to some degree patterned or textured. Researchers have made extensive efforts to fabricate circuitry on objects with different geometries [87], but the textures and patterns of these surfaces have barely been considered. In Figure 4.3 a, We have tested the drawing quality on four samples of sandpaper with 80, 150, 320, 1000 grits. We have used the 4mm pen to draw a 6cm long pattern on each sandpaper for 10 times and observed that the drawing quality is dramatically affected by surfaces with different levels of roughness. It was challenging to achieve smooth and consistent drawings on the 80 grits surfaces. For the smoothest 1000 grits surface, much sharper drawing edges were achieved.

Surface Topology

Besides surface roughness, target surface topology is also a major factor which needs to be considered when fabricating electronics on everyday vertical surfaces. In response to this design challenge, our circuit drawing system is equipped with a linear actuator and a pressure sensor, enabling the system to draw patterns across different surface heights. In Figure 4.3 b, we have shown experiments on ceramic tiles with three different surface patterns, with resistance of 65Ω , 80Ω and 134Ω from top to bottom respectively. These experiments determined how much height difference and how much transition angle between two adjacent surfaces the drawing system can handle. Based on the testing results, our circuit drawing system can handle roughly 1 to 4mm height differences, and $0-60^\circ$ transition angles.

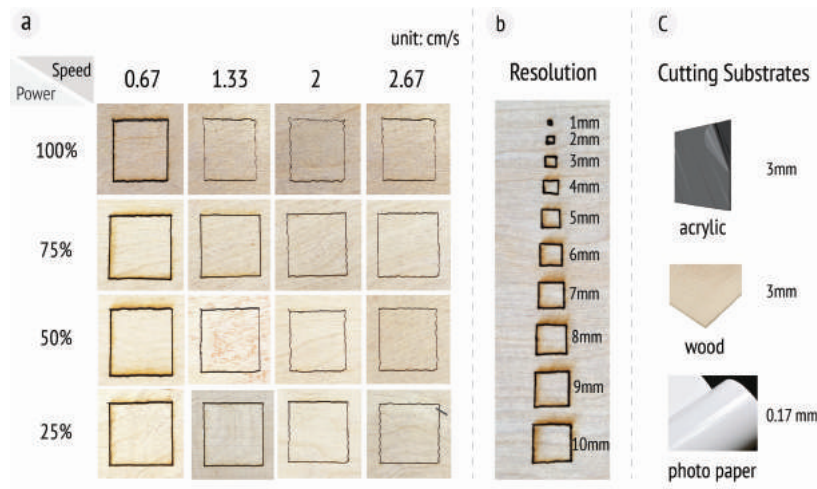


Figure 4.4: laser cutting head testing: (a) Speed and power testing. (b) Resolution testing. (c) Substrates that laser cutting head can cut.

4.4 APPLICATIONS

We have showcased five application examples enabled by Duco system. These applications mainly cover three key circuit fabrication domains that are greatly favored by the enlargement of the functional surface areas or spaces: 1) human-scale sensing [8, 41, 98];

2) energy harvesting [99]; and 3) 3D interactive artifact [31]. These five application examples are carefully chosen to highlight the advantages of using the Duco system: negating human intervention, supporting complex and accurate circuitry design, supporting multi-material/multi-tool and constructing circuits from 2D to 3D, from single-layer to multi-layer.

4.4.1 Interactive Piano

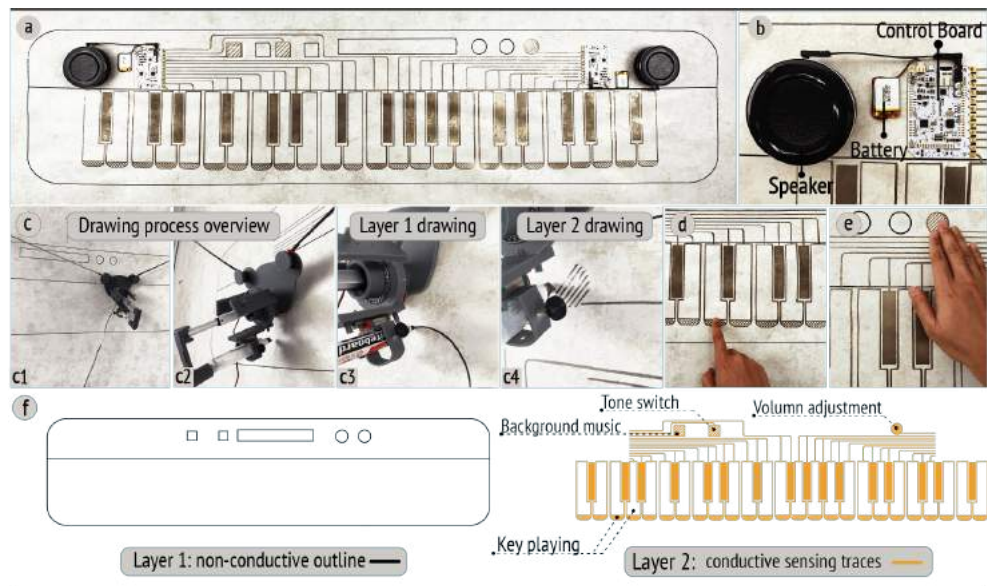


Figure 4.5: Interactive Piano: (a) Overview of the system. (b) The control board, the battery and the portable speaker connections. (c) The drawing process overview. (d) Playing the capacitive keys. (e) Tuning the volume. (f) The schematics of two layers and their functions.

Many interactive panels, exhibitions, and art setups have demonstrated novel ways of embodied interactions, which are also favored by utilizing large interactive areas or spaces. Our inspiration came from well-known art installations [100, 101, 102]. Aiming at providing unconventional interactivity, in Figure 4.5, we present an untethered interactive piano with a size of 160cm by 32cm drawn on wall paper by using two separate pens, a normal black marker for non-functional outlines, and a conductive pen for the functional piano keys and connections. This application highlights the ability of Duco system in draw-

ing complex but accurate circuitry patterns, which becomes very challenging to make by adopting the existing large-scale circuit fabrication method that relying on human inputs and stencils. When fabricating the interactive piano, we first used the 4mm black marker to draw the outline, and then switch to the 4mm marker loaded with the conductive ink to draw the rest of the interactive patterns. The interactive piano exhibits multiple functions including white and black key playing, background music playing, tone switching, and volume adjusting. We wired up a pair of portable speakers, a 400 mAh Lithium battery and a Bare Conductive Touch Board [103] on each side of the printed piano.

4.4.2 Interactive Coffee Maker Control

As IoT devices become increasingly prevalent these days, more home appliances became "smart" that allow people to control or manipulate the functions remotely (*e.g.*, smart lighting system, temperature control, or button control). Here we showcase an interactive coffee maker controller (96cm by 68cm) drawn by Duco on our office's wall which is covered by blue wall paint. We used the black and conductive markers to draw the non-functional and functional patterns respectively. Then, we wired up the drawing to an ESP32 board by using the jumper wires and silver epoxy. Thanks to the end-user programming platform IFTTT [104] and Smarter Coffee Maker [105], we achieved demonstrating a remote controller including various functions of the coffee maker by creating different applets through the IFTTT (*e.g.*, start/pause the brewing, change the brewing strength or adjust the brewing size). As shown in Figure 4.6 c, we are controlling a coffee maker located in the community kitchen of our floor by using the control panel that we drew on the wall in our office. We believe this not only provides a novel and playful interaction with an IoT device remotely, but also demonstrates a vision to locate controls for multiple home IoT appliances to be centralised.

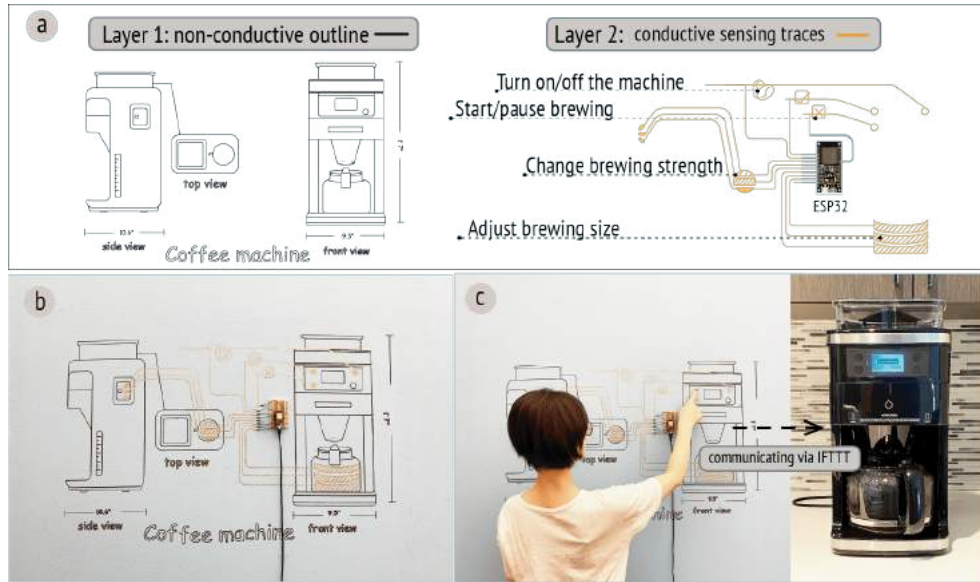


Figure 4.6: Interactive Coffee Maker Control: (a) Demonstration the drawing and schematics of two layers and their functions. (b) The overview look of the coffee maker controller. (c) Brewing coffee remotely by using the controller.

4.4.3 Capacitive Sensing Wall

In order to augment the sensing capability on everyday surfaces, HCI researchers have manually painted or brushed conductive materials onto the wall surfaces to passively detect indoor human activity or gesture [41, 8]. While those techniques enable large-scale human activity sensing, the lack of autonomous fabrication tools hinders a possibility for further enlarging the sensing area. The capacitive sensing wall application features the strength of Duco's automation, scalable working area and support multi-tool tasks. After we upload a design file to the interface, Duco frees users' hand by taking a task of drawing the conductive layer(s) and the drawing/curing of the insulation layer automatically. The capacitive sensing wall is a 15 by 8 grid pattern inspired by *SmartSkin* with a dimension of 200cm by 110cm. It consists of two (top and bottom) conductive layers and an insulation layer in the middle [106], shown in Figure 4.7 (c,d). We highlighted the pen brush and UV LED to automatically draw and cure the dielectric ink in Figure 4.7 b. An Arduino Mega 2560 [107] and multiplexer [108] were used as the main hardware components to wire up

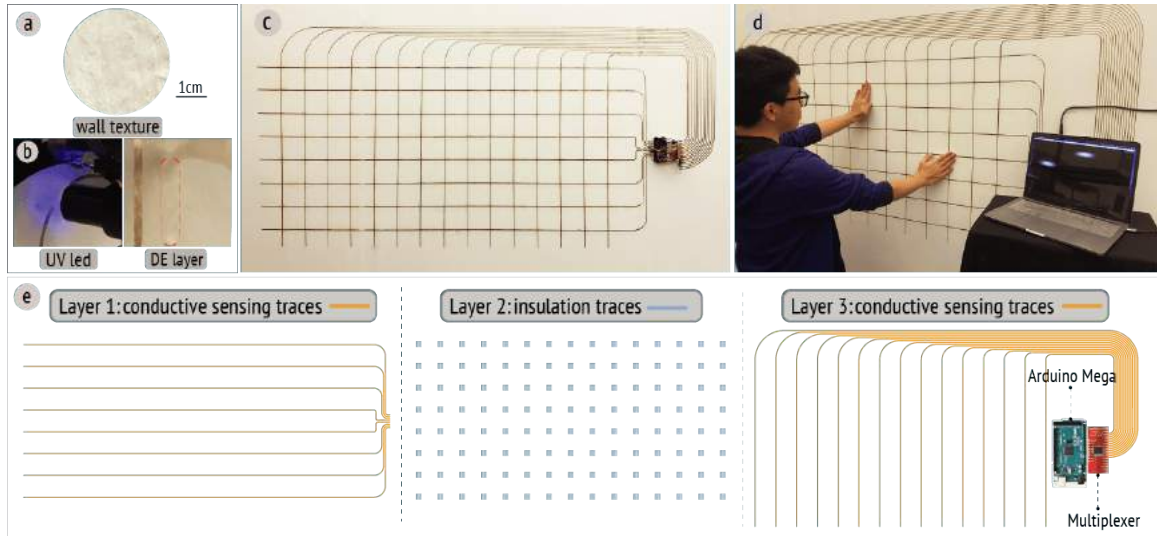


Figure 4.7: Capacitive Sensing Wall: (a) Zoom-in look of the surface texture of wall. (b) Zoom-in look of UV curing and dielectric ink brushing. (c) Overview of the sensing wall. (d) Human touch is detected by the capacitive sensing wall. (e) Detailed schematic for each drawing layer.

the system.

4.4.4 FM Energy Harvester

Among most of the vertical separation materials, glass plays a special role. Unlike normal walls or wooden frames which functioning as space dividers, glass surfaces like windows must allow people to see through. Here, we design a wide-band, quasi-isotropic, kilometer-range FM energy harvester printed on a 120cm by 120cm glass sheet by utilizing the 4mm conductive marker, (Figure 4.8). Duco, as a digital fabrication system, features the capability of making drawings with high precision. Unlike other applications, energy harvester requires the patterns to meet the precise length, width or even the direction/location on a graph to achieve the desired RF characteristics (*e.g.*, all antennas we designed in the energy harvester pattern correspond to a specific wavelength, they are different in terms of length, width, location and pointing direction). The drawing results meet our simulation well which made it able to harvest energy from surrounding FM towers omnidirectionally. We purposely made the thin-trace design of this energy harvesting pattern to harvest energy

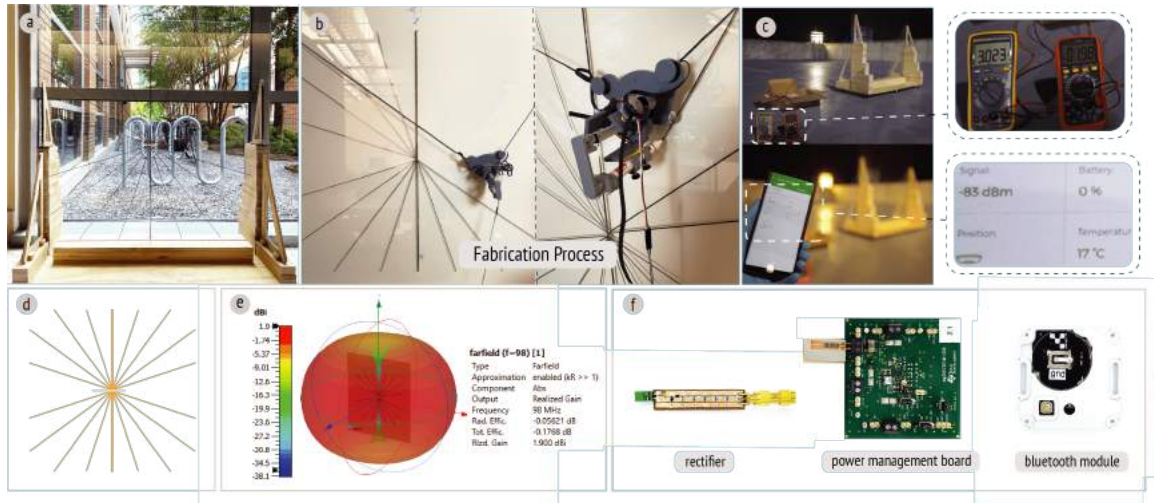


Figure 4.8: Printed FM Energy Harvester on glass: (a) The front view of the printed FM energy harvester with components mounted. (b) The fabrication process for the energy harvester. (c) When the energy harvester is capturing energy and powering up a blue-tooth module with embedded temperature and location sensor. (d) The design for the energy harvester. (e) The simulation result of the FM energy harvester (f) A closer view of the electrical components: the rectifier, the power management board and the blue-tooth module.

and at the same time will not block the normal view through the glass. Radio frequency energy harvesters favor utilizing larger surface areas for harvesting more energy. We envision the possibilities of using our circuit drawing system to fabricate energy harvesters across the entire outside surface of a glass-covered building to harvest free energy from the ambient environment as a "printed battery" to support other activities within the building. Figure 4.8 f shows the printed energy harvester pattern wired up with a rectifier, a power management board with capacitors, and a blue-tooth module that we would like to power up. Also, Figure 4.8 c presents our field test, in which we successfully powered the blue-tooth module with embedded thermometer and accelerometer. To our best knowledge, we are the first one utilizing low-cost autonomous platform to fabricate this energy harvester on glass, which can achieve a competitive power of around $200 \mu\text{W}$ in outdoor rooftop locations and $60 \mu\text{W}$ in indoor rooftop locations.

4.4.5 3D Interactive Lamp

Many daily objects can be assembled from multiple flat pieces (*e.g.*, desk, chair, lamp, shelf and etc.). Researchers have demonstrated embedding sensing capabilities into these objects, however, most of these interactive objects are limited by the existing fabrication machines, which are at the same time taking up plenty of plane spaces. We demonstrate a 110cm tall interactive lamp in Figure 4.9. We take the advantage of the vertical space as our main fabrication site. For the fabrication process, we firstly hang a 2mm thick black acrylic board with a dimension of 125cm by 60cm onto a wall by using double-sided tape. We start by drawing the interactive patterns on the acrylic sheet (shown in Figure 4.9 a, b), following by automatically switch to our 5.5 W laser cutting head to cut the outlines (shown in Figure 4.9 b). We used four acrylic sheets in total, with first three sheets producing two lamp shades each, and the last acrylic sheet producing the lamp base which is composed of two semi-circle pieces, shown in Figure 4.9 e. The entire process is completed autonomously with involving minimal human intervention. After we finish the drawing and cutting tasks, the pieces are assembled by using liquid glue, and then we connect the traces to the Bare Conductive Touch Board by using silver epoxy. Figure 4.9 c shows the assembled look of the lamp when in its turned on state by touching the capacitive pattern that we drew. We also would like to note for the fumes generated by the laser cutting process, similar to many commercial desktop laser cutter/engraver [109], the laser diode we implement will only generate a small amount of fumes, but a vacuuming system is strongly recommended when operating the system with more powerful laser cutting heads.

4.5 DISCUSSION

We have demonstrated five application examples to highlight the key strength of using Duco system in making large-scale circuits. Here we discuss several other critical factors when operating the system, including the total fabrication time, the working area and the

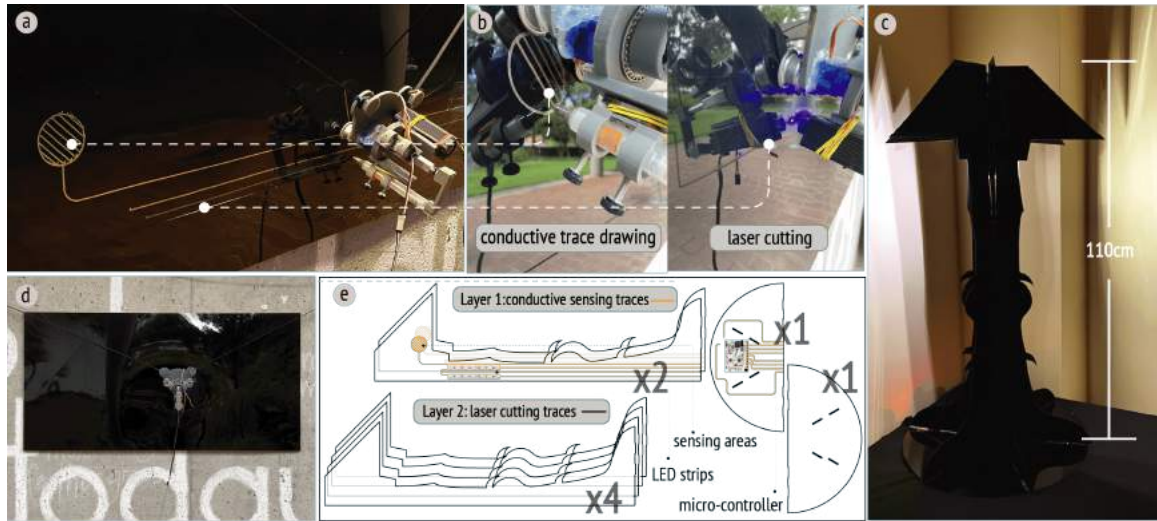


Figure 4.9: 3D Interactive Lamp: (a) An overview when the system is drawing the circuits. (b) A zoom-in look of the drawing and laser cutting areas. (c) When the lamp is turned on via capacitive sensor. (d) The overview of the fabrication setup. (e) Detailed decomposition of the assembly.

requirements for initial setup.

Net Fabrication Time. With conventional fabrication approaches, large-scale circuits would require significant human efforts. Manual calibrations, masking, and drawing must be carried out, which not only waste time but are also prone to errors. Similar to many digital fabrication techniques such as 3D printing, Duco frees users from laborious manual efforts by offloading the drawing process to autonomous robotic mechanisms. We believe the automation of the drawing process is a critical breakthrough, even though there might not be a significant reduction on net fabrication time. All of the application examples presented here adopted a recommended optimal drawing speed of 10.72 cm/s. At this speed, the interactive piano can take up to 3 hours (15 minutes for the non-conductive outline, 2 hour and 45 minutes for the conductive parts) to complete the drawing process while the coffee maker control takes 2 hours (1 hour and 10 minutes for the non-conductive outline, 50 minutes for the conductive parts), the FM energy harvester takes 50 minutes, 5.5 hours for the entire interactive lamp (25 minutes for drawing and 35 minutes for cutting of each lamp shade, 1 hour 10 minutes for the base), and 7.5 hours for the capacitive sensing

wall (1.5 hour and 1 hour for the top and bottom conductive layer, 5 hours for the insulation layer). It is noteworthy that the curing process for the insulation layer takes a substantial length of time. This length of time is not only due to the 30 seconds curing time at each of the 120 overlapping circuit trace nodes, but also because we repeated this process three times to ensure the insulation layer's performance. Even though the drawing process does not require human intervention, further fabrication time reduction will be necessary for the system improvement. One direction for improvement would utilize more advanced path planning algorithms. The drawing time for the interactive piano application was shrunk from 6 hours (by using the path planning algorithm reported in *Polargraph* [110]) to 3 hours (by using our modified algorithm respectively). With this experimental confirmation, we believe there is still room on the software front to further cut down the fabrication time. Another direction for improvement could be increasing the moving speed of Duco. In this work, we are mainly adopting the optimal drawing speed for our application examples but, one can apply a higher speed for the fabrication which inevitably will sacrifice the drawing quality.

Working Surfaces & Areas. With our goal of augmenting vertical everyday surfaces, we realized that not all the vertical surfaces are completely flat. Practical surface extrusions such as hanging frames, LED decorations, or wall mounted lamps, can all block the drawing path for Duco. The current system setup does not support a camera to detect these existing objects or an advanced path planning algorithm to avoid these objects. Also, daily surfaces can easily have transition from one type to another (*e.g.*, from a wall to its connected window glass), so far Duco is not able to handle these surfaces transitions with a major vertical gap in between. Additionally, the current drawing area is slightly smaller than the anchors' setup area due to certain geometrically extreme locations (*e.g.*, the area above Duco's initial starting point and the areas close to the anchors/ weights). When we carry out drawing tasks, a 20-centimeter gap on the two sides, and the area above Duco's starting point are marked as non-optimal drawing areas which are also reflected in our in-

terface. Our future efforts will focus on making advancements in Duco's hardware and software designs to work with a wider spectrum of real-life surfaces.

Initial Machine Setup. As previously introduced, the two anchors and their corresponding motors are required to be manually mounted on the top two corners of the drawing canvas. They are to be mounted horizontally and at the same height, with the distance between the two anchors needing to be measured. Through our working experience, this is by far a time consuming step which in general consumes 20-30 minutes. Additionally, this step prevents Duco from providing a completely autonomous fabrication experience. We propose in the future to utilize small robots to drive the anchors to the designated locations and apply a vacuuming system to fix the anchor.

CHAPTER 5

PITAS: RENEWABLE SENSING AND ACTUATING EMBEDDED ROBOTIC SHEET FOR PHYSICAL INFORMATION COMMUNICATION

PITAS integrates both input sensing and active shape output within a single sheet, and this soft silicone-based system endows PITAS with great adaptability to different materials (*e.g.*, thermochromic pigments, tactile add-ons) for different purposes. Additionally, the bottom conductive layer makes PITAS system "heating ready", so one can simply attach electrodes selectively for different swell sizes or locations. The generic robotic sheet form factor and the associated cutting fabrication approaches further enable applications ranging from making 2D-3D shape-changing artifacts to augmenting everyday objects. Within the wide range of applications, PITAS can also go beyond a single space to convey physical information across multiple locations. Prior work has demonstrated that materiality plays a critical role in emotional interactions – how we perceive, interpret, and feel about information [111, 112]. So, we also investigate how non-expert makers could create their own physical telecommunication devices, as well as explore the unique and feasible affordances PITAS can provide.

Although PITAS is a custom synthetic sheet that was prepared in the lab, it would be possible to mass-produce the sheets to make them widely available in electronics or craft retail stores, especially given the simplicity of the sheet fabrication process. Like copper tape or other craft sheet materials, those who enjoy DIY-making projects could purchase a roll and use it as needed, apply widely available cutting methods, and connect it with existing electronics and hardware parts for self-sensing and actuating projects.

5.1 System Overview

PITAS is a sensing and actuating embedded synthetic sheet that is capable of conveying different types of physical information about **shape**, **temperature**, **color** and **texture** to users (Figure 5.1). The fabrication method starts with a simple pre-processing of the material (*e.g.*, mixing the phase transition material and the conductive silicone). The focus is on transforming the materials into a synthetic thin-sheet form factor after pre-processing them, because sheets are easy to store and reuse. It also enables novice users who don't have mold-casting experience or 3D modeling knowledge to explore making their own sensing and actuating devices by manually cutting the sheets or utilizing a commodity vinyl/laser cutter. For those who want to investigate more advanced 3D shapes, PITAS also supports the use of 3D printing as an optional fabrication method.

Commercially available components (*e.g.*, ESP32, relays, and a portable router) were mostly used to build the hardware system, to provide a cloud server for communication, and a mobile app to visualize the transmitted data.

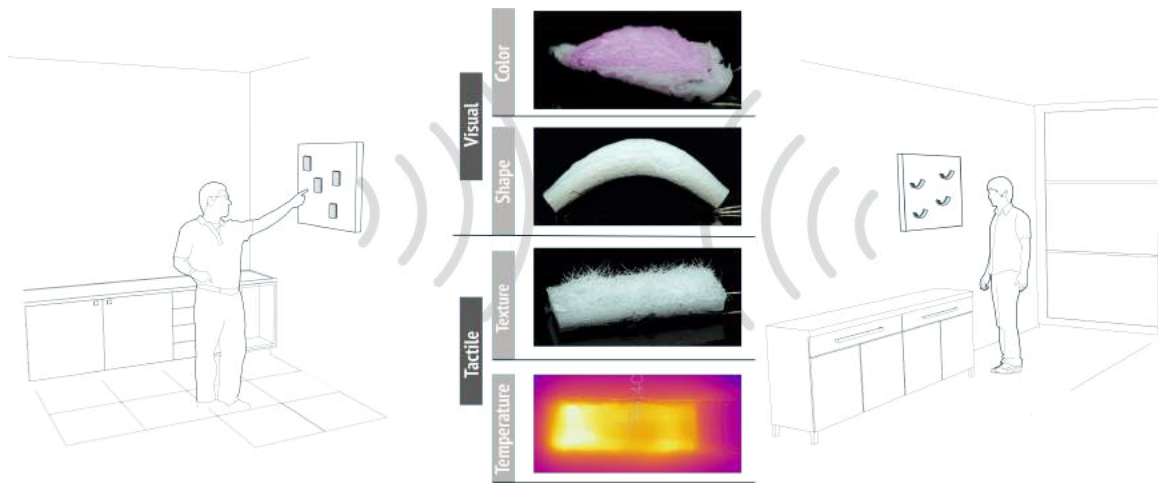


Figure 5.1: Overview of the PITAS system.

5.2 Fabrication Pipeline

5.2.1 Phase Transition Actuator

The most well-known example of phase change materials is paraffin which was mostly used for self-regulating vents in greenhouses. *Soft material for soft actuators* [113] has introduced a new type of phase transition actuating mechanism, which was mainly adopted for our PITAS system. Illustrated in Figure 5.2 a, two-part platinum-catalyzed silicone elastomer smooth-on Ecoflex 0050 was chosen as the matrix material. Because of its excellent wettability with ethanol, it allows the system to maintain ethanol from escaping after curing, which also ensures an even distribution of the ethanol within the silicone matrix. Here, we mainly used 20 vol% of ethanol to the entire matrix as our receipt. 20 vol% of ethanol was first hand-mixed with 40 vol% of Ecoflex 0050A by using a stirrer for 2-3 minutes, and then with 40 vol% Ecoflex 0050B. The entire matrix will take approximately 3 hours to cure, and the material cost is 3 cents per gram.

Working Mechanism

When Miriyev et al. first introduced *Soft materials for soft actuators* [113], the main fabrication method was mold-casting, and there is one follow-up work talking about the possibility of 3D printing the systems [114]. For all these existing works, the main form factor of the system is relatively bulky, taking up substantial space, which limits the response time of the system. Since heat will need to penetrate the entire thick matrix. Also, the existing mold-casting approach can lower the motivation for the real users to use them since they have to make the material every time. Another big issue for the existing method is the heating wire problem. The original work was using the Ni–Cr spiral wire to heat up the system. However, how to place this rigid resistive heating wire became a critical challenge for the system design. Here, we propose a new way of utilizing this system by pre-making the phase transition actuator into thin sheets with desired thickness (*e.g.*, 1mm-5mm) and

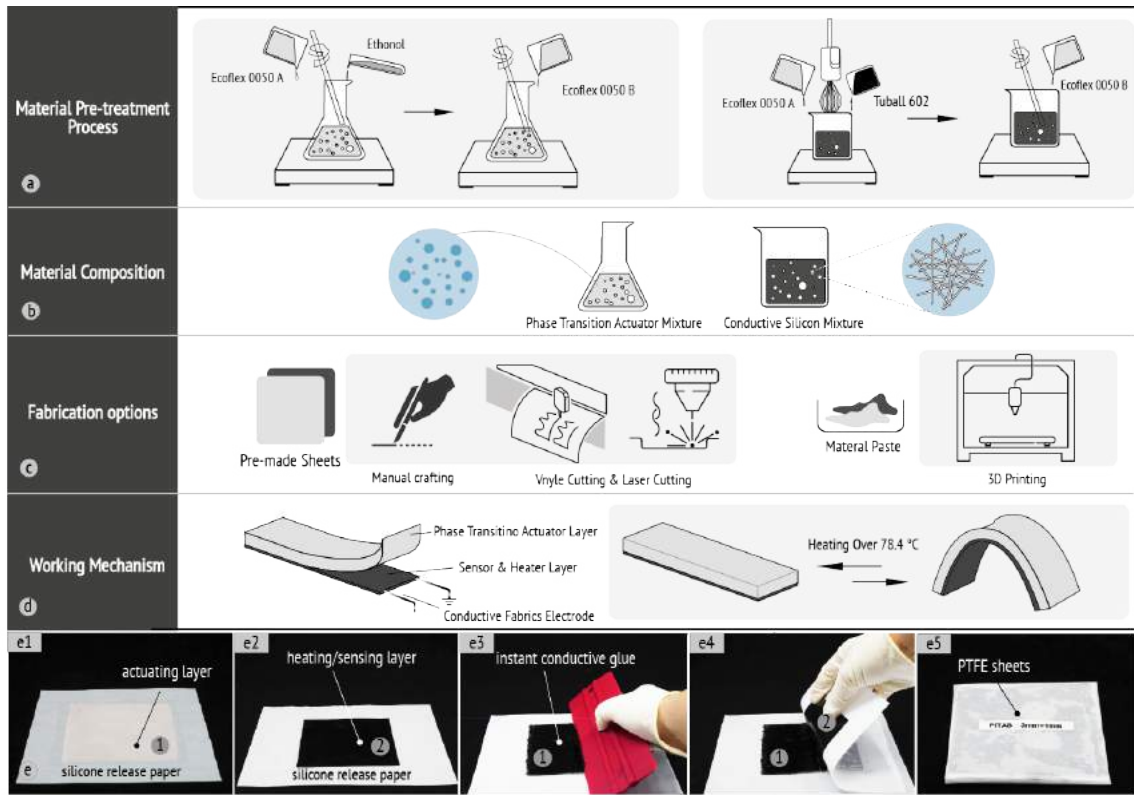


Figure 5.2: (a) Material preparation step for phase transition actuator and conductive silicone; (b) The material composition; (c) The two main fabrication options: 2D cutting & 3D printing; (d) The fundamental working mechanism for the system; (e) Detailed fabrication process.

pre-making another thin sheet of conductive silicone material (*e.g.*, 1mm), and utilize the instant conductive glue that we made to stack the sheets together to form a new "robotic material" sheet, which allows the users to achieve high volume production and can easily store the material anywhere for later fabrication tasks. We have also detailed the sheets preparation process in Figure 5.2 e, where actuating sheet and sensing/heating sheet are pre-molded and attached to silicone release sheets. Instant conductive glue is used to bond two sheets together to form our final PITAS "robotic material" sheet.

The fundamental working mechanism is that ethanol, as the core actuating material, spreads inside the silicone matrix and forms bubbles occupied by ethanol vapors and air. When heating the material over its boiling temperature of 78.4 °C, ethanol boils and the local pressure inside the bubbles grows, forcing the elastic silicone elastomer matrix to

comply by expansion to reduce the pressure. Since the new composite material contains conductive silicone layers, users can directly use this layer as the heater to heat up the system. Meanwhile, another big advantage for this layer is that we can also utilize this layer as the sensor to sense the input from the users (*e.g.*, touch, press, slide). Additionally, we have also considered using Novec 7000 as a replacement for ethanol, which is an engineered fluid with much lower boiling point (34 °C) from 3M company and has been used as a popular candidate for phase transition actuators [115]. However, the high air permeability for Ecoflex 0050 made it not compatible with Novec 7000, which will start to degrade during the mixing/curing steps and most of liquid will escape from the matrix after 2-3 hours [116]. A latex membrane or teflon sheet instead of Ecoflex 0050 should be applied as barriers/container to cover the device [117].

Actuator Design Space

We have showcased four categories of design primitives of PITAS, which are selected to represent different visual or tactile information that PITAS can deliver. We also would like to note that these actuator examples are inherently based on the same heating/actuating mechanism for PITAS while by endowing it with different additions (*e.g.*, thermochromic pigments, tactile add-ons). In Figure 5.3, we have shown: (1) Shape primitives: PITAS can be cut into various thin-sheet shapes to form different 2D shape-changing modules or layered up to assembly 3D structure where people can control each layer locally, or combine with other material as an additional layer or geometric extensions (*e.g.*, *paper*). (2) Heating primitives: On the same sheet, PITAS can be triggered selectively. For example, the first three primitives under the heating category are of the exact same size, but by alternating the location of the electrodes, one can achieve different swell sizes of PITAS, while for the rest examples, one can also choose to selectively trigger different spots of PITAS for different types of deformation. (3) Color-change primitives: PITAS is a heating-based system, made it a perfect system to combine with thermochromic pigments to leverage the visual

information communication. We show how to enable the deformation and the color change at the same time. (4) Surface texture primitives: With the unique advantages of silicone’s adaptability, we show how we can simply alter the PITAS’ surface features to enhance the tactile information it can communicate.

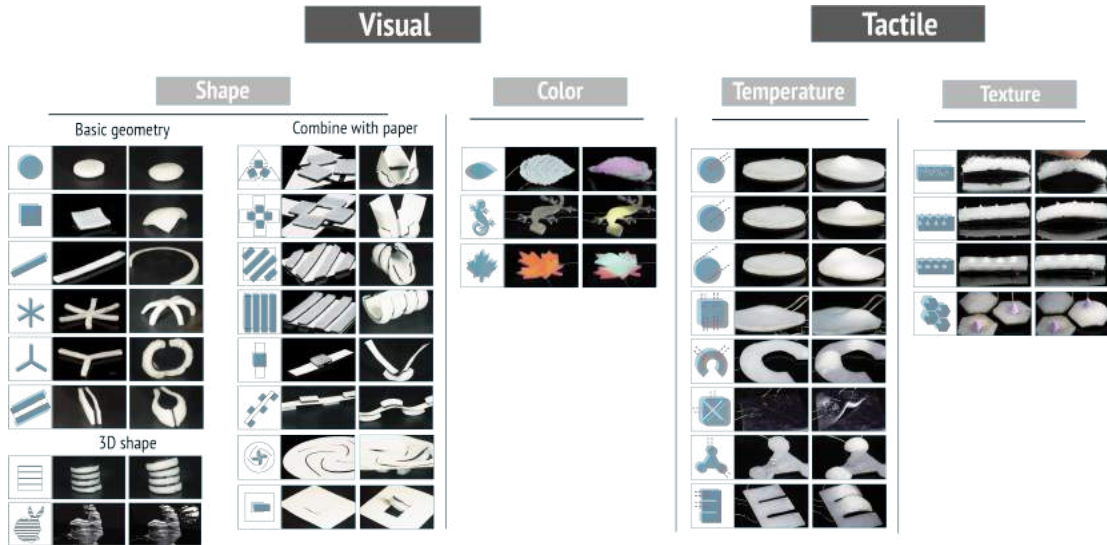


Figure 5.3: Four categories of PITAS design primitives.

5.2.2 Sensor & Heater

There are many existing methods to make conductive silicone, including creating channels for embedding conductive liquid, mixing with carbon nano-tube or carbon fibers. However, to maintain the simplicity of fabrication and utilize the most accessible materials/tooling, we only considered methods that do not involve multiple steps of chemical synthesis or require machines that are not highly accessible.

Mixing with carbon nanotube and carbon fibers became the optimal options, which have both been adopted by the HCI community [118, 21]. Between these two material options, carbon fiber will dramatically reduce the stretch-ability of the silicone, so carbon nano-tubes show a brighter future. We used Tuball 602, which is a commodity graphene nanotube-formulated conductive filler specially designed for making conductive liquid silicone rubbers (LSR). We chose these specific carbon nano-tubes for the following reasons.

First, it provides fine dispersion of nanotubes in the host matrix. Second, it's commercially available at a low price (35 cents per gram). Third, it requires low dosages (0.3 wt%-5 wt%) which also reduces the effect on the softness of the silicone. Finally, it comes as a paste form instead of powder which reduces the inhalation safety concern for the material. We mainly utilize the 3 wt% of Tuball 602 to mix with 48.5 wt% Ecoflex 0050 A and B by using an overhead stirring machine, as our conductive silicone sheet, which serves the function both as a heater and as a sensor.

Sensing Modalities

In Figure 5.4, we present different sensing modalities. It is noteworthy that we used a vinyl cutter to cut the different shapes of the sensors shown in Figure 5.4 b-c within one path. Our sensing modalities are mostly based on two commonly used sensing techniques: resistive sensing and capacitive sensing. Figure 5.4 b shows two types of resistive sensing including stretching and bending, and Figure 5.4 c shows three types of capacitive sensing including simple touch, pressure sensing and sliding. We have also included the continuous raw data for both resistive (stretch) sensing and capacitive (touch, press) sensing in Figure 5.4 e.

5.2.3 Instant Conductive Glue & Electrode

How to connect soft material interfaces with electrodes is always troublesome because of the high deformability and the local fragility of the material. Researchers have tested a wide range of connection routines such as silicone glues for pneumatic systems, silver epoxy or liquid metal (EGaIn) for printed electronics, and soldering paste for shape memory alloy (SMA) systems [119, 2, 120, 30]. However, most of the current connection methods are either not deformable (*e.g.*, silver epoxy) or can cause leakage (*e.g.*, EGaIn). So, to better support users to instantly connect the current system with electrodes, we have developed an instant conductive glue made of Ecoflex 0035 fast. We mixed the 0035 fast A with 4% of Tuball 602 for 30 min and loaded it into the syringe to store it. When mixing with

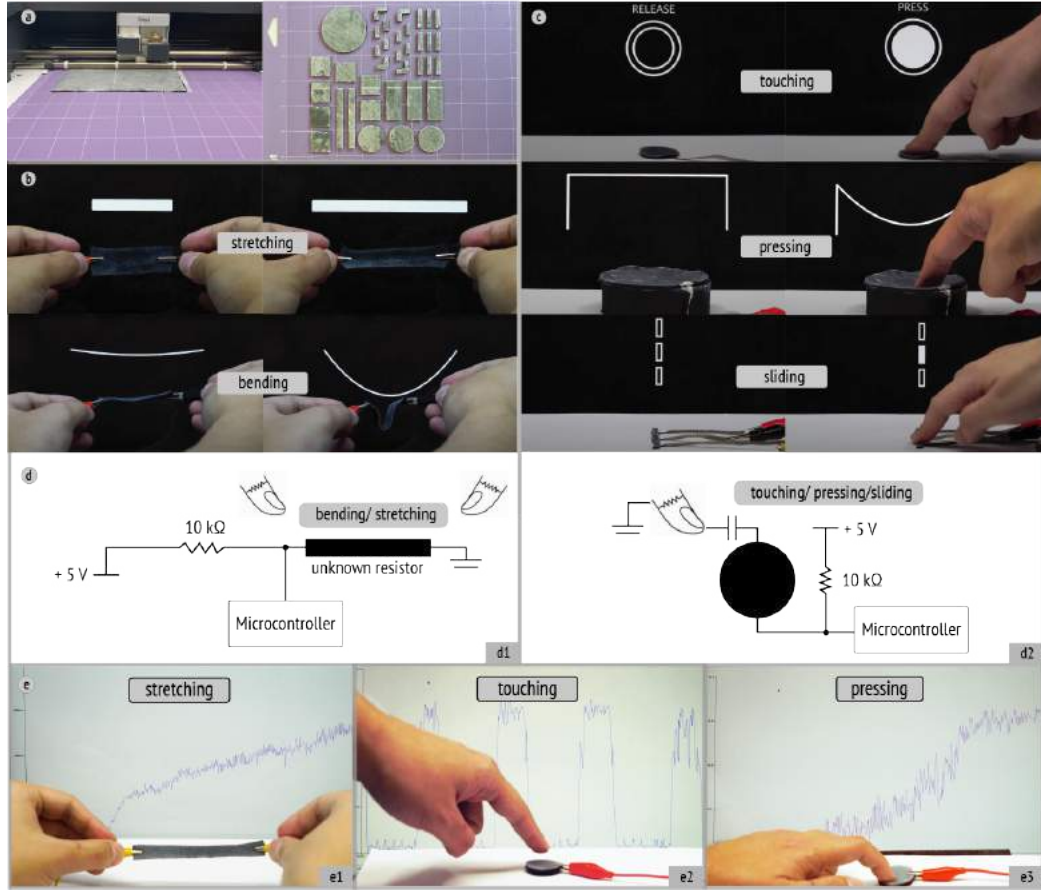


Figure 5.4: (a) Vinyl cutting process for the sensing samples; (b) Two example resistive sensing modalities: stretching and bending; (c) Three example capacitive sensing modalities: touching, pressing and sliding; (d) schematics for both sensing approaches; (e) Raw sensing data for resistive (stretch) sensing and capacitive (touch, press) sensing.

an equal amount of Ecoflex 0035 fast B, it will cure within 10 minutes, which can serve the function of instantly gluing the electrodes to our PITAS system (Figure 5.5 a). Also, after tested 12 samples ($3.4\text{cm} \times 0.8\text{cm} \times 0.18\text{cm}$), the instant conductive adhesive shows a conductivity of $0.013 \pm 0.002 \text{ S/cm}$. For the conductive electrode choice, we mainly considered the flexibility of materials that can be easily made into desired shapes and is malleable enough not to intervene in the deformability of the system. In Figure 5.5 b-d, we have tested three different types of conductive-fabrics-based connection methods, *Ag conductive hoop-and-loop*, *Zeven+30 conductive copper fabrics* from [121] and *Silver-Coated Vectran Thread* [122]. The first two options are easy to cut into various shapes

since they are both purchased in sheets, which can be cut by a vinyl cutter to meet different shape requirements. Conductive thread can be a replacement for the copper wire which is a common electrode connection for the electronics system, while the thread is more deformable and easier to get glued to our system.



Figure 5.5: (a) Two parts of the instant conductive adhesive; (b) Conductive hook & loop connection method; (c) Conductive fabrics connection method; (d) Conductive thread connection method.

5.2.4 Fabrication Methods

Our goal is to develop accessible fabrication methods to enable non-expert users to explore making various devices using our PITAS system. We considered three factors when choosing and testing the fabrication methods: 1) machine or tool cost; 2) whether the machines are commercially available and can fit into the home environment; 3) the net fabrication time.

Vinyl Cutting and Laser Cutting Based Method

Vinyl cutters support promising outcomes in the DIY community especially considering their low machine cost and the small space required for the machine setup, which serves as a great tool for cutting different thin-sheet materials (*e.g.*, fabrics, paper, cardboard). However, cutting silicone is not common due to the visco-elastic properties of silicone, which make it challenging to cut through the material by a normal cutting blade, also through the experiments, we observed the scrolling mechanism tend to peel off the silicone sheets from the cutting board because of silicone's high surface energy which made it hard to get adhered to normal surfaces. To tackle these fabrication issues, we bond the silicone

sheet in between two sheets of parchment paper. We also found a rotary blade can provide much better-cutting results compared to normal cutting blades [123]. With the machine setup, we are able to consistently cut through up to 3mm silicone sheet which typically contains 1mm conductive silicone sheet and 2mm phase transition actuator sheet (shown in Figure 5.6 b). We also observed the rotary blade will sometimes overcut the sample, so we suggest keeping a 5mm gap in between two adjacent cutting lines.

Laser cutting is another subtractive fabrication method for cutting silicone material into desired shapes. Compared to a vinyl cutter which only deals with sheet materials, a laser cutter can cut a wider range of materials and thicknesses with higher precision. However, although laser cutters are widely available in community-based maker spaces, laser cutters are more expensive and take up substantial spaces, so we treat this fabrication method as our secondary cutting method.

For our experiment, we used an Epilog FusionPro laser cutter. The cutting power could range from 20% to 50%, and the speed can range from 30% to 80%. For different material thicknesses, different combinations of cutting power, speed, and times should be applied, but certain combinations are more preferred than others. For example, for cutting a 4mm sheet (1mm conductive sheet and 3mm phase transition actuator sheet), 50% power, 50% speed for 4 times and 30% power, 65% speed for 5 times can both cut the sheet through. We prefer the lower power one since our phase transition actuator sheet is heat sensitive. Higher power would take the risk of evaporating the embedded ethanol around the cutting edges of the sample. Also, lower power will generate less cutting ashes from the conductive silicone sheet. We also recognize the conductive sheet layer is harder to cut through than the phase transition side, so we recommend cutting this stubborn layer first to avoid overcutting on the phase transition actuator layer.

Manual cutting

Among all cutting methods, manual cutting is the most accessible and rapidly available option. By using simple tools (*e.g.*, rulers, scissors, crafting knives, or even compass circle cutters), one can cut PITAS into desire shapes without the installations and operation of any machines. Besides accessibility, the manual crafting experience is also a good way to let people experience the proposed material system without any further process. This reflects great tinkerability by immediate feedback of materials.

Optional 3D Printing Method

Silicone 3D printing is a widely used fabrication method, but limited resources are yet in the market. The printing technique is available but not matured or accessible enough and mostly limited within research labs. Due to its less accessible manner, we tend to include 3D printing as an optional fabrication method. We searched the market and used Hyrel system 30M as our silicone printer. 3D printing PITAS requires printing process for both the actuating layer and the sensing/heating layer. Because of the high viscosity of the sensing/heating layer, one can directly load the material to the syringe to print. We normally choose to use the 16 gauge syringe tip as our main printing tip, but one can use tips with different diameters for wider or thinner traces. We also recommend to use the disposable sterile syringe instead of the metal extruder from Hyrel (*e.g.*, EMO-25 extruder), since the two-part silicone will ultimately cure inside the extruder. For printing the actuating layer, we choose to add 3% silicone thickening agent (THI-VEX, Smooth-On) to part A to thicken the material and make it more printable. For the machine setup, two key factors should be considered: the flow rate multiplier and proper Z height. For example, the conductive silicone material is very viscous and requires a material flow rate multiplier of 5 in the Hyrel system while for printing the actuating layer, a lower flow rate multiplier of 2 can be applied. Proper Z height also plays an important role for achieving good contact between two consecutive layers, and we have used 0.3mm as our main Z height value in the system.





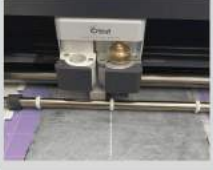




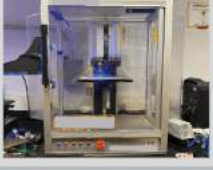


	Machine	Fabrication Detail	Failure Type	
Manual Cutting a			 under cut	Accessibility Design space Fabrication speed
Vinyl Cutting b			 over cut	Accessibility Design space Fabrication speed
Laser Cutting c			 burning ashes	Accessibility Design space Fabrication speed
3D Printing d			 improper Z height	Accessibility Design space Fabrication speed

Figure 5.6: Four different fabrication approaches: (a) manual crafting; (b) vinyl cutting; (c) laser cutting; (d) optional 3D printing.

5.3 System Characterization

5.3.1 Electrical Properties For the Conductive Silicone

Conductivity Test

Making electrically or thermally conductive elastomeric materials has been thoroughly studied in material science community. Researchers have tried to embed fillers including graphite powders, carbon nanotubes [21, 124], carbon fibers [118] or liquid metal (EGaIn) [125]. Most of the existing methods require 10%-15% of the filler material to be added to elastomer matrix, and mostly require complicated mixing steps and operation environment. We chose a graphene nanotube-formulated silicone filler Tuball 602 as our conductive filler

for its low dosage requirement, simplicity of the mixing process, and efficient conductivity. Most carbon nanotubes are powders and have safety concerns for inhalation, which may bring them in contact with the cardiovascular system, and normally requiring fume hood and other protections when processing the material. Tuball 602 contains single-layer rolled-up sheets of graphene that are more than 5 μm in length. Tuball 602, when sold, is already mixed with a matrix material that made the Tuball 602 a paste instead of powder. Another great advantage is the simple mixing method for Tuball. According to its guideline, one can simply adopt a mechanical stirrer to mix the Tuball filler to the silicone elastomer. Also, Tuball requires very low working dosage from 0.3–5%, and our conductivity test in Figure 5.7 a has shown the results with different dosages from 0.5-3.5% by mixing the Tuball 602 with Smooth-on 0050. For each dosage, we have tested 10 samples with a dimension of 3.4cm by 0.8cm by 0.18cm each. Conductive epoxy and a small piece of conductive fabrics are attached to both sides of the sample, and two-probe measurement setup is applied. For the conductive silicone layer, we mainly adopted 2.5-3% as our main recipe. The conductivity can further go down by increasing the dosage to 3.5% or more, but the material cost and the stiffness of conductive silicone material will also go up as a trade-off.

Heating & Cooling Time

PITAS is a heating based system, relying on the heat to penetrate the entire matrix to trigger the phase transition and the overall deformation. So heating process plays an essential role in the actuation process. We have tested five different types of sample with different dimensions from 1.5cm by 0.75cm, 1.5cm by 1.5cm, 1.5cm by 3cm, 1.5cm by 4.5cm and 1.5cm by 6cm (See Figure 5.7), each sample contains 1mm of phase transition layer and 1mm conductive silicone layer. We evaluated how different heating dimension along with different electrodes distance can affect the heating/cooling rate and how different provided power can affect the heating/cool rate. Figure 5.7 b & d shows a clear trend for the heating

time. When the heating area for the sample is smaller, which at the same time means the distance between two electrodes are closer, the heating time is much faster. Similarly, for a fixed heating dimension, the more power we provide, the faster heating rate we can achieve. Regarding the cooling rate, we can see the cooling difference between different samples, but it's not significant within one sample set when they are heated with different power. Our interpretation is since even the samples are heated with different amount of power, but we stop the heating process and start counting the cooling time when they reach 90°C, so the cooling rate performs similarly for different power. In Figure 5.7 c, we also provided the entire heating & cooling curve for the sample with dimension of 1cm by 3cm and it shows the cooling process takes substantial time. For example, the heating time for the sample at 5W takes around 25 seconds to reach 90°C while the cooling time takes almost 260 seconds to cool down back to the room temperature.

5.3.2 Mechanical Properties For the Phase Transition Actuator

Bending Test

On top of the test that we carried out for the heater, we have also tested how different volumes of the actuator can cause differences in the deformation. Since our focus is on the thin-sheet form factor for the PITAS system, in Figure 5.7 a and b, we have included testing samples of 1.5cm by 4.5cm dimension and with different actuating layer thickness ranging from 1mm to 5mm. Also the samples have a 1mm conductive silicone layer as the heater. As we have observed that 3mm and 4mm samples perform the best results, we speculate when the actuator is getting thicker, it becomes more difficult to uniformly heat up the entire matrix. Another aspect from this actuating results is the heat dissipation time from the conductive silicone heater to the phase transition layer. For example, The full actuation time for the 1mm sample is around 90s, while the 3mm sample will take almost 220s to get fully actuated.

Force Quantification

Ethanol/silicone based phase transition actuating system benefits from its high stress (up to 1.3 MPa) [113], which can play an important role when fabricating tactile devices to deliver information. However, we would like to note that since we keep a thin sheet form factor, it would not achieve the stress level reported in the previous paper [113]. Nevertheless, the phase transition actuator system is relying on the vapor pressure generated by the ethanol to delivery force, so one can stack up multiple layers of the material in order to achieve bigger force, but will inevitably lose the benefit of PITA's thin form factor. We have carried out the force testing for PITAS with a sample dimension of 1.5cm by 4.5cm, and we adopted 3mm thickness from the bending test results. The setup for the testing is shown in Figure 5.8 c. We put the PITAS sample beneath the force gauge, and consistently apply 3W to heat up the samples and we achieved the force curve on the right side of Figure 5.8 c. The maximum force detected by the force gauge is around 1.5N for our sample and we have repeated this test for 10 times and achieved an average of maximum force of 1.2 ± 0.2 N.

5.4 Communication & Control Methods

Our hardware system consists of two core parts: (1) a device that can measure conductivity, actuate phase transition, and communicate to other devices over the Internet, and (2) a cloud server that receives, store, and retrieve the sensing data. Although the proposed system is currently based on a ESP32 module, our approach can be easily adapted to other embedded platforms.

Device: We used ESP32, a widely-used, off-the-shelf, and open-source hardware platform [126]. When a participant connects a phase transition module, the device measures its conductivity 20 times using the analog-to-digital conversion function in ESP32 and averages the values to determine the baseline of the module. This initial calibration is required since the conductivity of each module may vary due to its shape, size, and thickness. After

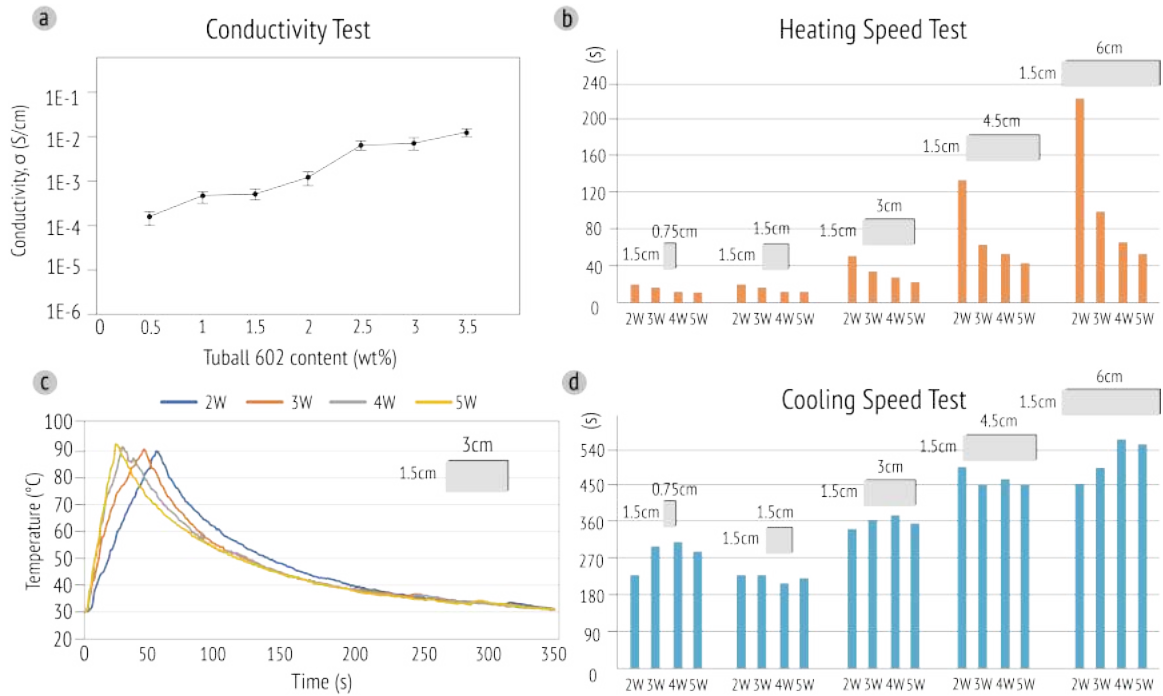


Figure 5.7: (a) Conductivity test results; (b) Heating speed test for five sample with different sizes; (c) Temperature curve for different input power; (d) Cooling speed test for five sample with different sizes

that, the participant can press the surface of the phase transition module to actuate the phase transition in another device. Though we simply detected the resistive or capacitive change, the sensing materials used in this study has a great potential to recognize various gestures and motions through simple machine learning and signal processing techniques [127]. For actuation, we connect the power source using an on/off relay switch. Note that the voltage value in this study is relatively high (*e.g.*, 60V), but the required current is relatively low (*e.g.*, 50mA). Therefore, a battery-powered actuation can be developed in the future using DC-DC voltage converters. All data communication was done through Wi-Fi.

Cloud Server: We developed the server part using a RESTful API based on Spring Framework [128]. This part allows a device to communicate with other devices anywhere with the Internet connection. For the sake of experimentation, we paired two devices. At first, a device sends its node identification number and sensing information to the server. Then the server transmits the data to another mapped device to change the phase of the

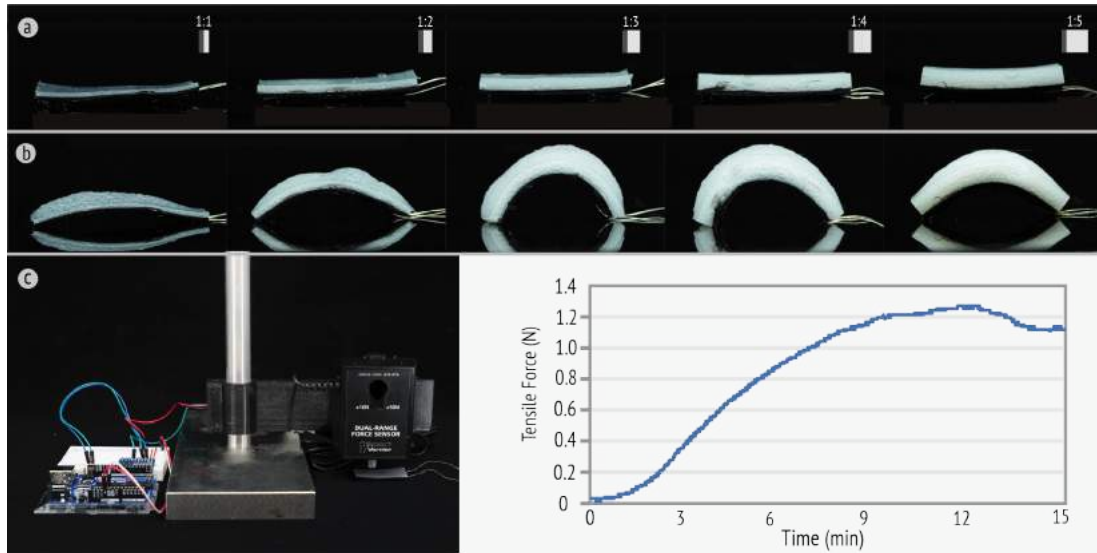


Figure 5.8: (a) Five phase transition actuator sample with different thickness; (b) Different bending curvatures achieved by the phase transition actuators; (c) The force testing setup and the results for the 3mm phase transition actuator sample.

device. Since our communication system is in the form of a star topology, system designers can easily modify the communication architecture to 1-1, 1-N, or N-N formats in the future.

5.5 Application

We also showcase two application examples that highlight the potential use cases of PITAS, and each application artifact exemplifies different actuation and sensing methods for PITAS (Figure 5.10).

5.5.1 Home decor artifact for emotional communication: 3D artificial rose

Inspired by the aesthetic demonstration from *Thermorph* [15], we developed an artificial rose whose petals and leaves are made by 3mm by 1mm PITAS sheet with embedded thermochromic pigments. When touching or bending the petals or leaves, people can remotely deliver the emotions of missing each other (with petals blossoming and color turning into pink from colorless, Figure 5.11 b) or share melancholy or loneliness (with leaves hang-

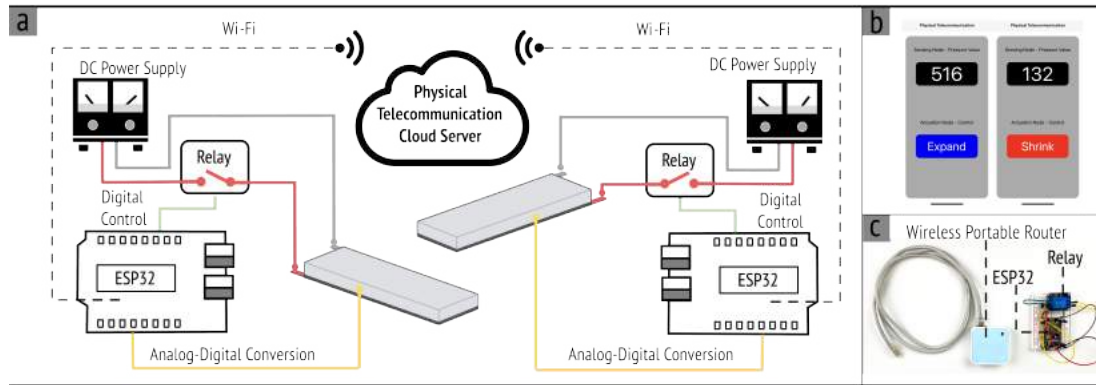


Figure 5.9: (a) Configuration of hardware system; (b) A mobile application to visualize the sensing data; (c) An actual device that participants used in the workshops.

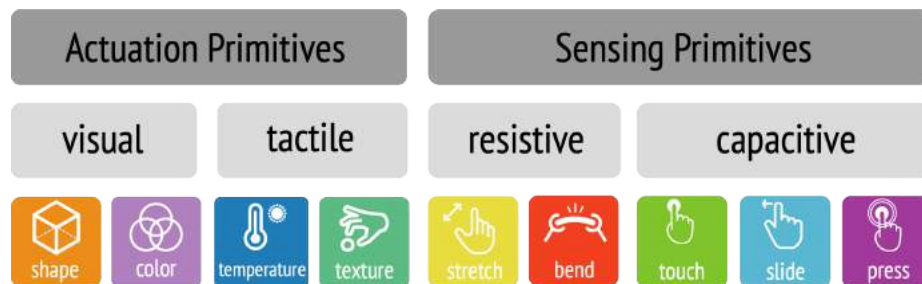


Figure 5.10: Overview of the actuation and sensing modules for PITAS

ing down and turning to yellow from green, Figure 5.11 c). This application is intended to evoke an emotional interaction enabled by the adaptability and deform-ability of PITAS that can be endowed with thermochromic functionality and rolled up into desired 3D shapes.

5.5.2 Office accessory for information delivery: Actuatable sticky notes

One key feature of PITAS is how easy and accessible it is for novice users. They can customize it into desired shapes to actuate daily objects by simply using scissors or a craft knife to cut. We demonstrate this by using a pair of scissors to manually cut PITAS sheet into different shapes and place them onto Post-it notes with different arrangements to remotely synchronize different stages of a task shown in Figure 5.12 a. Users are able to remotely update the status of their work and communicate it to his/her team. This is done with a cut-and-attach approach in which modules are fabricated by hand without involving additional fabrication machines, shown in Figure 5.12 b. In this example, a long strip of PITAS placed



Figure 5.11: (a) Overview of the artificial rose and leaves fabricated by PITAS; (b) Delivering color change (colorless to pink) and flower blossom to partners remotely when missing each other; (c) Delivering the depression by enabling the color change (green to yellow) and leaf hanging down remotely.

in the middle of a Post-it note causes a bigger curl in the middle. A strip placed diagonally causes a side flip of the Post-it note, while two short strips cause a wider but smaller curl. These can represent an accomplished, stuck, or in-progress task respectively.



Figure 5.12: (a) Different actuation modalities; (b) Remotely synchronize the task progress by tapping or bending the Post-in note with PITAS attached on the back.

5.6 Limitation & Future Work

In addition to the insights that we gained from running the workshop, we have also observed certain weaknesses that PITAS can improve in the future:

Material Preparation As previously mentioned, the current version of PITAS is prepared by the researchers. Even the mixing steps for both the phase transition layer and the conductive silicone layer are not complicated – only requiring simple mixing stirrers, these pre-process steps are still constraining PITAS from being adopted by a broader spectrum of users. Also, the current PITAS sheets are mostly molded, which does not always provide consistent layer thickness. We believe a film applicator can be a good candidate to make the PITAS with more uniform thickness like the one has been used from *Silicon Device* [39]. We also envision that PITAS or a similar type of actuating and sensing embedded materials can be commercially available for direct purchase in the near future.

Driving Voltage Even comparing with some other types of soft material system (*e.g.*, electroactive polymers), which usually required over 1kv or more to drive the deformation, PITAS demands low voltage. However, the voltage requirement (*e.g.*, for a 1.5cm by 4.5cm sample) is still usually around 50V, which is a limiting factor and further constraints the practical usage of PITAS. This can be tackled by further adding higher dosage of conductive materials to reduce the resistance of the conductive silicone layer, but inevitably can sacrifice the softness of the system. Also, this high voltage requirement makes direct touch to the conductive silicone layer very dangerous, especially for any potential on-body applications. A thin silicone coating which can act as the dielectric/protection layer should be applied if users will be in contact to the conductive silicone side.

Actuation Speed PITAS mainly aims at showing the possibilities for DIY different types of physical telecommunication modules with taking the material advantages by providing large strain, high adaptability to different inclusions or sensing/actuating embedded. However, the current mechanism has been limited by its actuation speed. The current actuation time is at the order of minutes. To speed up the actuation cycle, mixing the conductive material, ethanol and the silicone matrix all together will help with the heat distribution throughout the system much better, and that would be a next step for us to investigate.

Material Preparation and Use Safety The material preparation steps for the conductive

sheets and the instant conductive glue of PITAS involve manipulation of Tuball 602, containing single-wall carbon nanotubes which is traditionally categorized into carcinogenic materials that can damage the cardiovascular system [21]. Even for Tuball 602 matrix, the carbon nanotubes are already encapsulated within a resin carrier instead of free powders, to reduce its airborne exposure potential. However, when preparing the sheets or processing the fabrication (*e.g.*, laser cutting, hand cutting), one should complete the necessary safe handling procedures and wear proper personal protective equipment (protective gloves, goggles, masks) and must be under a good ventilation environment (*e.g.*, fume hood). We list the official material process document from Tuball here (Safe Handling and Use of Tuball Guideline).

CHAPTER 6

FUNCTIONAL DESTRUCTION: UTILIZING SUSTAINABLE MATERIALS' PHYSICAL TRANSIENCY FOR ELECTRONICS APPLICATIONS

6.1 Introduction

Advances in manufacturing methods for electronics most often aim to produce highly integrated and reliable devices for long-term use. While these features have brought benefits to customers, they also have many side effects. One of these is e-waste, which is the fastest-growing waste stream in the world with 53.6 Mt. (million metric tonnes) generated in 2020 [129]. Significant effort has been put toward e-waste recycling, but the composition of electronic devices makes the recycling process far more challenging than that of other materials like metals and cardboard. This is exacerbated by the increasing rate at which we produce smart devices, leading to much more e-waste than today's recycling methods can handle. Material science has contributed a range of sustainable materials which may alleviate some of the impact these electronics have, but this overall approach of "build components which will last for a long time" means an object's physical form often outlasts its usefulness.

The goal of this work is to explore transiency as an alternative to traditional electronics. Transient electronics are designed with destruction in mind. That is to say, the disposal of the hardware is integral and intrinsic to its design. In this schema, a device exists for only as long as it's needed. Given this, transient electronics naturally have a place in our future; however, less explored is how such electronics can enable interactivity, what HCI researchers can do with them, and how sustainable materials may be utilized to deliver all this. We examine these questions by utilizing well-understood materials — ones that are known to researchers, practitioners, and designers alike for more traditional uses — in the new context of enabling interaction in sustainable transient electronics. Some of these

materials, like polyvinyl alcohol (PVA) or carbon powder, are often overlooked as possible solutions for sustainable transiency because they so often are part of more traditional electronic systems. That is to say, they are not always sustainable when used in their more traditional contexts. For others, their sustainability is impacted by their supply chain. Wax, for example, is not inherently unsustainable; while paraffin wax is traditionally the result of a crude oil-intensive process, its sustainable alternative, beeswax, is the natural byproduct of honey bees.

In recent years, there has been a rise in HCI research with a focus on sustainability and unmaking [81, 130, 131]. These works emphasize the disassembly of an object or structure comprised of entirely decomposable components. For example, Song et al. leverage the inherent material properties of natural materials, including paper, leaf skeletons, and chitosan, along with silver nanowires to create a thin-sheet heater that backyard decomposes [82]. The work in unmaking and sustainable HCI greatly inspired this work, and through our exploration emerged a similar complementary idea we call *functional destruction*: the ability for the core functionality of a device to exist within its prescribed transient destruction. Destruction is not usually considered a functional part of a device, but for transient electronics, designing for a given method of destruction is necessary. We not only aimed to enable conventional interactions through transient means, but also to genuinely consider what interactivity may be enhanced, or in some cases enabled, with the introduction of destruction as an intentional part of design.

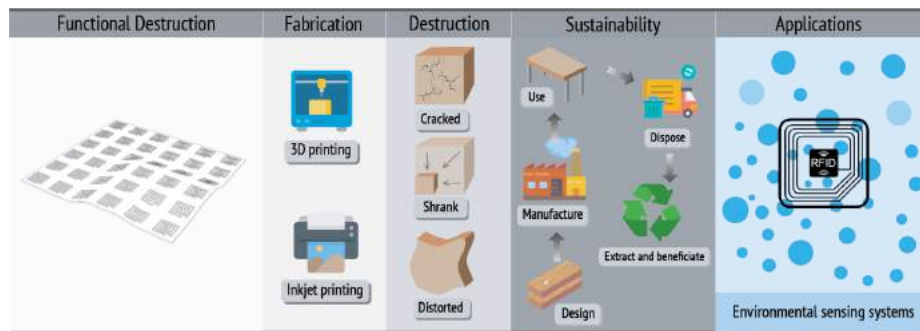


Figure 6.1: The overview for functional destruction, including fabrication methods, destruction types, sustainable cycles, and potential application domain.

In this work, we have investigated how materials, fabrication tools and methods, and different types of destruction (melting, dissolving, etc.) can be combined to make devices with sustainability, transiency, and interactivity at the core. We introduce three practical approaches to building such devices, all of which are accessible to HCI researchers, and many of which are highly manufacturable. Our methods include inkjet printing conductive traces on water-soluble PVA sheets, laser-transferring edible gold foil onto 3D printed chocolates, and fabricating electronic devices using natural beeswax. We demonstrate applications of these methods which take advantage of each material's physical transiency for functional goals. For example, water-soluble electronics that can be used for water-leakage sensing, edible chocolate electronics which destroy data contained in a circuit through digestion, and beeswax-based temperature sensors which melt away after use. Lastly, we implemented a metallic resonator design in all three material systems enabling fully passive and chipless RF detection in each context. Such chipless RFID technology requires no soldering process or non-recyclable components and allows each of these embodiments to interact with other systems.

The main contributions include:

- A method of utilizing inkjet printing to directly print silver nanoparticles onto PVA sheets, making water-soluble electronics.
- A process and formulation for a natural beeswax-based conductor which can be configured into a range of meltable electronics.
- A process to apply conductive gold foil onto chocolate, 3D printed or otherwise, for making edible electronics.
- Demonstration and validation of passive wireless interaction with all three different substrates (PVA, beeswax, and chocolate).



Figure 6.2: Overview of the design space for functional destruction, including detailed destruction types, sustainable electronic materials selections, available fabrication methods, and the potential application spaces.

6.2 Functional Destruction: Design Space and Overview

6.2.1 Design considerations for destruction

The goal of this work is to utilize the physical destruction of circuits for functional purposes in order to mitigate the sustainability issues caused by more permanent electronics used today. Sustainability is an increasingly pressing global concern that demands particular attention when discussing energy and material-intensive efforts. Since the design approaches of everyday objects in HCI may affect mass-produced products, rethinking the life-cycle of such objects become especially critical. As such, before presenting our practical approaches, we first explore what the design space looks like, how to harness known digital fabrication materials and tools, and how this could be integrated into the sustainability cycle for functional applications.

The Design Space of Destruction

Broadly, destruction in transient electronics is mostly described as "physically disappearing" without any other design considerations [132]. We apply a more structured meaning to destruction which we'll define through **1) destruction types, 2) destruction affecting factors, 3) stimuli types and 4) post-destruction processes**. When developing this design space, we primarily refer to existing destruction types for today's transient electronics (such as melting and dissolving) and were greatly inspired by the design space discussed in [81]; however, we're particularly focused on how designing for destruction can affect the functionality of transient electronics in addition to the environmental benefit [81].

Destruction Types

The first destruction types are **dissolve and melt**, which are the primary destruction types used in this work. These include the dissolving of PVA and chocolate when exposed to water and stomach acid respectively, or the melting of beeswax when near heat. Dissolving is an especially common way for today's transient circuitry to visually disappear, usually accompanied by the destruction of the associated circuits [133]. We also recognize that there are other types of destruction that can be utilized for functional purposes, such as **crack**, which usually happens to more brittle and plastic substrate-based electronics. Alternately, **expand** and **shrink** are two types that require the substrates to be more elastic and permit a range of deformation before being directly separated into pieces [134]. **Wrinkle** and **distort** are two similar and less severe destruction types as the functionality of the circuits can often be restored. We summarised these in Figure 6.2 as an initial set of destruction types; a set that is by no means exhaustive but which is sufficient to describe our exploration.

Destruction Affecting Factors

Primarily, destruction types and their severity are determined by the **chemical composition** of the device materials, where the substrate material plays a dominant role. For example,

PVA or silk film-based transient electronics can be dissolved in the order of 100 seconds [135], but PLGA, which is another water-soluble polymer, may require several days to dissolve [136]. Beyond composition, **geometry** of the device is another variable that impacts destruction and may be tweaked to achieve desirable behavior. For example, PVA-based electronics placed on the surface of water will dissolve at a rate proportional to their thickness. Varying this thickness allows timed destruction. Similarly, 3D PVA structures dissolve faster when the surface area in contact with the dissolving stimuli is increased, this can be tuned by adding pores.

Stimuli Types

Triggering destruction usually requires stimuli, which range from specialty chemicals to water, to heat, and even mechanical actuation. Sometimes, these stimuli are experienced naturally, which we call **passive** activation. These stimuli may be heat from sun, water from a broken pipe, or other scenarios where the destruction senses a feature of the world around it. Alternatively, these stimuli may be applied **on-demand**. This may mean activating a heating element with a remote control or eating the device to intentionally destroy the circuit. Whether passive or on-demand, the destruction type, and destruction affecting factors remain unchanged, only the activation source is impacted by a given stimuli choice.

Post-Destruction Processes

When a transient device is destroyed, there is usually some minimal post-product that must be considered. For example, a dissolvable electronic may leave a non-toxic residue, but that doesn't mean you should dissolve it in a fish tank. For today's transient electronics, some attention is paid to the post-destruction phase, but we believe that significant consideration of post-destruction is highly merited to ensure life-cycle sustainability. We encountered three types of post-destruction activity in our exploration: **recycle**, **degrade**, and **enhance**. If a device is destroyed via degradation, the post-product of the device will remain in the

intended environment without causing harm to it; for example, natural bio-degradation caused by microorganisms such as bacteria and fungi, or a more human-intention-driven process like composting. Recycling involves re-obtaining the device materials and re-processing them into new devices; for example, melting the beeswax-based devices and reconfiguring them into new shapes with new functionality. Enhance is a special type of degradation, where the destroyed device is beneficial to the environment; for example, a device that, when digested (like the chocolate circuits), provides nutrition to a person.

6.2.2 Sustainable Material Considerations

Many materials chosen for making transient electronic substrates are bio-compatible and highly sustainable; however, not all materials in transient electronics can biodegrade into water, carbon dioxide, or biomass. Materials like metal and metal nanowires, while used in quantities so small they are not usually an environmental risk, are technically not biodegradable. This presents a challenge to truly sustainable functional destruction, but one which other material-focused works are actively working to overcome through developments in paper, silk, chitin and silver nanowires (Ag NWs), magnesium, and conductive polymers such as PEDOT:PSS.

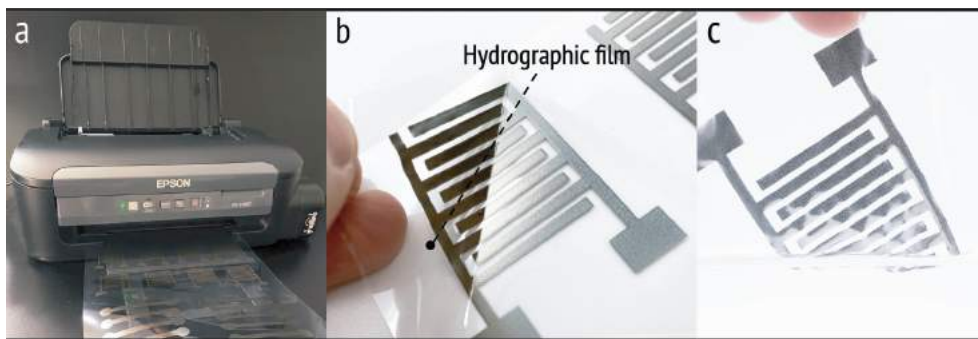


Figure 6.3: The overview for inkjet printing water-soluble electronics, where conductive patterns are (a) printed on hydrographic films, (b) peeled off from the PET backing, and (c) directly dissolved in water.

6.2.3 Using Highly Accessible Materials & Tools

Most current transient electronics fabrication methods and materials require lab spaces. For example, to prepare a common silk substrate, researchers need to rinse and dissolve the silk fibroin in a special solution, dialyze it with distilled water for a couple of days, followed by centrifugation and filtration steps. These steps often require domain experts who need a fundamental understanding of how to prepare and process materials, as well as how to properly dispose of the byproducts [132]. For non-experts, simply following the procedures described in the literature will almost certainly cause frustration, material waste, and inappropriate material disposal. While these lab-centric efforts are critical for the future of transient electronics with better performance, we believe to broaden the impact and design space we must allow a wider spectrum of designers to use these electronics, elevating the importance of accessible materials.

6.2.4 Application Domains

Functional destruction aims to leverage transient electronics, utilizing the destruction process to enable interactivity. We believe this creates opportunities to rethink the designs and applications of the interactive devices from a more sustainable perspective. In Figure 6.2, we propose four example application spaces for functional destruction.

The first application domain is data storage. A usual requirement for data storage is also a method for securely deleting data. Systems built with transient materials have the potential to be naturally or on-demand physically destroyed to sanitize this stored data. The second application domain is biomedical, where utilizing bio-compatible materials may allow implantable monitoring systems with designed transiency for short-term to long-term health monitoring. Environmental sensing is the third application domain, as most current permanent sensors face retrieval challenges when deployed in large quantities or to hard-to-reach areas (*e.g.*, mountains, large infrastructure); Functional destruction-based sensors can leverage the environmental stimuli as both sensor triggers and a solution to retrieval

challenges (*e.g.*, water sensing which both activates and destroys the sensor. The last application domain we propose is re-configurable electronics, where this reconfigurability can span from small shape changes (*e.g.*, shrinkage or expansion functions as a volume sensor) to entire device re-shaping (*e.g.*, changing from one type of sensor to another both functionally and physically).

6.2.5 Design Space in Practice

We take these application domains and consider them within our design space, leading us to primarily consider materials that will cause minimal environmental impact (*e.g.*, biodegradable, compostable) while remaining highly accessible to a broad spectrum of users without space or lab requirements. We do so through three independent approaches. In our first approach, we utilize home-safe inkjet printing water-soluble electronics. Inkjet printing has been widely used to quickly prototype electronics in HCI [30], and we directly print sintering-free Ag nanoparticle inks to off-the-shelf PVA sheets by using a common inkjet printer. With this approach, users can make passive-trigger water detection sensors, where water will both cause the destruction of the system through dissolving, and also act as the trigger to activate a water-leakage alert. In another approach, we use a natural beeswax substrate to achieve reconfigurable interactive devices with both compostable graphite powders and the same sintering-free Ag nanoparticles. The fabrication methods involved are simple conductive pattern transferal and mixing at kitchen-safe temperatures. Our third method demonstrates how to use both off-the-shelf edible gold leaf and chocolate substrate to make edible electronics, where on-demand eating and digesting will physically destroy the data stored within the system (*e.g.*, RFID). Each of these approaches has its own sustainability implications, functional limitations, and benefits which we will discuss in depth.

section Inkjet Printing Water-soluble Electronics Water has been widely used as a catalyst for the destruction of transient electronics [132]. Beyond being just a dissolving

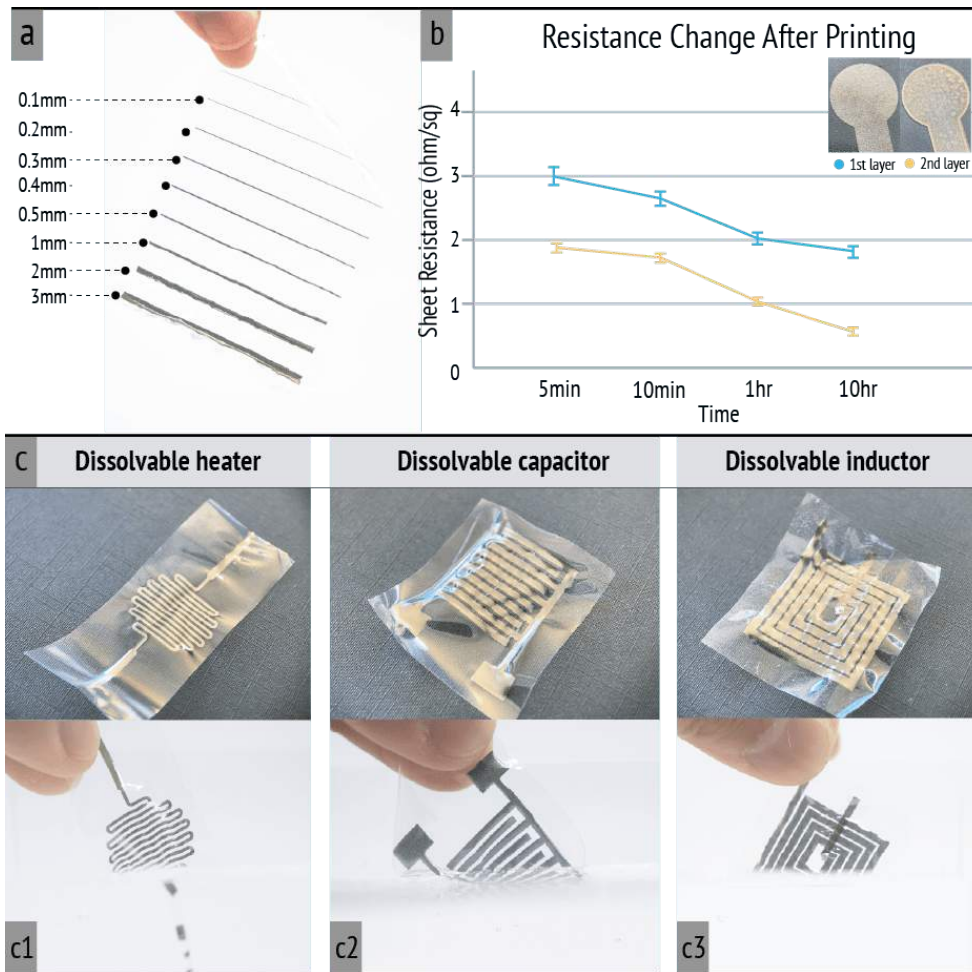


Figure 6.4: (a) Printing resolution. (b) Resistance change over time for printing once and twice. (c) Printed devices.

medium, the presence of water can also indicate certain information or activity (*e.g.*, water leakage). Our first investigation for functional destruction was to design a circuit that is both water-soluble and can be used for detecting the presence of water at the same time. There are many existing fabrication methods for making water-triggered transient electronics, but the fabrication process for them usually requires the use of complicated tools and processes along with deep materials science knowledge [132].

Inkjet printing has been adopted by researchers as a tool to create versatile printed electronics by replacing traditional ink with functional ones [30]. Due to the inkjet printer's affordable cost, reliability, and rapid printing speed, a combination of commodity inkjet

printers and off-the-shelf functional inks have been widely used within the HCI community for electronics prototyping purposes [29]. Standard heat-sintering inks require an annealing process following the print to evaporate solvents and stabilizing polymers surrounding the conductive particles [87]. Annealing allows a wide range of substrate materials for printing but materials choices are limited to those that can withstand annealing temperatures. The process adds additional time to fabrication and requires a heat source for annealing.

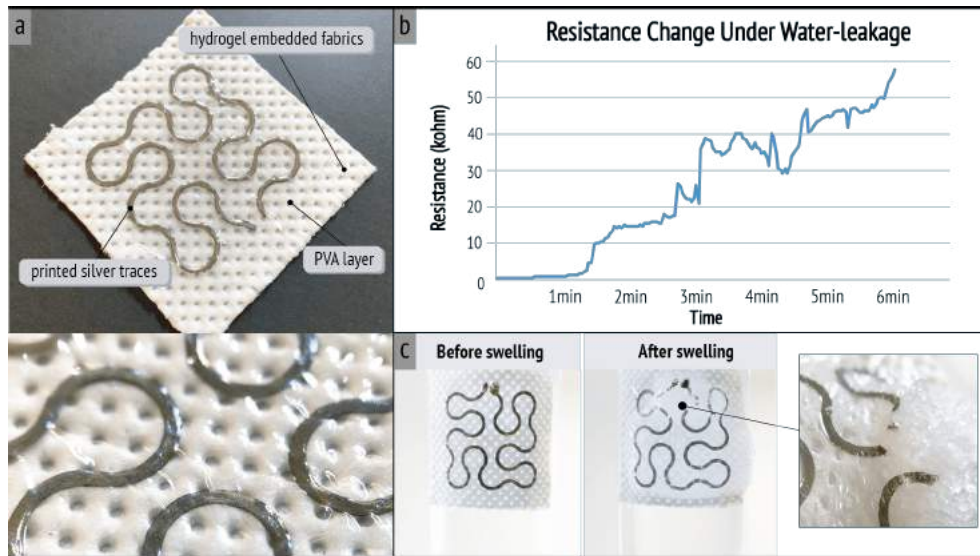


Figure 6.5: (a) PVA-hydrogel combined printed water leakage sensor. (b) Resistance changes when there is a water leakage. (c) The sensor before and after swelling from the water leakage.

A chemical sintering (or sintering-free) method enabled by the silver nanoparticle ink (Mitsubishi Paper Mills NBSIJ-MU01) provides a simpler process with no post-treatment requirements. Printed traces will usually become conductive within a minute [30], though the conductivity will slightly increase along with time as the chemical sintering continues. The downside is this technique requires the substrate to be specially coated with sintering agents, limiting this technique to Mitsubishi PET sheets or photo paper only. Hydrographic film, a water-soluble film (typically PVA), contains a surface layer similar to the required sintering agents for the ink from Mitsubishi. Hydrographic film is commonly used as the printing and transferring medium for making patterns on 3D surfaces and objects, and

HCI researchers have extended this method for patterning circuits or displays on objects with 3D surface structures [87]. We repurposed these PVA films and their surface coating (sintering layer) to inkjet print conductive traces without any post-treatment. The PVA-based hydrographic films provide a water-soluble substrate to create transient electronics. We used a commodity inkjet printer (Epson PX-S160T), Mitsubishi silver nanoparticle ink, and off-the-shelf hydrographic films [137] to create our prototype. The hydrographic film is composed of a PVA printing layer and a PET backing. One can print any circuit pattern and peel the PVA layer off of the backing (shown in Figure 6.3b). The resulting printed circuits can then be destroyed when the PVA dissolves in water (shown in Figure 6.3c). For more details on the silver ink printing method, please refer to prior work [30, 2].

Using this technique, we fabricated and tested a set of circuits to better understand their electrical characteristics. All patterns tested were 60 mm in length with variant widths from 3 mm to 0.1 mm. 0.1 mm was established as the lower limit of resolution, with a printed trace measured at 900Ω (shown in Figure 6.4a). In (Figure 6.4b), we printed single-line patterns with widths of 3 mm for 15 samples with both one and two printing layers. We measured the resistance in a simple two-probe set up and reported the average values. As can be seen from the plot, resistance values decrease rapidly after printing and then continue to slowly decrease in the 10-hour period measured. The lowest resistance after 10 hours for one layer and two layers were $1.73 \Omega/\text{sq}$ and $0.57 \Omega/\text{sq}$ respectively. We further demonstrated the versatility of this technique to create transient devices by creating a single-layer serpentine-based heater, a single-layer capacitor, and a two-layer inductor that is interconnected with silver epoxy (CW2400) (Figure 6.4c).

The PVA's solubility in water, destroying the conductive traces as it dissolves, can provide a functional application such as water leakage detection. As shown in Figure 6.5a, we printed 120° Peano curves and attached the film to a super-porous hydrogel-embedded fabric [138]. Peano curves were chosen to enhance the stretchability of the device [139]. The hydrogel layer serves two functions in this water-leakage detection scenario. First, as

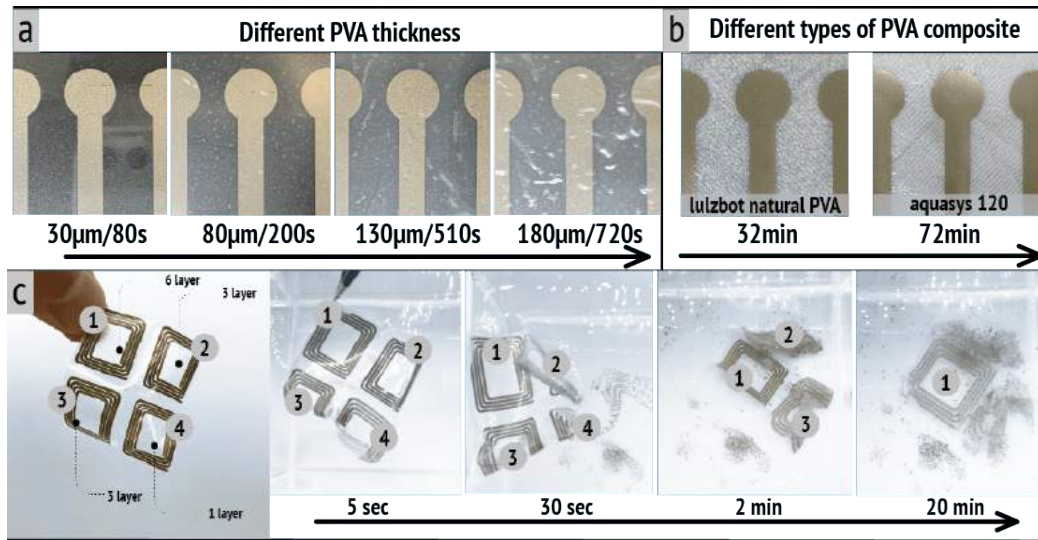


Figure 6.6: (a) PVA sheets with different layer thicknesses. (b) 3D printed different PVA composites. (c) Demonstration of the computational dissolvability within the same sheet.

shown in Figure 6.5c, after we attach the device to the pipe, the hydrogel will slow down the leak by absorbing the water. Second, as the hydrogel absorbs the water and expands, the physical deformation will trigger a resistance change. Gradually, the water will pass through the hydrogel and dissolve the PVA sheet, increasing the trace resistance. The measurement shown in Figure 6.5b is the resistance from the conductive trace after exposure to water, providing a clear output signaling that water is present.

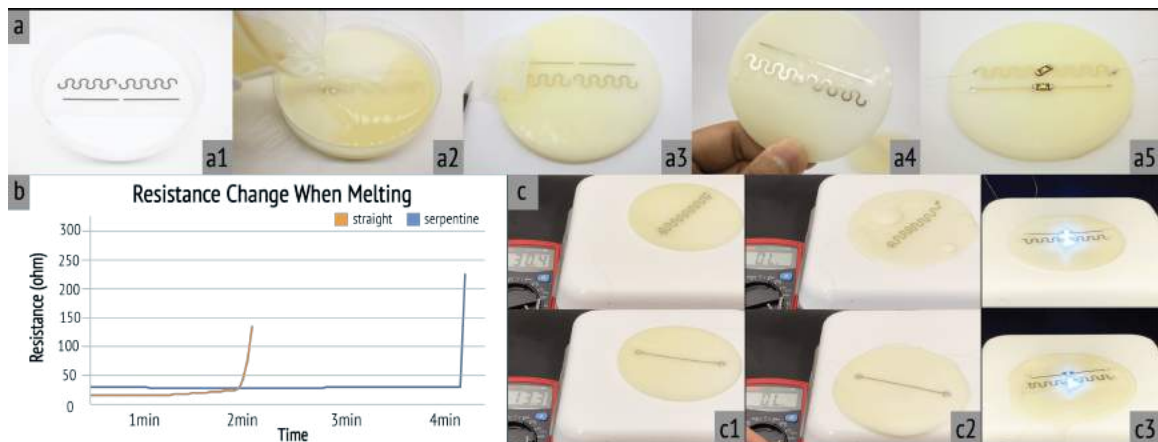


Figure 6.7: (a) Detailed print-transferring fabrication method for highly conductive circuitry on beeswax. (b) Resistance change for straight and serpentine patterns respectively. (c) Demonstration of when the patterns are melted on a hot plate.

The results and other existing literature [140] motivated us to investigate the computational aspects of transient electronics. As shown in Figure 6.6a, a print on a 30-micron thick hydrographic film can be implemented as a one-time use sensor with uniform dissolvability taking around 80 seconds to dissolve when submerged in water. In Figure 6.6a, we tested stacking PVA sheets to increase the total PVA thickness and thereby change the dissolving time of the entire device. We also explored the effects of the substrate material composition on PVA-based transient devices by 3D printing different types of PVA filaments. In Figure 6.6b, we first 3D printed a thin sheet of PVA layer (around 1 mm) by using different PVA filaments, and attached the inkjet printed hydrographic sheet onto the 3D printed PVA sheet to achieve different dissolving rates. In Figure 6.6c, we also demonstrated within the same water-soluble sheet, that areas with different PVA thicknesses will dissolve sequentially. This points to the idea of computational transiency, in which the disappearance can be highly programmatic and enhance functionality in the destruction process; for example, so that a PVA moisture sensor may map to a different amount of water exposure.

6.3 Beeswax based heat-meltable electronics

Besides water, heat is another very common and natural resource. Researchers have tried to mix conductive fillers (*e.g.*, carbon nanofiber, microparticles of tungsten) with wax and other materials to make functional devices [141, 142], but, as with water-soluble electronics, the materials and fabrication methods are not very accessible and mainly limited to the lab. We propose our second approach for functional destruction by taking natural beeswax as the primary substrate, and by either transferring highly conductive traces to beeswax or mixing compostable graphite powders for a more resistive beeswax-graphite composite.

Our first approach for making beeswax-based electronics was transferring inkjet-printed silver nanoparticle traces to beeswax substrates [143]. We leveraged the print-transferring method described in Silver Tape [2] by first using a commodity inkjet printer to print conductive traces onto customized Mitsubishi PET film. We then poured melted beeswax

directly onto the printed side of the film and waited for the wax to solidify. The PET sheet can then be peeled from the beeswax to finish the transfer step and the trace is ready to be mounted with other electronic components. The detailed fabrication process is shown in Figure 6.7a. To our knowledge, we are the first to demonstrate making highly conductive circuitry on a wax substrate by a simple print-transferring approach. The most exciting result of this approach is that the conductive traces will remain stable and the resistance will start to dramatically increase only when approaching the circuit's breaking point. Using serpentine traces with this approach will relieve the local stress concentration and make the circuit more stable. As shown in Figure 6.7b and c, we have tested the resistance change for both straight and serpentine conductive traces by placing the samples on a hot plate at 75°C, and both have shown a slight increase in resistance, rising from 12.3 Ω to 26.8 Ω and 27.1 Ω to 30.2 Ω for straight and serpentine lines respectively. Testing the variance in the resistance across 10 samples of 5cm by 0.5cm, we achieved a sheet resistance of $0.21 \pm 0.01 \Omega/\text{sq}$ and $0.24 \pm 0.03 \Omega/\text{sq}$ before and after the circuits were transferred onto the beeswax substrates, respectively. These variances are relatively small and show the reliability of the transfer process. The serpentine design increases the endurance of the device before its cut-off point. Changing the circuit's path can therefore allow a designer to control the time it takes for a device to be destroyed.

We also developed an approach to directly mix graphite powder [144] with beeswax to form a composite material. The mixing steps are simple. We first melt beeswax pellets at 75°C and pour the graphite powder into the beeswax once it is completely melted. We use a magnetic stirrer to mix the beeswax and the graphite powder under 1000 rpm for 30 minutes, where the stirring speed might vary for different graphite dosage (*Note: Graphite powders used in our approach are around 44 microns particle size and need to be handled carefully by wearing safety protection equipment in a well-ventilated environment*). Until it becomes a uniform liquid, one can mold the wax into various shapes or use a film applicator to form thin-sheet wax. The detailed mixing and shaping steps are summarized in Figure 6.8a. We

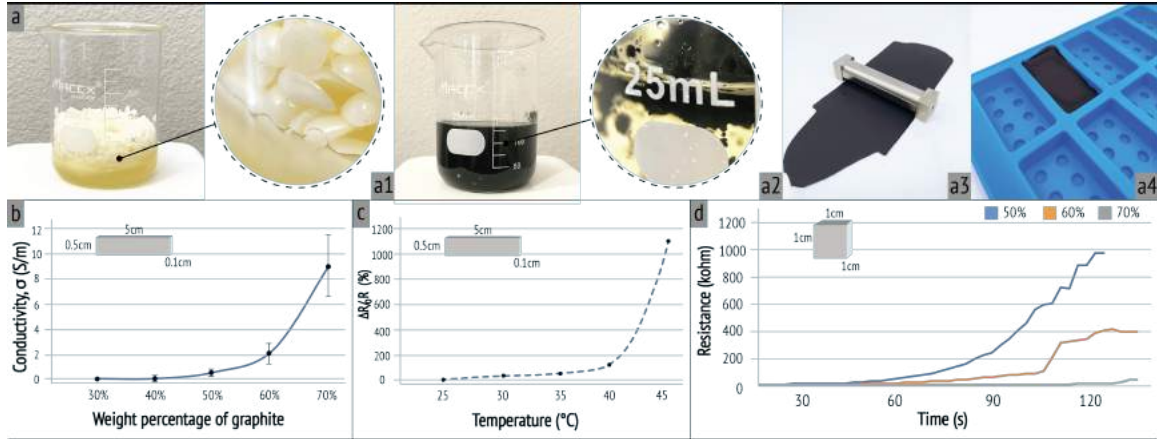


Figure 6.8: (a) Mixing steps for making the beeswax-graphite composite and the post-mixing shaping methods. (b) Conductivity testing results for different ratios of graphite powder. (c) Testing results for the resistance change under different heating temperatures. (d) Testing results of the resistance change over time for different graphite powder ratios.

first tested how different ratios of the graphite powder to beeswax will affect the conductivity of the composite. As shown in Figure 6.8b, we tested 10 samples with dimensions of 5cm by 1cm by 0.1cm by using a two-probe setup. The results show that the higher the amount of graphite powder is, the more conductive the composite will be. Unlike the first print-transferring approach, which can maintain stable conductivity for the circuit when under external heating stimuli, this beeswax-graphite composite is sensitive to heat. As shown in Figure 6.8c, the resistance increases with temperature across all graphite powder ratios (results for 50% weight ratio samples shown in this figure). After testing the samples with different graphite ratios under 60°C, lower ratios yielded a higher final resistance and a steeper curve as shown in Figure 6.8d). Especially for the first 100 seconds, the resistance increase and heating time are almost linearly dependent, which could potentially make this beeswax-graphite composite a physical thermistor.

6.4 Chocolate-based Edible Electronics

By combining these approaches for making both highly conductive or more resistive beeswax, we showcase how they can be combined to form a self-destroying circuit configuration



Figure 6.9: Demonstration of creating a self-destructing circuit from Beeswax: (a) The front LED circuitry side; (b) backside to show the Beeswax-graphite composite is sealed inside; (c) The LEDs are on; (d) The circuits are damaged and the LEDs turn off. (e) The Beeswax-graphite heater reaches 50°C under thermal camera.

(Figure 6.9). We first transferred the inkjet-printed silver nanoparticle traces onto the beeswax and connected it to three LEDs (shown in Figure 6.9a). We also sealed a piece of the beeswax-graphite composite inside the device, which is shown as the black area in Figure 6.9a and b. Normally, the LEDs are powered and light up, but when we also power the heating element in the device made of the beeswax-graphite composite, it starts to melt the circuit and ultimately damages its functionality. In Figure 6.9d, we show that the silver traces and the beeswax substrate are melted. To further validate this self-destructing behavior, we fabricated four identical devices with the configuration shown in Figure 6.9. We recorded the temperature ($40.3 \pm 4.4^\circ\text{C}$) and the time ($142.5 \pm 45.0\text{s}$) for the devices to start to melt and shut down the first LED, the time ($756.2 \pm 320.7\text{s}$) to shut off the entire device, and the peak temperature it achieved ($53.3 \pm 3.7^\circ\text{C}$). Note that the LEDs shown in this beeswax-based approach are conventional SMD LEDs that are not biodegradable and were utilized solely for demonstration purposes. We further discuss possible sustainable replacement options for conventional components in our later discussion.

We also demonstrated three additional interactive devices made from this conductive beeswax separately, including an LED, a capacitive touch sensor, and a resistive bending sensor. As shown in the first column of Figure 6.10, we used a silicone mold to cast the beeswax-graphite composite into different LEGO brick shapes, where one LED is embedded in the middle non-conductive beeswax. We connect the power to the two conductive beeswax bricks that are placed on both sides. Similarly, we cast a spiral-shaped button as a capacitive touch sensor, where the capacitive change is read through Arduino’s Capacitive

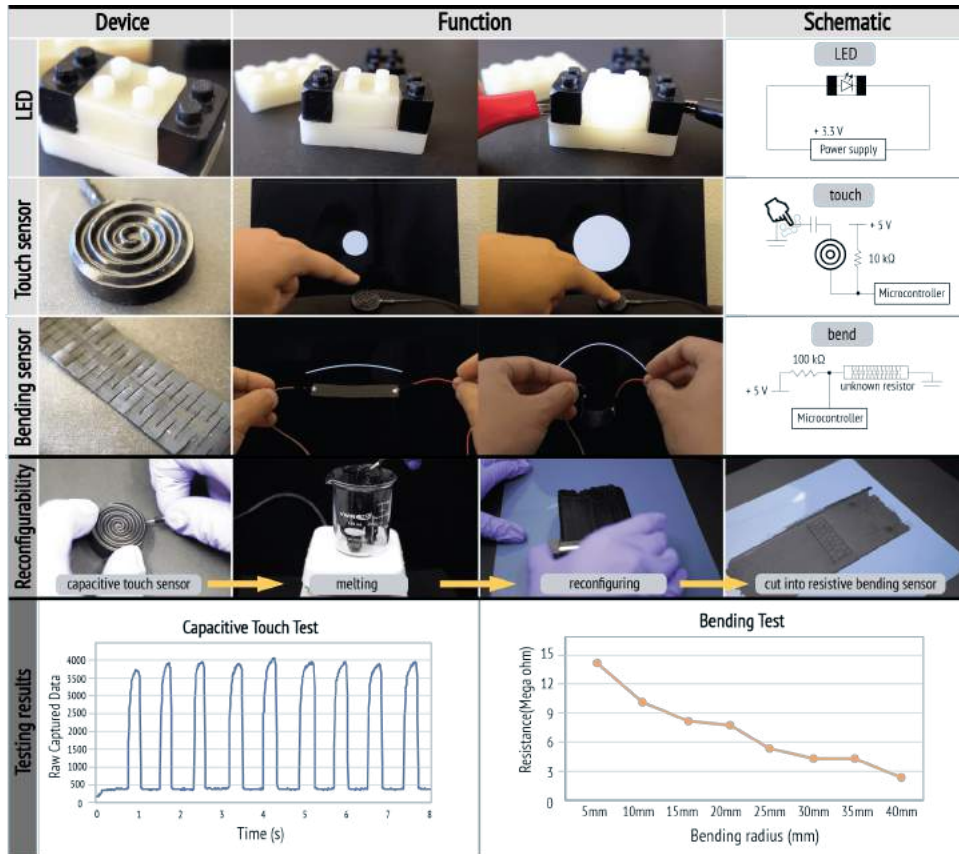


Figure 6.10: Demonstration of the devices made out of the beeswax-graphite composite and the re-configuring process including (1) an LED, (2) a capacitive touch sensor, (3) a resistive bending sensor with digital output displayed in background, Row 4: re-configuring process for the conductive beeswax sensors, and Row 5: the capacitive touch and bending test results.

Sensing Library. Wax itself is not typically bendable in its commonly used bulky form factor, but here we use a 1000-micron film applicator to make thin-sheet wax and manually cut it with kirigami cuts to make it more flexible. We showcase this bending sensor in the third row of Figure 6.10, where the resistive changes are read from a voltage-dividing circuit connected to an Arduino. Another exciting feature of these interactive devices is their recyclability. As seen in the fourth row of Figure 6.10, each device can be melted and re-shaped into forms with different functionality. For example, we melted a capacitive touch sensor and re-cast the material into a resistive bending sensor. Besides the compostable nature of beeswax and graphite, this recyclability feature adds a new layer of sustainability

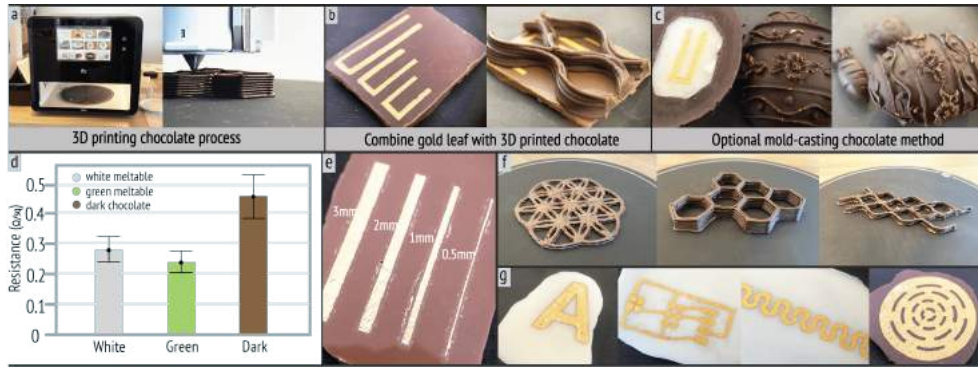


Figure 6.11: Overview of the chocolate-based edible electronics: (a) 3D printing chocolate. (b) Assembling the 3D printed parts with the edible gold leaf that creates the electrode. (c) Optional chocolate mold-casting method. (d, e) Basic resistance and resolution testing for applying edible gold leaf onto different chocolates. (f, g) Demonstration of versatile 3D printed chocolate geometries and laser-cut edible gold leaf.

to beeswax-based interactive devices.

Lastly, we evaluated the basic behavior of these touch and bending sensors. To test the capacitive touch sensor we used an Arduino UNO and the Arduino Capacitance Library to create a touch-sensitive button. To test the bend sensor, we measured the resistance change with a multimeter when a 7cm by 2cm sample with 50% graphite is put under different bending radii; as the bending radius increases from 5mm to 40mm, the resistance decreases from 14.5 $M\Omega$ to 2.1 $M\Omega$, accordingly.

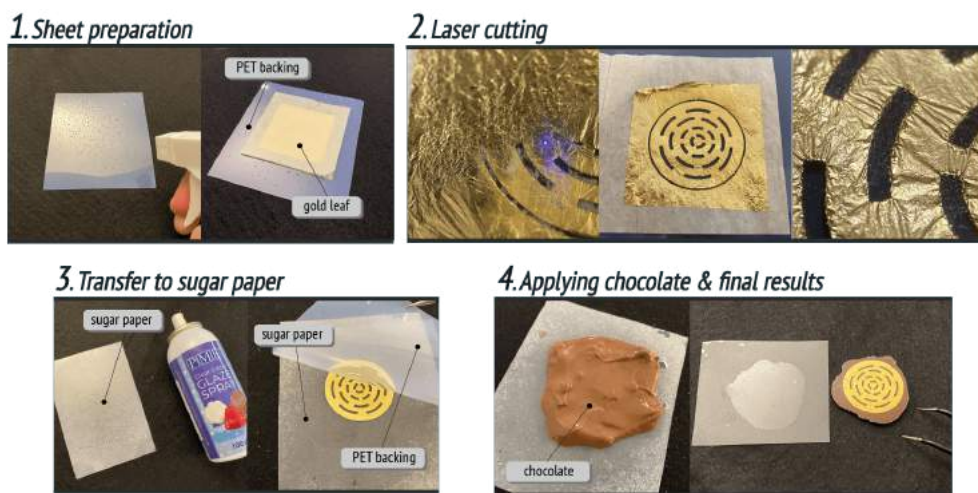


Figure 6.12: Detailed fabrication pipeline: 1) Sheet preparation, 2) Laser cutting/etching, 3) sugar paper transferal, and 4) final chocolate transfer steps.

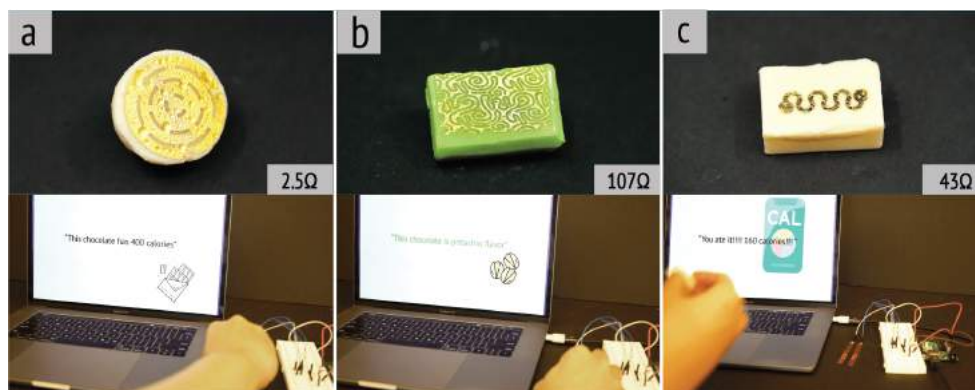


Figure 6.13: (a) The circular pattern can be read to provide the calories contained in the chocolate. (b) The mesh pattern can be read to provide the chocolate flavor. (c) The wavy pattern can be read to confirm the presence or consumption of the chocolate.

Wearable and implantable electronics are drawing increasing attention due to their broad applicability, like health monitoring (*e.g.*, diagnostics, therapy), decoration (*e.g.*, color-change, LED) or access/device control (*e.g.*, RFID, input touchpad/slider) [24]. Edible electronics are of particular interest to us in this work due to the destructive nature of the digestive process [145, 146]. Our third approach for functional destruction combines edible gold leaf as an electrode material with 3D-printed chocolate for edible electronics, which can be used to destroy sensitive information stored on the electronics during digestion. Printed chocolate, along with being a popular snack, can contain identifiable information (*e.g.*, access control with RFID) for users to obtain temporary access to areas or objects, which can be eaten and therefore destroyed when no longer needed. In Figure 6.11a and b, we show how we can apply gold leaf to flat chocolate and then use a food 3D printer to print arbitrary shapes on top. Alternatively, as shown in Figure 6.11c, one can also use food mold-casting to construct the electronics-embedded chocolate. Our example utilizes a flat white chocolate surface exposed to the gold leaf pattern through mold-casting.

As described in [146], several material options can be used as edible electrode materials (*e.g.*, gold leaf, activated charcoal, carbonized cotton). In this proposed method, we used edible gold leaf [147] as our electrode material. The fabrication challenge comes from the ultra-thin nature of the gold leaf and its sensitivity to static charges, which makes the gold

leaf difficult to manipulate. Several previous HCI papers demonstrated how to use tattoo paper or toner to form the edible gold leaf into shapes [148, 24], but inevitably involved non-edible materials in the fabrication process. We first tested several edible glues to adhere gold leaf, but because of the low adhesion, the resolution suffers. For this reason, we developed a laser-based fabrication pipeline to pattern the edible gold leaf with any arbitrary shapes. As shown in step 1 of Figure 6.12, the gold leaf adhered to a PET sheet with some water; this PET sheet is utilized as the substrate throughout the fabrication process to keep the gold leaf flat. We then used a laser cutter to either directly vector cut the contour of the design or engrave away the unwanted areas. We mainly implement this step by using the Laser Pecker Pro L1, which is a low-cost personal laser cutter [149], but any laser cutter can be used. After we obtain the gold leaf with the desired pattern, we utilize commercial sugar paper as a transfer medium. We use a spray glaze to add adhesiveness to the sugar paper before transferring the gold leaf. After the gold foil pattern is transferred to the sugar paper (as shown in the third step of Figure 6.12), we apply hot chocolate onto the gold leaf side. Finally, when the chocolate has cooled, we can peel it off from the sugar paper. The results of our initial testing of this type of device (*i.e.*, resistivity, resolution) are included in Figure 6.11d and e. We measured and report the sheet resistance when the edible gold leaf is applied to three different chocolate substrates: white meltables, green meltables, and dark chocolate (90% Cocoa), where we achieved 0.28 Ω/sq , 0.23 Ω/sq and 0.45 Ω/sq respectively. We tested 10 samples with dimensions of 3cm by 0.3cm using a two-probe setup. We also determined the thinnest trace we can achieve through the laser-transfer process is 0.5mm wide. Additionally, we demonstrated several edible gold foil patterns transferred to different chocolates (shown in Figure 6.11g).

As 3D food printers are becoming more available, we believe combining 3D-printed chocolate with the transferred edible gold foil could create new opportunities for edible electronics. We investigated by using a Foodini commercial food 3D printer to print versatile 3D chocolate shapes which can be easily combined with the edible gold foil. As shown

in Figure 6.11f, we showcased several chocolate designs that are 3D printed, which can be assembled with edible gold foil. For example, in the second picture of Figure 6.11b, we have added a wave 3D printed chocolate design to the edible gold foil.

With different edible conductive patterns formed on chocolates (shown in Figure 6.13), we demonstrate how information can be encoded. For example, the circular pattern shown in Figure 6.13a has resistance around 2.5ω ; when this specific resistance is looped in the circuit, the system recognizes the value and looks up the calories contained in the chocolate. Similarly, flavor (in this case, pistachio) can be indicated when a different resistance (107ohm) is connected to the system (Figure 6.13b). Another approach is the recognize the lack of chocolate, which we've done with the wavy pattern (shown in Figure 6.13c); here, the circuit being broken indicates the chocolate has been taken for eating; this can be extended to detect how much of the chocolate is left, where the trace changing as bites are taken predictably changes the resistance. These demonstrations are based on Arduino UNO and a simple voltage divider from which we can measure the different resistance of each gold leaf pattern when make contact with two copper tape electrodes we placed on the table. Note that for this demonstration, the sugar paper transfer shown in Figure 6.12 step 3 has been replaced with a more laborious manual transfer process which may be used when direct contact with the foil is required.

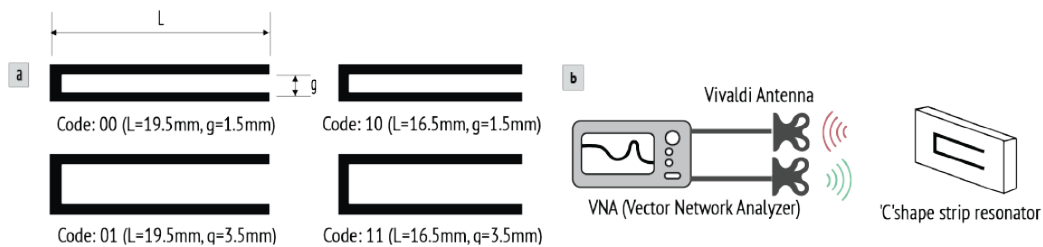


Figure 6.14: (a) Four code primitives designed by Vena et al. [150], where we demonstrated Code '01'. (b) Our experimental setup.

6.5 Fully Passive, Chipless RFID Implementation

We have demonstrated three approaches for making transient devices with a wide range of sensing and input functionality triggered by their destruction. However, all of these devices required a physical connection to an external system that can provide the necessary intelligence and power to make these devices functional. For example, the water-leakage sensor design in Figure 6.5 is connected using silver epoxy and two copper wires, and the current configuration requires a consistent power supply for operation. To address this issue, we created a *chipless RFID tag* using a simple "C" shape to eliminate the need for additional connections or wires and enable fully passive operation of the transient electronic sensors.

6.5.1 Principles of Chipless RFID

The basic operating principle of RFID is that an antenna transmits a radio signal to a tag and measures the reflected signals. In most commercial cases, the tag controls the shape of the reflected waveform using a tiny chip [151]. However, unique antenna patterns based on time- or frequency-domain reflectometry can also change the reflected waveform and eventually eliminate the need for a chip [152]. By doing so, such RFID tags can be easily printed and destroyed in an eco-friendly manner. Among various tag data encoding methods (*e.g.*, on-off keying, phase modulation), we chose a hybrid coding technique that changes the magnitude of the resonance peaks in the radar cross section (RCS). Vena et al. designed C-shape metallic strip resonators (which we will refer to as our "C" shape resonator) that can resonate between 2.5 GHz and 7.5 GHz. This design allows us to encode 22.9 bits in a dimension of 2 cm x 4 cm through absence/presence and frequency shift coding techniques [150, 153]. We selected one of Vena et al.'s code primitives *01*, shown in Figure 6.14a, since it can be easily differentiated among all the primitives. Thus, we integrated it into the three substrates (*i.e.*, PVA film, beeswax, and chocolate) proposed in this work. Although

we examine only one primitive type, it allows us to confirm the potential of our proposed technique for other primitive code types as the detection mechanisms are identical.

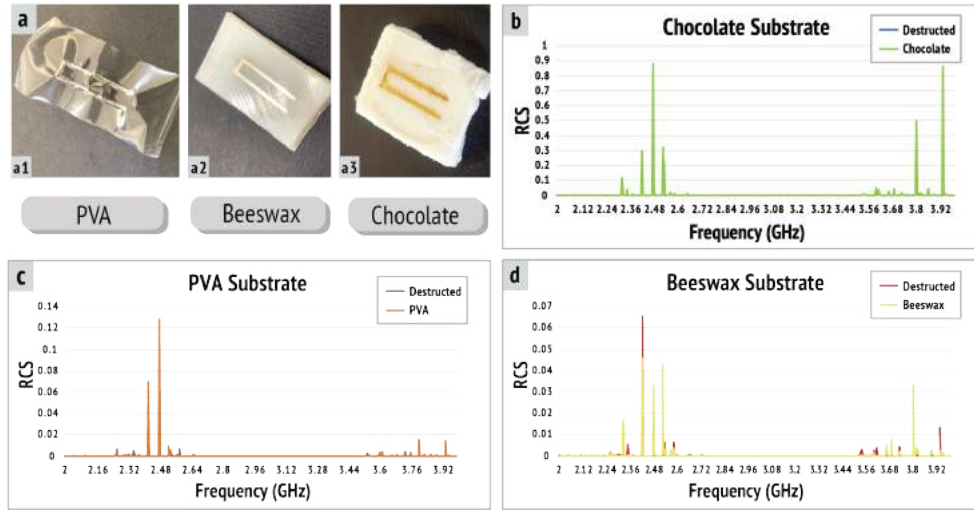


Figure 6.15: (a) "C" shape resonator design on PVA, beeswax, and chocolate substrates. (b-d) RCS measurements results.

6.5.2 Experimental Setup

In our experiment, we used a LibreVNA Vector Network Analyzer(VNA) that provides a 100kHz to 6GHz ultra-wide frequency range. This VNA has two ports—one to transmit RF signals and another one to receive its reflected waveform, and we connected two directional ultra-wideband Vivaldi antennas (appliedEM UWB400-D) that can be operated from 400 MHz to 8 GHz with a gain of 9.6 dBi. In order to recognize the code *01*, it was necessary to measure the frequency range of 2-4 GHz [150]. We were able to analyze the RF signals in that frequency band through this VNA-antenna combination. The transmit power delivered by the VNA is 0 dBm, and the received signals in frequency were recorded while placing the three tags (*i.e.*, b-d in Figure 6.15) at a distance of 45 cm from both antennas as shown in Figure 6.14e. Vena et al. evaluated this chipless tag design inside an anechoic chamber but also argued that the tag can also be evaluated outside the anechoic chamber if all environmental static noise can be removed. Thus, targeting real-world environment conditions, our testing setup is in a normal single room and we measured the reflected RF waveform,

the so-called complex S_{21} parameter, a total of three times in three conditions: 1) $S_{21}^{isolation}$ means the reflected RF waveform without any objects, 2) S_{21}^{ref} means with a metal sphere as a reference object, and 3) S_{21}^{tag} means with the three tags (*i.e.*, (b)-(d) in Figure 6.14) designed in this study. With this measurement, the complex RCS value of the tag, σ^{tag} can be obtained using the following equation,

$$\sigma^{tag} = \left[\frac{S_{21}^{tag} - S_{21}^{isolation}}{S_{21}^{ref} - S_{21}^{isolation}} \right] \cdot \sigma^{ref}$$

where σ^{ref} is the complex RCS value of the metallic sphere that is equal to πr_{sphere}^2 .

6.5.3 Results

In the theoretical analysis, the code *01* was expected to present a resonance peak at 2.5 GHz. Vena et al. implemented this code with one layer of copper conductive trace and FR-4 substrate with a thickness of 0.8 mm and empirically confirmed the peak at the target frequency range. Although we changed the material of the conductive trace and substrate, we also confirmed the peak of the reflected waveform at a similar frequency, 2.48 GHz as shown in Figure 6.15. Note that the plots in Figure 6.15 can also be presented in a logarithmic scale as the unit of dBsm, but this representation may visualize insignificant waveforms. Compared to the destroyed tags, we observed significant changes in the tags manufactured with a PVA film and with chocolate. Although the tag made with beeswax returned the weakest signals, we were able to recognize the difference before and after destruction by focusing only on the changes around 2.48 GHz. As presented in Figure 6.15, we used Mitsubishi silver nano-particle ink (NBSIJ-MU01) on PVA substrate, the same Mitsubishi ink on beeswax substrate presented in section section 6.3 and edible gold foil for the chocolate substrate in section section 6.4. Because of the higher conductivity of the gold foil, the RCS values in Figure 6.15c were much higher than the others. Note that we turned off all wireless devices in the area during the measurements. However, we were not able to completely control other wireless devices (*e.g.*, Wi-Fi access point, Bluetooth

devices) in adjacent houses. The RF signals from such devices may induce a measurement error.

The implementation of the resonator on three substrates is not aiming to deliver a novel RFID design, but rather a natural approach to further leverage the sustainability of our three applications and other similar transient devices. For example, in our PVA-based water leakage sensing example shown in Figure 6.5, the system setup requires a micro-controller and voltage divider constantly powered and connected through conventional metal wire. This does not only limit the design space of this sticker type of sensor but also counters our vision of sustainable transiency. However, with this passive RFID approach, we envision users can easily attach the PVA-hydrogel patch with a printed "C" shape resonator design to the areas which might have potential water-leakage risk without worrying about the wire connection and power supply to every device. Similarly, the current configuration for the chocolate example (Figure 6.13) requires extra hardware, which is not feasible for any applications within our body. Our chipless RFID design may help signal the destruction of the device during digestion. Other potential applications might include encoding information through different resonator designs: for example, in the self-destroying beeswax-based, the LEDs which currently represent information can be replaced with new resonator primitives to encode different information.

CHAPTER 7

RECY-CTRONICS: DESIGNING FULLY RECYCLABLE ELECTRONICS WITH VARIED FORM FACTORS

7.1 Introduction

The aspiration for 21st-century computing is its seamless integration into our everyday life (*e.g.*, smart lock, smart home hub), a vision steadily coming to fruition with the proliferation of today's computational devices, serving users both locally and through the internet. However, the current landscape of connected devices (an average of 22 per U.S household in 2022) and global e-waste (53.6 million metric tons (Mt) by 2020) paints a bleak picture. The rapid expansion of IoT (Internet of Things) devices has resulted in environmental hazards surpassing our capacity to manage them sustainably. At the same time, as we venture into emerging fields like AI (Artificial Intelligence) and strive for fully immersive user experiences, the number of devices and subsequent waste will only escalate. Estimates indicate IoT devices could reach a trillion by 2035. This raises concerns of how to handle the disposal of these devices when they eventually become obsolete or malfunction. Addressing these questions is essential to building a sustainable future where technological advancement aligns with responsible environmental practices.

Human-Computer Interaction (HCI) has a long history of prototyping various interactive devices, with a recent rise in promoting the development of sustainable ones. Traditionally, a significant portion of interactive devices rely on plastic housings (*e.g.*, ABS, HDPE), conventional PCBs with FR4 and SMD components, and batteries containing harmful elements like lithium and lead. Improper processing or disposal of these components can pose serious environmental hazards, contributing to plastic waste, E-waste, and lithium battery pollution. Recognizing the environmental impact, researchers in HCI have been ac-

tively advocating for sustainable practices and reducing reliance on conventional materials in device manufacturing. For example, researchers have proposed transient and decomposable devices with more sustainable material options, such as chitosan or beeswax to make wireless charged heater [82] or transient sensors [4]. The focus of these works lie in transiency and biodegradability, prioritizing environmental sustainability over functionality or longevity.

In this work, we develop and integrate a set of materials, fabrication tools, and manufacturing processes to enable the accessible fabrication of recyclable electronic interactive devices. The disintegration of the electronics is not viewed as the end of the the lifespan of the constituent materials; rather it marks the beginning of another circuit’s physical and functional creation. Our aim is that these devices are designed for recycling efficiency—unlike traditional electronics—eliminating the need for sophisticated machinery or intricate chemical processes. To this end, we have chosen commercially available room-temperature liquid metals (RTLMs), particularly eutectic gallium-indium (EGaIn) —known for their conductive properties— and poly(vinyl alcohol) (PVA) —as both substrate and encapsulation materials —in the creation of recyclable electronics.

Our innovations extend beyond traditional thin-sheet electronics, introducing three distinct form factors: sheets, foam, and tubes. We also introduce design strategies to customize devices’ mechanical properties, ranging from rigid sheet electronics to flexible, compressible interactive foams, as well as highly stretchable tube sensors and actuators. Each form factor is tailored to meet different application needs while ensuring complete recyclability, showcasing our commitment to reducing electronic waste through innovative design and material selection.

The main contributions of this work are:

- Integration of PVA and LM to enable the creation of fully and easily recyclable electronics across three distinct form factors: sheet, foam and tube.
- Introduction of a formulation facilitating the production of three types of recyclable

electronics with various properties: rigid, flexible, and stretchable .

- Development of a process recycle three different forms of electronics with high recycling rate.
- A life cycle assessment (LCA) case study for the recyclable sheet-based proximity sensor, validating the approach's efficacy using industry standard tools.

7.2 General Recy-ctronics Design Rules

Electronic devices have become pervasive in our daily lives, offering convenience while also giving rise to an inescapable tension between the rising quantity of these devices and the resulting waste they generate at the end of their life cycle. A central challenge in the realm of electronics recycling today stems from the prevailing focus on functionality, durability, and affordability during device creation, often at the expense of considering their sustainability at the end of their lifespan. Many devices were designed without prioritizing characteristics like "ease of repair" and "recyclability." In this section, we set three general design criteria for Recy-ctronics.

1. *Recyclability over functionality*: To enable "greener" electronics, we will prioritize materials selection, fabrication approaches that can ensure easy, high rate recycling process, but meanwhile secure devices' functionality.
2. *Versatile form factors and mechanical versatility*: We aim to use recyclable materials to enable a wide range of electronics including form factors and mechanical properties.
3. *Highly accessible approaches and tools*: For Recy-ctronics, to support a broad spectrum of users, we expect our materials and tools selection can be low-cost, off-the-shelf parts, and easy to use.

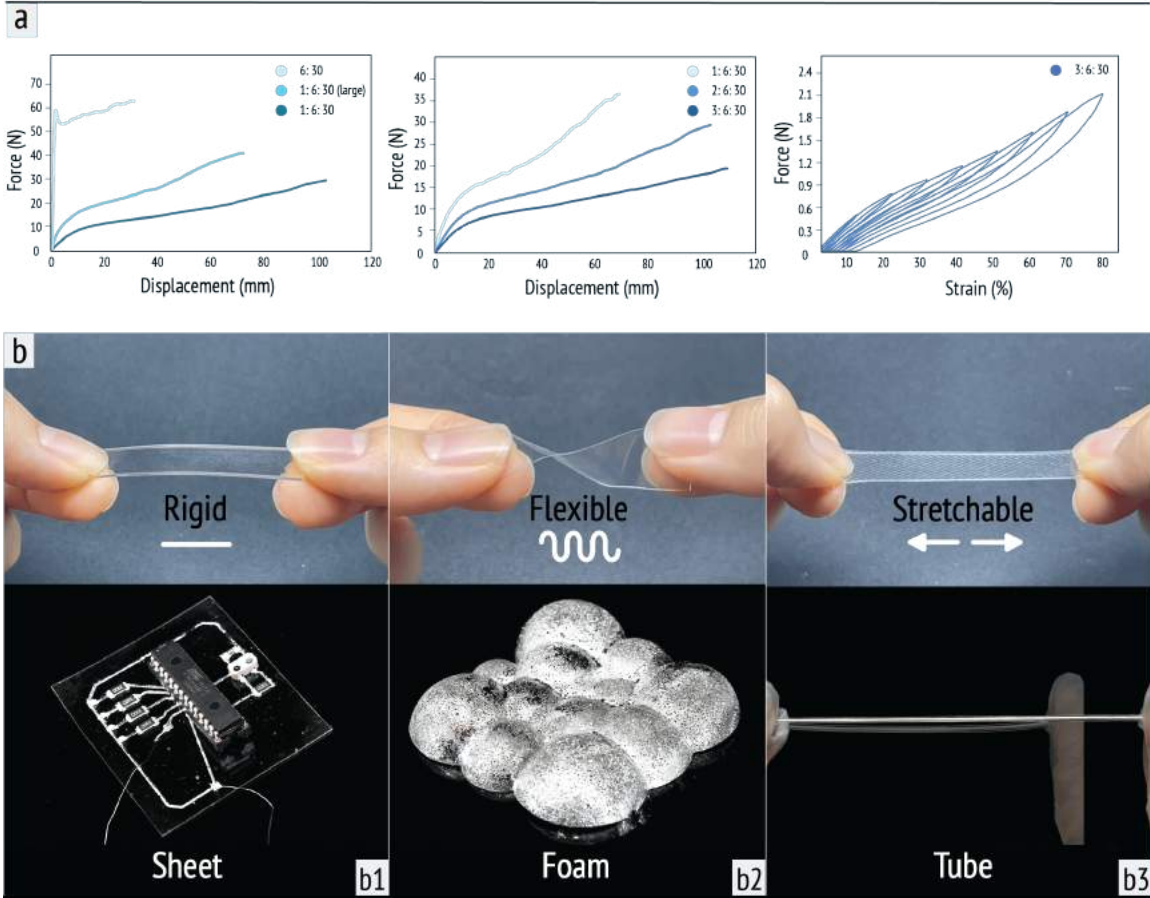


Figure 7.1: General design strategy. (a) Load versus strain curve under uniaxial deformation for different types of PVA and Cyclic loading to increasing strains as a function of strain. (b) Demonstration of PVA's mechanical flexibility (rigid, highly flexible, stretchable) for versatile types of devices (sheet, foam, tube).

7.2.1 Recycling approach for Recy-ctronics

The definition of electronics recycling nowadays is indeed broad, which mainly referred as e-waste recycling, pertaining to the retrieval of valuable materials and components from discarded electronic devices. However, when viewed through a more fundamental material lens, recycling processes can be further classified based on whether the items retain their original functionality. Recycling plastics as an example, approximately a decade ago, diverse strategies for recycling plastics were grouped into different categories: 1) primary, 2) secondary, 3) tertiary, and 4) energy recovery [154]. Primary recycling mainly involves

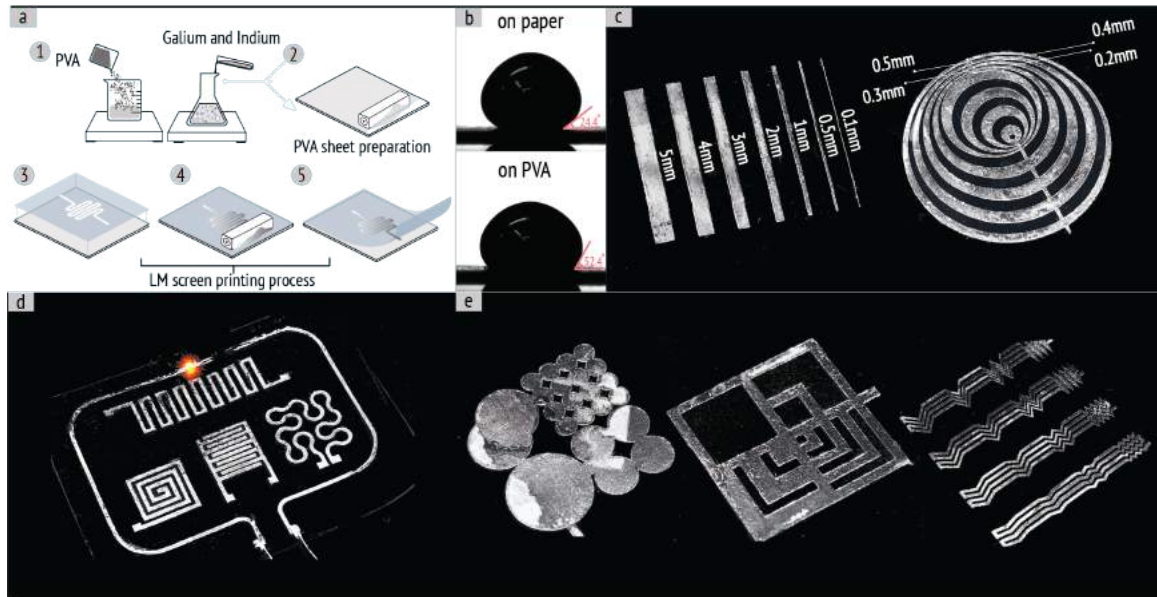


Figure 7.2: Sheet fabrication and basic characterization. (a) Fabrication process for making recyclable electronics with thin-sheet form factor. (b) Contact angle between LM and different substrates. (c) Resolution testing for trace width and gap width. (d,e) Different device and pattern design primitives.

reprocessing materials to generate substances with the same intended function. In contrast, secondary recycling yields materials repurposed for uses differing from the original plastic, often referred to as "downcycling". Tertiary recycling predominantly employs chemical processes, encompassing methods like hydrolysis, pyrolysis, hydrocracking, and gasification, to recover individual components or monomers. This approach presents opportunities for "upcycling" the original materials, leading to the production of potential higher-grade products. The fourth method, energy recovery, also termed quaternary recycling or incineration, involves harnessing heat as a form of energy recuperation. Recy-ctronics focuses mainly on primary and can be extended to secondary recycling processes. This means prioritizing electronics that can be recycled while retaining their initial functionality, with minimal or controlled levels of impurities. Of particular significance is our emphasis on facilitating recycling ease without any complicated procedures or chemical involvement, which can greatly enhance electronics prototyping experience [155].

7.2.2 Versatile electronics from simple materials

Electronics encompass a spectrum of components including semiconductors like silicon, metals like copper and gold, plastics, ceramics, glass, and rare earth elements. These materials are combined to form structures such as printed circuit boards (PCBs), connected by solder joints and powered by battery systems. Each component's characteristics, encompassing materials, shapes, and sizes, exhibit variations. In this work, Recy-ctronics not only highlights ease of recycling and the quality of recycled materials, we also emphasize the flexibility, which we mean the capacity of materials to be adapted into diverse interactive devices.

Polyvinyl Alcohol (PVA) stands as a synthetic polymer originating from vinyl acetate, synthesized via a distinct polymerization process. Unlike conventional polymerization routes, PVA emerges through the dissolution of polyvinyl acetate (PVAc) in alcohol like methanol, followed by treatment with an alkaline catalyst such as sodium hydroxide. This unique process grants PVA remarkable attributes including high water solubility, adeptness in forming films, and recyclability [156]. These qualities have made PVA to be a favored material for transient electronics, serving as substrates and encapsulation mediums [157], which also made us to choose PVA as the main material for Recy-ctronics. Besides the easy-to-dissolve nature of PVA, the mechanical versatility of PVA is also another key factor. As illustrated in Figure 7.1 a, showcasing how we can tailor the mechanical property of PVA through the simple adjustments in material composition and fabrication approaches. In general, for making PVA based substrates, a blend of glycerol/glycerin, de-ionized water, and PVA powder constitutes the primary components. Each component plays a different roles to enable diverse material properties.

As shown in Figure Figure 7.1 a, we have conducted a series of tests on diverse PVA samples with varying compositions. As shown in the first graph of Figure Figure 7.1 a, if with the same recipe (glycerin: PVA: de-ionized = 1: 6: 30), PVA featuring a higher molecular weight (*i.e.* M.W. 88,000-97,000) exhibits a higher elastic modulus, ultimate stress,

and meanwhile demonstrates lower stretchability. Interestingly, within the same figure, if no glycerin is added, PVA behaves as non-elastic materials with clear yield stress and much higher Young's modulus, makes it a great option as rigid sheet material. Additionally, the overall stretchability can be augmented by increasing the proportion of glycerin, which is a typical plasticizer, during the PVA mixing process. As shown in the second graph of Figure 7.1 a, it is clear when more glycerin is added to the system, more elastic and "softer" the material will become. Furthermore, on the right side of Figure 7.1 a, we have carried out a cyclic testing for PVA samples with a recipe of glycerin: PVA: de-ionized water ratio of 3: 6: 30. The sample underwent two cycles of increasing strain levels: 10%, 20%, 30%, 40%, 50%, 60%, 70%, and 80%. These tests revealed minimal plastic deformation of the sample during the process. All the testing specimen were prepared in dog-bone shape (ASTM D412A) and tested on a materials testing machine (Instron Universal Testing Systems 68SC-05) at a strain rate of 20mm/min.

In this section, we aim to provide a simple strategy to easily tailor the mechanical property of PVA, which is a crucial step to enable a wide range of devices and applications. In general, shown in Figure 7.1 b, by varying the composition of PVA, one can achieve electronics materials from rigid, to flexible to highly stretchable. This high tun-ability can also favor different forms of interactive devices we aim to make. For example, for making sheet-based electronics, more rigid and non-elastic recipe can be used, while for fabricating foam-based electronics, we will mostly use flexible recipe to enable the compressing behavior for foams and for tubes we prefer more stretchable recipe due to the typical stretchable application domains for this specific form factor.

7.3 Sheet

Even in today's electronics landscape, various form factors are present, yet planar geometry remains as the main form factor (PCB board). Our initial exploration centers on exploring using Recy-ctronics approach to make some of today's electronics more sustainable. As

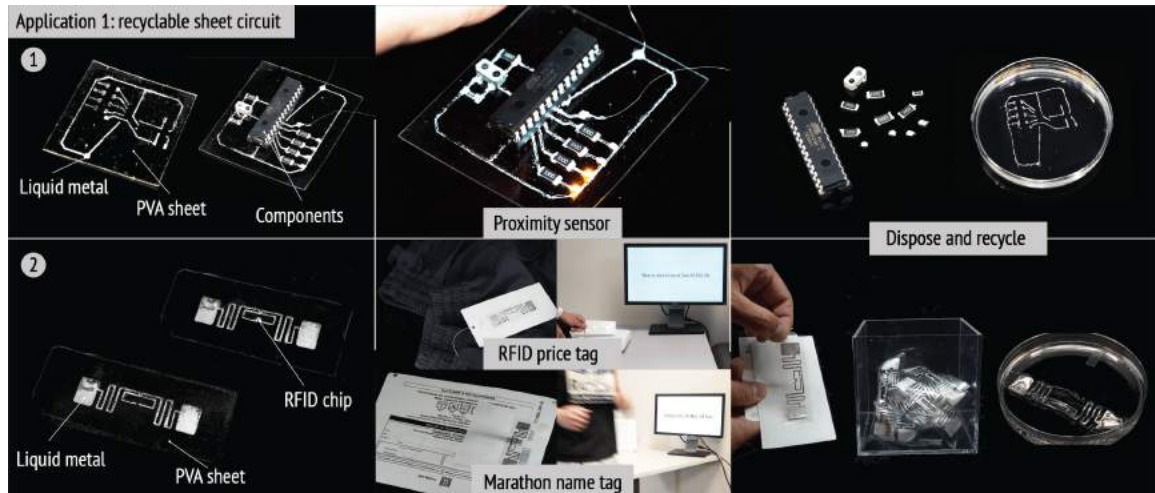


Figure 7.3: Sheet application. (1) Recyclable Sheet-based proximity sensor that responds to finger position. (2) Recyclable RFID tag used in two different application scenarios, including recyclable RFID clothing price tags and marathon RFID tracker. Both the proximity sensor and RFID tags are collected and recycled.

shown in the initial step of Figure 7.2 a, both PVA and LM are prepared through mixing and stirring processes. In the formulation of PVA, a blend of glycerin, de-ionized water, and PVA powder constitutes the primary components. For crafting flexible and moderately stretchable thin sheets, a typical recipe involves a glycerin: PVA powder: de-ionized water ratio of 1: 6: 30. The LM involves the combination of pure Gallium and Indium in a weight ratio of 3: 1. Employing a magnetic stirrer (Thermo Scientific Cimarec stirring hot plate), PVA is subjected to mixing at 80°C for approximately 2 hours, while LM undergoes a 160°C overnight stirring process. Once both materials attain the desired state, a film applicator (GLTL four-sided coating applicator) is utilized to form a PVA film. This film is allowed to cure either at room temperature overnight or in an oven for 4 hours at 60°C depending on thickness. Subsequently, a stencil (Selizo low tack transfer paper) is applied to the PVA sheet, onto which LM is evenly brushed with the assistance of a rubber roller. The stencil is removed post circuit completion (shown in Figure 7.2 a). We conducted preliminary tests to examine the printing resolution for trace and gap widths, achieving a minimum trace width of 0.1mm and a smallest gap width of 0.2mm (Figure 7.2

c). Moreover, we present several printed electronics device design- LED, inductor, capacitor and heater pattern (Figure 7.2 d). We have also explored some pattern designs including interconnected circles, squares and waves with different density—showcasing the design and fabrication potential inherent in the utilization of PVA and LM (Figure 7.2 e). It also shows great adhesion and intrinsic mechanical compatibility between PVA and the room-temperature LM. Usually, because of the high surface energy of LM, it barely get attached to other surfaces. As shown in Figure 7.2 b, the contact angle of PVA and LM is $52.4 \pm 4.2^\circ$ (ramé-hart Contact Angle Goniometer), indicating a relatively good adhesive between PVA and LM, and as a comparison, the contact angle between LM and the copy paper is also measured, which is much smaller ($24.4 \pm 2.5^\circ$). With this great adhesion between LM and PVA sheet, we have also achieved a sheet resistance of $0.013 \pm 0.002 \Omega/\text{sq}$, where 20 samples with 40cm by 0.5cm dimension were tested (B&k Precision 891 LCR Meter).

7.3.1 Application 1: Recyclable Sheet Electronics— from multiple components to minimal components

Our primary goal is to enable the transformation of the current Printed Circuit Boards (PCBs) into easily recyclable alternatives using PVA and LM. In this section, we highlight two distinct circuit designs to demonstrate the versatility of Recy-ctronics in prototyping electronics with varying component complexities—from those with many components to those with minimal components.

As shown in the top row of Figure 7.3, we first introduce a proximity sensor circuit featuring an OPB733TR, which integrates both an infrared LED and an NPN phototransistor. This sensor activates additional LEDs as a hand or object passes over it, with the lights dimming once the object is removed. This interaction is managed by a standard Microcontroller Unit (MCU), specifically an ATMEGA328P-PU. To enhance compatibility with the sheet circuit, a socket is added for the MCU, ensuring a flat connection between the MCU and the sheet substrate. This assembly is bonded using commercial silver epoxy.

This particular circuit design incorporates twelve electronic components in total, including the phototransistor, the MCU, four Surface-Mount Device (SMD) LEDs, and six SMD resistors. The PVA substrate used in this specific circuit design has a dimension of 5.5cm x 4.5cm x 0.5mm, made from a mixture excluding glycerin (PVA: de-ionized water = 1: 5). Also, all components are designed for easy disassembly and reuse, and the substrate dissolves entirely in water within ten minutes, enabled by the PVA circuit's recyclable nature (shown on the right side of Figure 7.3).

Besides the proximity sensing circuit which can exemplify most of today's circuit, there are also electronics that with minimal to no components, but serving crucial role in our everyday life. Passive RFID technology is one typical example, which has gained widespread adoption in various everyday scenarios (such as key fobs, door access, chipless payments, etc.), primarily due to its technological benefits. Firstly, it operates without the need for a battery. When an RFID reader is in proximity, the tag becomes instantly powered, enabling it to transmit the data stored within it back to the reader. Secondly, its design is notably slim, enabling seamless integration of the RFID tag into thin and flat devices (like clothing price tags, apartment key fobs, etc.). Lastly, the production cost of the RFID tag is very economical, facilitating large-scale manufacturing. These benefits make RFID not only a promising commercial product in almost all industry branches, also draws attention in using RFID for interaction, including tracking 20 objects and identifying their movements [158], utilising RFID to build interaction with smart devices [159].

However, the widespread adoption of RFID tags has also brought about concerns regarding their end-of-life waste management. Recent research highlights that selected logistics centers alone contribute to an annual generation of 5.7 tons of e-waste from discarded radio frequency identifiers on received pallets, with this waste containing 139 kg of metal components. Our primary objective is to address this issue by introducing easily recyclable RFID tags, specifically targeting two key scenarios. Illustrated in the second row of Figure 7.3, we have affixed recyclable ultra-high-frequency (UHF) RFID tags to clothing price

tags and marathon name tags. After these RFID tags have fulfilled their purpose, users can conveniently deposit them into designated collection bins (depicted in the third column of Figure 7.3), initiating a process of dissolution and subsequent recycling.

As shown in Figure 7.3, we fabricated the RFID tags utilizing PVA as the substrate, overlaying it with a LM pattern. Employing the Impinj Monza 4QT chip, which can either be retrieved prior to RFID device dissolution or recycled subsequently, added to the fabrication process. Our measurement approach employed an ultra-high-frequency (UHF) RF reader, specifically the Impinj Speedway R420 RFID reader paired with the Laird S9028PCR antenna, encompassing the radio frequency range spanning 902MHz to 958MHz. Leveraging the Octane SDK, we established a comprehensive system that not only reads UHF RFID tags but also furnishes pertinent feedback. As presented in the central column of Figure 7.3 b, we conducted replicative scenarios involving the utilization of our recyclable RFID tags in shopping and marathon runner information tracking. Remarkably, in both scenarios, the recyclable RFIDs consistently exhibited robust detectability by our reader systems. Also, the fabrication process is similar as the proximity sensor example. However, considering most of today's commercial RFID tags are in a more flexible form, so we fabricated the RFID on a more flexible substrate recipe (glycerin: PVA: deionized water = 1: 6: 30), which can be more conformally attached to the price tag or marathon name tag.

7.4 Foam

Besides sheet form factors, which is more of conventional form factor for printed circuits, foam, with its inherent porous composition and responsive elasticity, has garnered significant attention in HCI, offering diverse avenues for crafting interactive devices. Nakamaru et al. showcases foam devices coated with conductive ink, enabling volumetric alterations for detecting a spectrum of user inputs: compression, bending, torsion, and even shearing [160]. In this section, our study aims to use PVA and LM to enable fully recyclable

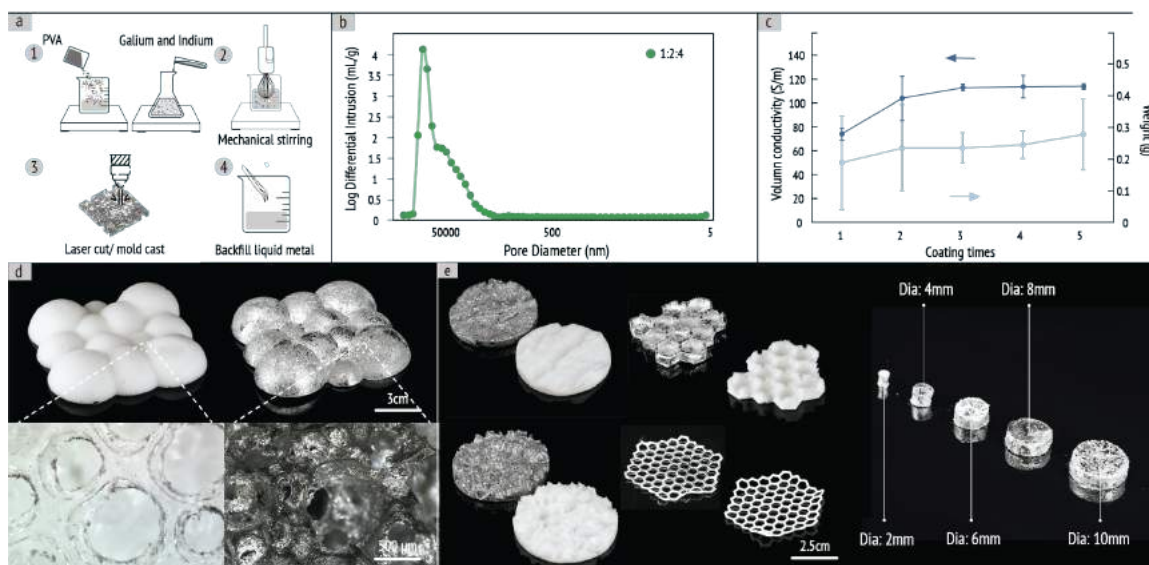


Figure 7.4: Foam fabrication and basic characterization. (a) Fabrication process for making recyclable foam electronics. (b) The pore diameter for the 1:2:4 foam recipe. (c) The conductivity testing for the interactive foam. (d,e) Different types and dimensions of recyclable interactive foams through mold casting or laser cutting.

interactive foam structures.

As shown in Figure 7.4 a, the fabrication process starts by preparing both the PVA material and LM. The sequential steps are similar to the ones described in the sheet fabrication section. However, a major difference arises in the formulation for PVA and how we coat the LM. To ensure the foam's stability during the curing phases of PVA, we reduce the use of water content coupled with an increased glycerin proportion. The main recipe we adopt in this study covers a blend of glycerin: PVA: de-ionized water in a ratio of 1: 2: 4. Once the PVA solution is prepared, a mechanical stirrer operating at approximately 2000rpm for 6 minutes serves to transform the PVA solution into a spongy and porous configuration. It's noteworthy that we had also tested adding nano-cellulose fibers (NCF) and surface surfactants (such as Sodium dodecyl sulfate) which can effectively maintain the structure of the recyclable foam during the curing process, meaning no foam bubbles will collapse during the curing step but will complicate the material synthesising and also the subsequent recycling process. After the complete drying process of the PVA foam, which is thickness

dependent (typically spanning 1 day at room temperature for a 2mm foam), laser cutting can be employed to shape the foam into versatile geometries. Concluding the process, as shown in Figure 7.4 a, step 4, the foam is immersed in LM, with an additional vacuum treatment to back-fill the LM into the foam's internal voids. Figure 7.4 b and c shows two testing results, including the pore concentration for the 1: 2: 4 foam, which is mainly around 55000nm (AutoPore 9520 Mercury intrusion porosimeter) and also the conductivity and weight changes across different back-fill times. It is worth noting that as we back-fill more times, LM will flow and attach to more voids within the PVA foam, making the foam more conductive. For shaping the foams into different geometries, not only laser cutting, foams can also be mold-casted, shown in Figure 7.4 d and e, we have introduced different recyclable interactive foams with various sizes, geometries or even surface textures.

7.4.1 Foam-based Electronics Primitives

Foam, with its unique bouncy property, can enable unique multifunctional sensing capabilities. Here, we present four innovative conductive foam designs. We initiated our exploration by showcasing a basic square foam configuration as a pressure-sensitive unit, which can detect different levels of user-applied pressures (Figure 7.5 a). This foam pressure sensor is able to distinguish between light, moderate, and firm touches. Different than this fully LM-soaked pressure sensor, in Figure 7.5 b, we introduce a selectively conductive foam. Here, we utilized laser cutter to cut the four corners of the foam, selectively immerse these units into LM to make them conductive, and then reattaching them back to the original piece by using PVA solution as glue. This device now functions as a controller, offering four distinct input options. Both the pressure sensor and controller implementations rely on self-capacitance mechanism and the Arduino CapacitanceSensor Library, with data acquisition handled by an Arduino UNO (shown in Figure 7.5 a and b), and $1M\Omega$ resistor was used in the RC circuit.

Expanding beyond capacitive sensing, we showcase a mechanical-contact based switch

in Figure 7.5 c, where we present a three-layer foam structure comprising a fully conductive top layer, an insulating middle layer, and a bottom layer housing two separated conductive components. Utilizing on foam’s exceptional compressibility, applying pressure to the top conductive layer will make contact with the two lower terminal layers which further completes a closed-loop circuit. This configuration has the potential to serve as a functional light switch. While bending sensors have been frequently explored, it becomes challenging for using highly conductive LM which has minimal resistance variance during bending. In Figure 7.5 d, thanks to the laser cutting approach, we try to overcome this challenge by laser-cutting a strain-gauge-like pattern to amplify resistance changes along the bending direction. Both the mechanical-contact switch and the enhanced bending sensor (Figure 7.5 c and Figure 7.5 d) are implemented using Arduino UNO and voltage-dividing mechanisms. We have also included the characterization data for both sensors on the right side of Figure 7.5 c and d.

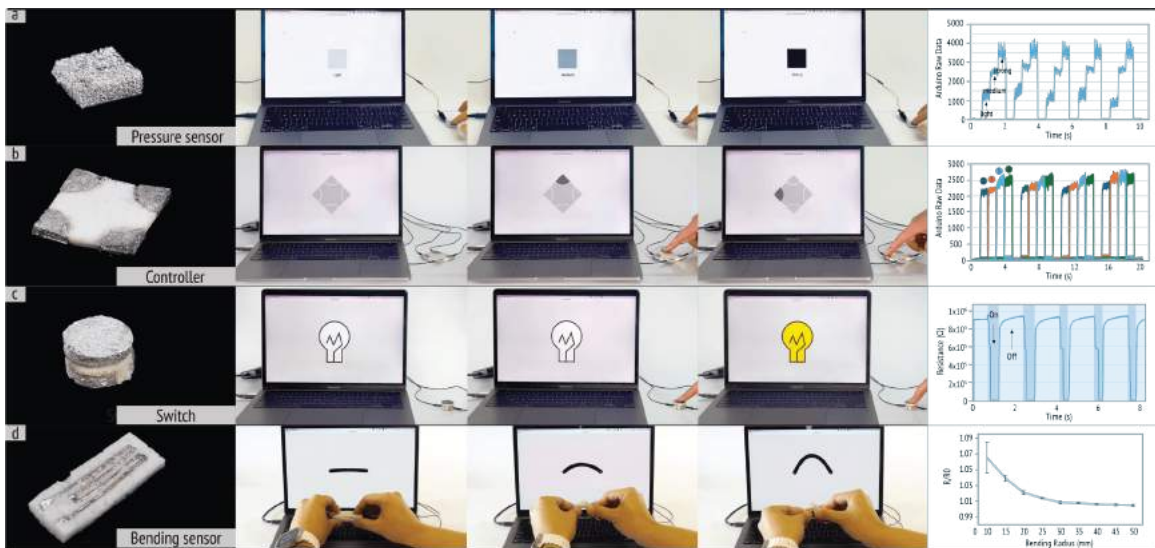


Figure 7.5: Foam sensing primitives. (a, b) Capacitive sensing based pressure sensor and controller and (c, d) Resistive sensing based mechanical contact switch and bending sensor.

7.4.2 Application 2: Recyclable Interactive Pen Tip

Foam has many distinctive qualities, encompassing its softness, cushioning attributes, and adaptability to the contours of objects or bodies. When interacting with foam-based devices, one of the most notable characteristics is the bouncy tactile feedback. Applying this mechanical property, we present an interactive pen featuring four distinct interactive and recyclable pen tips. We aim to address the existing gap in current drawing software, which typically offers a wide array of pen tools, while conventional interactive pens, such as the Apple Pencil, only provide rigid tips that do not replicate the tactile sensations associated with specific tools. As illustrated in Figure 7.6 a 1-4, we demonstrate four pen tips with varying foam properties designed to mimic the appearance of different drawing tools, such as a pencil, ballpoint pen, and brush. Also, we employed various formulations to create PVA foams with adjustable levels of hardness, enabling these four interactive pen tips to provide users with sensations closely resembling real pen tools. As shown in Figure 7.6 b, these pen tips can be affixed to 3D-printed pens, with a conductive foil and wire used to establish a capacitive coupling between the pen tips and the user's hand. The formulations utilized for creating hard, medium, soft and brush pen tips are as follows: glycerin: PVA: de-ionized water ratios of 0.5: 2: 4, 1: 2: 4, and 2.5: 2: 4, and 1: 2: 4 (small PVA molecules) respectively. We have also include the young's modules of these four different foams in Figure 7.6 c, showing their distinct hardness. It is important to note that only the pen tips are fully recyclable in this application, while the pen holder and the pen's body are 3D printed using black PLA materials.

7.5 Tube

Besides sheet and foam, Recy-ctronics is introducing a third form factor: tube. Tubes, tailored by their dimensions and diameter-to-length ratios, are versatile in applications, allowing for the creation of bending actuators [12] or integration into textiles for sensing

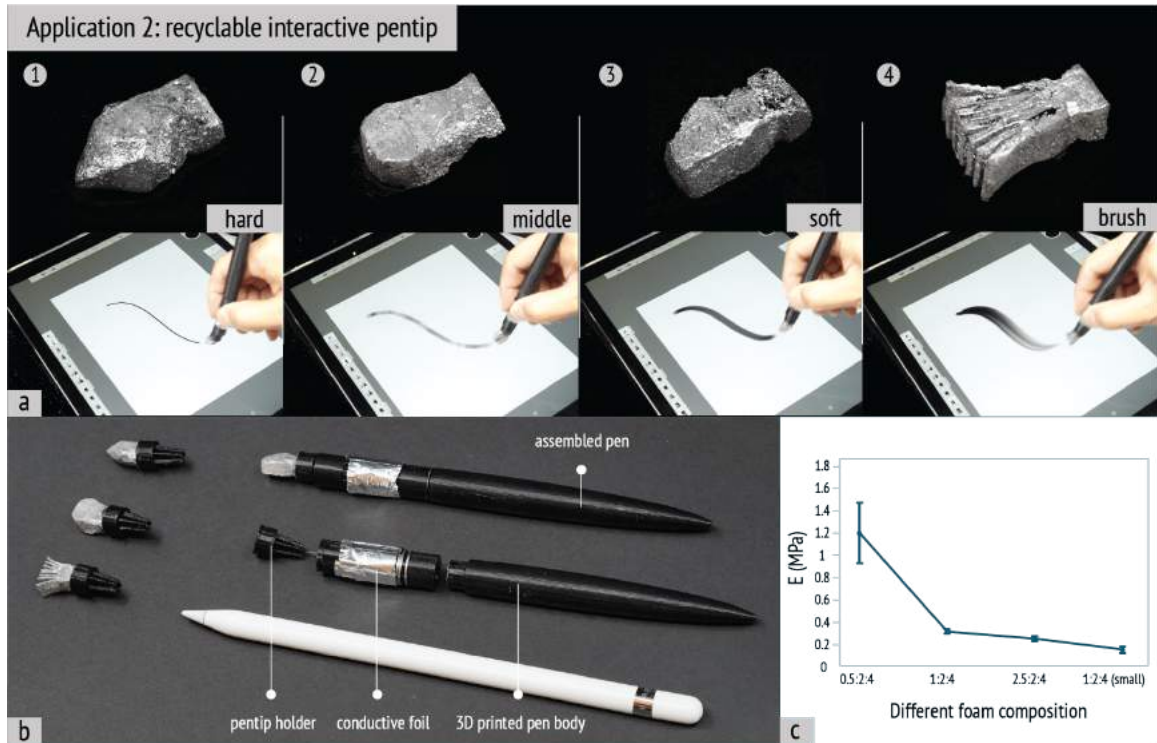


Figure 7.6: Recyclable interactive pen tip application. (a) From 1-4, we showcase recyclable interactive pen tips with different hardness and tactile feelings, from hard, medium, soft to brush feelings. (b) The disassembly look of the interactive pen for mobile devices with replaceable pen tips. (c) Young's modules for the foams with different material composition.

purposes [161]. This section focuses on utilizing PVA and LM-based tubes to develop various types of hand-weaving recyclable devices. The method for fabricating these recyclable tubes begins with the preparation of PVA solution and LM, similar to the processes for sheet and foam. We exemplify three different recipes for making different types of tubes in the third graph of Figure 7.7 f, where by varying the mix ratios, it is possible to produce tubes ranging from rigid and flexible to highly stretchable. While for most of the tubes used in this work, a mixture ratio of glycerin: PVA: de-ionized water = 3: 2: 3.5 is preferred for achieving high elasticity in this work.

The fabrication technique for tubes is straightforward, as illustrated in Figure 7.7 a. A simple casting method involves dipping a carbon fiber rod into the PVA solution. The process is complete once the PVA tube has cured and the curing time is similar to curing PVA

sheet which is also thickness dependent. As demonstrated in Figure 7.7 b, tubes of varying diameters can be produced by using carbon fiber rods of different sizes. Additionally, as shown in Figure 7.7 c, applying multiple layers of PVA allows for the creation of tubes with various wall thicknesses. While this tube casting method is limited to producing tubes up to one meter in length, corresponding to the length of our carbon fiber rod that is available, longer tubes can be fabricated by joining multiple tubes end-to-end. This is shown in Figure 7.7 d, where a 3-meter tube was assembled by connecting several tubes together by using PVA as an adhesive.

In this work, we present two types of tubes for making interactive devices: hollow tubes and LM-filled tubes. The stretchable LM-filled tubes can be utilised as strain sensors. Through experimentation, we detail the process by stretching these tubes to a 50% strain results in a resistance increase from approximately 0.74Ω to 0.82Ω (shown in first graph of Figure 7.7 f). Also, we explore the possibility of using LM-filled tubes for connecting LEDs. Unlike the circular tubes, we chose to use squared tubes that can align more compatibly with the geometry of standard SMD LEDs (as illustrated on the right side of Figure 7.7 e). Beyond sensors and LEDs which both rely on LM-filled tubes, we also showcased the application of using hollow PVA tubes in the development of recyclable pneumatic actuators. To enhance the functionality of these tube actuators, we add a constraining layer by using fishing lines, which will limit the axial tube deformation and only the longitudinal deformation is allowed. Besides, on the left side of Figure 7.7 e, we have investigated the design consideration for using tubes for fabricating devices. Tubes that are overly flexible with thin walls may easily get sharp bends, obstructing the flow of LM or air. Conversely, tubes that are too rigid pose difficulties in bending and integration into textiles, limiting their applicability in wearable technology and smart fabrics.

For building recyclable tube-based interactive devices, we present two applications. Firstly, we introduce a strain-sensor enabled haptic ring, as shown on the left side of Figure 7.8. This device comprises ten PVA tubes, each has 1.5mm in internal diameter (ID),

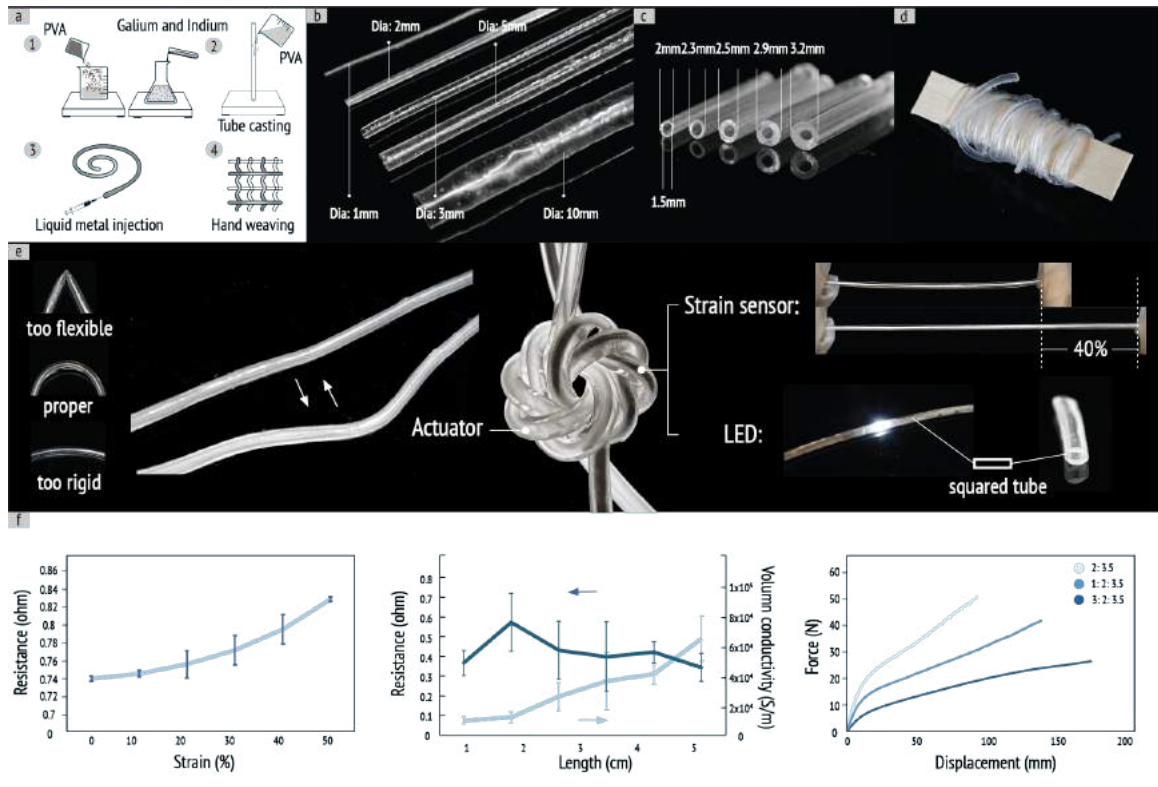


Figure 7.7: Tube fabrication and basic characterization. (a) Fabrication process for making recyclable tube electronics. (b-d) Recyclable tube with different diameters, wall thickness and length. (e) Three types of tube-based devices, including LED, sensor and actuator. (f) Basic electrical and mechanical testing results for tubes.

2.9 mm in outer diameter (OD), and 10cm in length. These tubes are hand-woven using PVA-based knots for secure connections. Five of these tubes are filled with LM, serving as strain sensors to detect users' finger movements. Additionally, a circular-shaped pneumatic actuator, fabricated from a thicker PVA tube (3mm ID, 6mm OD, and 20cm long), is integrated at the device's tail end. The pneumatic tube's axial movement is restrained with fishing wire, allowing the actuator to expand or contract around the finger. As a result, when a user bends their finger, the ring can automatically get loosened, enabling easy removal (illustrated at the bottom of Figure 7.8).

Secondly, we demonstrate an interactive LED setup, showcased on the right side of Figure 7.8. This setup is crafted by weaving four LM-filled PVA wires with conventional cotton yarns. Among these, two wires function as capacitive sensors, which we simply

implemented the self-capacitance mechanism and the Arduino CapacitiveSensor library is used. The remaining two LM-filled PVA wires serve as connectors for two SMD LEDs, where two squared PVA tubes are casted to fit the size of the LEDs. This configuration allows for the individual activation and deactivation of each LED by interacting with the corresponding capacitive sensing wire.

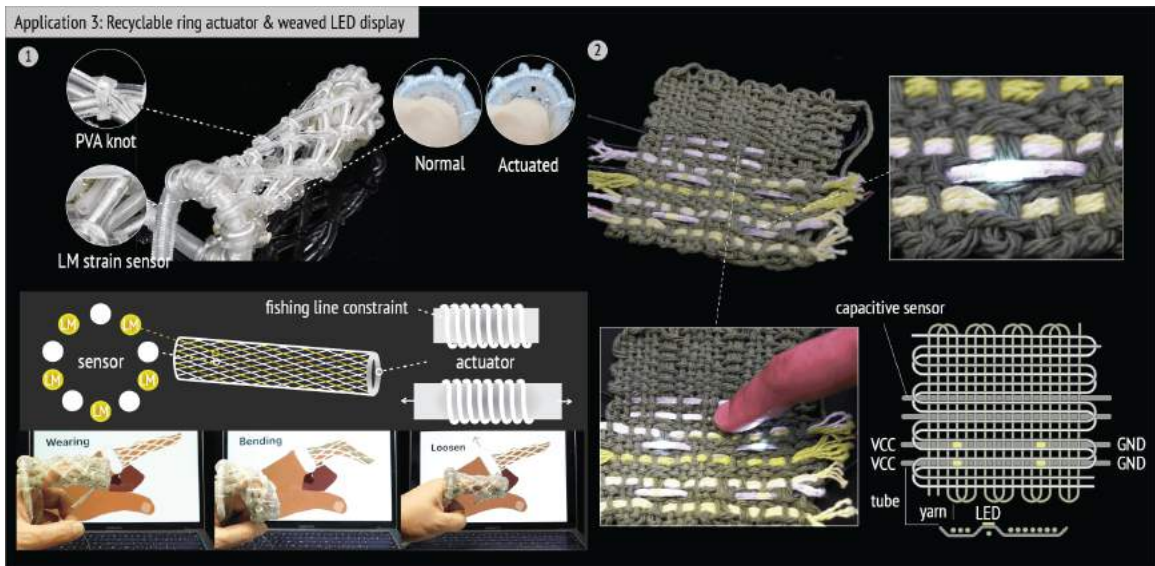


Figure 7.8: Two tube-based applications. (1) A fully recyclable sensor embedded haptic ring, and (2) An hand-weaved interactive LED.

7.6 Recycling Process

We have introduced Recy-ctronics for crafting interactive devices across varying form factors. These devices not only offer diverse interaction capabilities but are also designed with full recyclability in mind. The recycling process are the same for all three form factors—sheet, foam, and tube, while recycling rates, duration, and practical viability might differ among different form factors.

The recycling process follows prior literatures [157, 162, 163], which starts with detaching electronic components if there are any (*e.g.*, SMD, MCU, battery) from the substrates. Any material remnants on the pins of the components can be delicately eliminated

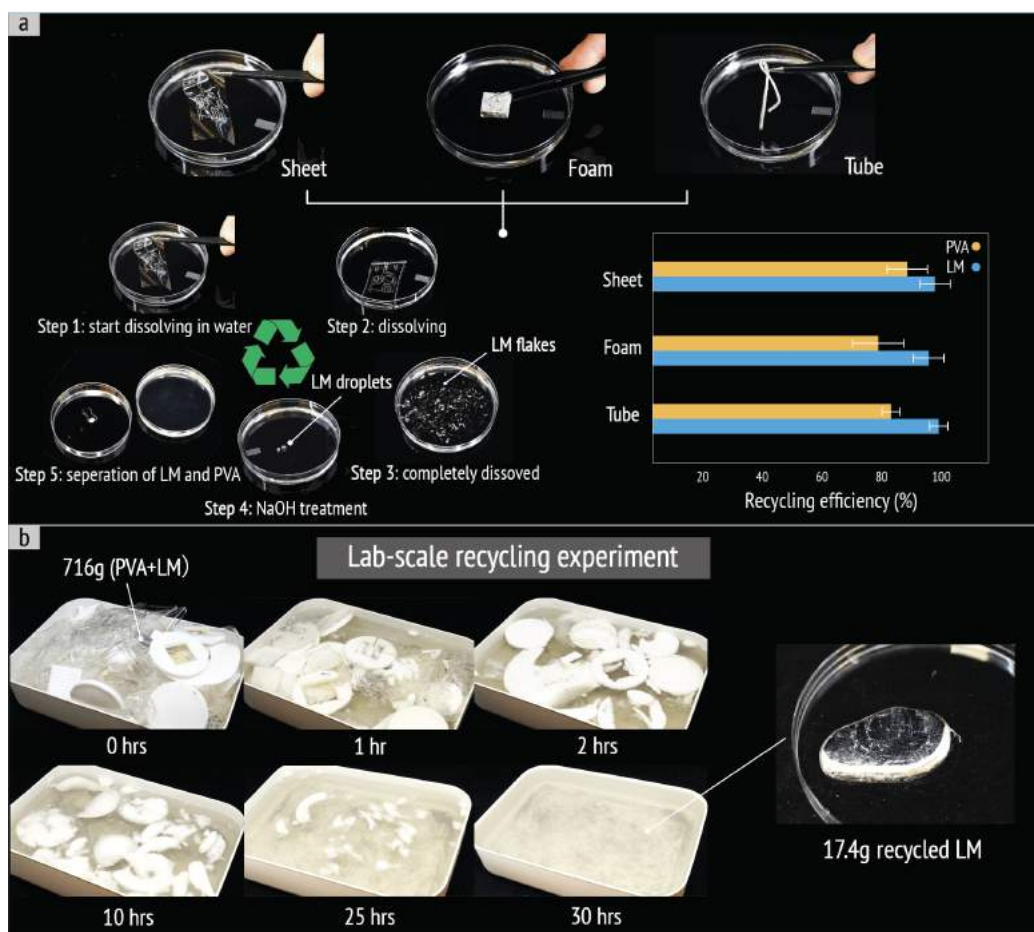


Figure 7.9: Recycling process. (a) All three form factors-sheet, foam and tube will undergo immersion in the water until complete dissolution. Then the LM and PVA will be separately collected to conclude the recycling process. (b) Lab-scale recycling experiment over two months.

using tweezers or by partially immersing them in water. Any components can be further dried out to prevent electrical failure under the condition of 80-90°C for one day in an laboratory oven. Then the entire device undergoes immersion in water until complete dissolution is achieved. Throughout this process, the dissolved device is subjected to thorough rinsing with fresh water, a step conducted 2-3 times to ensure the complete dissolution of PVA. The resulting PVA-enriched water is then collected, following the separation of the PVA-rich water from the residual LM fraction, approximately 5ml solution of 1mol% NaOH is added to the LM. The quantity of NaOH solution is contingent upon the device's

size. This NaOH serves the role of removing the oxidized layer on the LM, a thin Ga₂O₃ shell, thereby enabling the seamless recycling of the LM and ensuring high recycling efficiency. With the removal of the oxidized layer and the transformation of the LM into spherical form, one can retrieve the LM by using a syringe.

To assess the recycling performance across three distinct form factors, we carried out a comprehensive recycling testing. This encompassed recycling a LED pattern on a thin sheet, a cylindrical conductive foam, and a 4cm pipe. The recycling process was executed with six samples for each design, documenting and presenting the pre- and post-recycling weights of PVA and LM. As shown Figure 7.9, all three sample groups achieved a high recycling rate over 95% on average for LM, where we have achieved 97.5%, 96.1% and 98.6% for sheet, foam and tube respectively. Also the loss of PVA during the recycling process is higher, where we obtained 87.4%, 78.1% and 83.2% for sheet, foam and tube respectively. Among all the three types of interactive devices, tube group displayed the highest recycling rate for LM. This lower recycling rate for LM can potentially come from the foam's highly porosity structure which is mostly covered by LM, inducing more oxidised area comparing to sheets and tubes.

Beyond the individual device recycling test phase, we expanded our scope to include a batch of devices accumulated over two months, leading to the recovery of 17.4 grams of LM, as detailed in Figure 7.9b. This batch consisted of various device types (*e.g.*, sheets, foams, tubes) and miscellaneous non-device waste, totaling 716 grams. Within approximately 30 hours, all materials dissolved in water, which is later rinsed three times to transport the PVA-rich water from the LM remnants. It is worth nothing that we paid more attention in recycling LM for this experiment and saved the PVA solutions in containers for later prototyping use.

This lab-scale recycling initiative revealed several insights: (1) Complexity in Bulk Processing: Recycling a multitude of devices introduces complexities that we did not encounter in single-device recycling. The diverse mixture resulted in the emergence of un-

expected contaminants such as silver epoxy particles, paper scraps, and wires, requiring further filtration through a 200 mesh filter (around 75 microns). (2) Necessity for Improved Sorting: The heterogeneous nature of the waste highlighted the need for a better sorting system. Varied material compositions with different ratios of glycerin, PVA, and de-ionized water, suggest pre-recycling categorization could stabilize the material composition of recycled outputs. (3) Observations on LM Recycling: The bulk recycling process yielded a higher presence of oxidized substances and an increase in the resistance of the recycled LM, with a sheet resistance of $0.019 \pm 0.011 \Omega/\text{sq}$, (20 pieces of 40cm by 0.5cm samples), compared to the original LM's $0.013 \pm 0.002 \Omega/\text{sq}$, which might stem from the extended environmental exposure during waste accumulation. (4) Challenges in Dissolving PVA: We has observed that the dissolving process got dramatically slowed down after several hours and we have to add more water in the dissolving tank. Also, approaching the end of the dissolving stage, we picked up some remained PVA fragments and separately dissolved them in a beaker with hot water. Overall, this experience with recycling accumulated waste underlines the method's simplicity and efficiency, making it particularly suitable for maker environments.

	Scenario	
# of Circuits	N >= 1	
Parts List	Ours (PVA + LM + Electronic Components) N x (PVA + LM) + N x Electronic Components	Conventional (FR-4 + Copper + Electronic Components) N x (FR-4 + Copper) + N x Electronic Components
Raw Materials	N x PVA + N x LM	N x FR-4 + N x Copper
Manufacturing	N x Screen Printing	N x (Heat press + CNC + Etching + Copper Plating...)
Transport	-	-
Use	-	-
End of Life	Reuse (water-soluble PVA) and Reuse LM + Electronic Components	E-waste
Overall	Ours	Conventional

Figure 7.10: Comparative environmental impact analysis of Recy-ctronics sheet and conventional FR4 PCB.

7.7 Life Cycle Assessment

We undertake an environmental impact comparison (Figure 7.10) to juxtapose Recy-ctronics against conventional rigid PCB-based scenario using the case of the recyclable sheet-based proximity sensor presented in Figure 7.3. This comparison utilizes the recent concept of a comparative life-cycle assessment (LCA) [164] to underscore the environmental benefits of Recy-ctronics. FR-4, the most common PCB substrate, serves as the baseline for comparison. We assume identical dimensions to our substrate, i.e., 45mm x 55mm, and a standard thickness of 1.6 mm per dielectric layer. Various common LCA boundaries exist, including “cradle-to-gate” assessments, which encompass raw material extraction through product manufacturing, and “cradle-to-grave”, which extends to transport to the consumer, usage throughout the product’s lifetime, and end-of-life disposal. Given our focus on end-of-life recycling, we adopt a “cradle-to-grave” analysis as the primary scope of this comparison study.

In the initial phase of conducting comparative LCA, we compile a parts inventory of the recyclable sheet-based proximity sensor circuit and an FR-4 printed circuit board assembly (PCBA). As demonstrated in the previous section, the Recy-ctronics sheet effectively supports the standard MCU and sensor operation. Consequently, electronic components across both sensors can be canceled out in this environmental impact comparison as they are mostly identical. Thus, the sole distinction between Recy-ctronics sheet and conventional FR-4 circuitry in the raw material phase lies in the substrate, and conductive traces on the circuit board, which are PVA and LM for Recy-ctronics, and copper-clad FR-4, respectively. The environment impact of these parts is approximately equal in the raw material stages.

The first step of comparative LCA, We create a parts inventory of the recyclable sheet-based proximity sensor and a FR-4 sensor, we have shown in the previous section that Recy-ctronics sheet can support the successful operation of a standard MCU and sensor,

so the electronic components across could be canceled out in this environmental impact comparison as they are identical. Therefore, the only difference between Recy-ctronics sheet and conventional FR-4 circuit is the substrate and the conductive traces on the circuit board, and their corresponding manufacturing and end-of-life stage. We qualify them as PVA and LM for Recy-ctronics, and copper-clad FR-4, they are comparable in the raw material stages.

In the manufacturing stage, Recy-ctronics and conventional PCBs each possess pros and cons. For instance, Recy-ctronics employs screen printing to pattern circuits, a method that is faster for low quantity manufacturing and requires less expensive equipment and ecosystem. However, it lacks scalability compared to the conventional heat press and etching process, which can produce large quantities of parts or multiple boards simultaneously. From an environmental standpoint, screen printing proves more beneficial, as its required equipment consumes significantly less electricity, which contributes almost half of the global warming potential in conventional PCB manufacturing [165], compared to conventional PCB manufacturing equipment in factories [166].

We assume similar transportation and use life stages throughout the device's lifespan, as they are the same device. When both devices eventually reach the end-of-life stage. While FR-4 becomes e-waste, Recy-ctronics enables the reuse of its substrate (PVA) and conductive traces (LM), along with electronic components, owing to an accessible recycling process. As discussed before, the recycling process for Recy-ctronics is very straightforward with high recycling rate which only requires dissolving the device by immersing it in the water, reducing the oxidised layer outside LM and separating the two materials. This entire process is highly accessible without involving complicated tools/steps. For recycling FR-4, the collected PCBs are dismantled and shredded, followed by crushing and grinding to reduce them into finer particles. Subsequent stages involve air separation, screening, and magnetic and electrostatic separation techniques to isolate copper from non-metallic materials. Chemical processes, such as hydrometallurgical methods, are employed to leach out

copper, which is then refined for reuse. Meanwhile, the fiberglass component is processed separately to recover fiberglass materials for further applications [167].

In summary, Recy-ctronics offers substantial environmental benefits and potentials compared to the conventional, non-recyclable FR-4, particularly at the end-of-life stage.

CHAPTER 8

DISCUSSION

Mark Weiser’s visionary concept of seamlessly integrating technology into our everyday lives, objects, and routines has significantly influenced my work and that of many other researchers in ubiquitous and mobile computing. However, the reality of an increasing number of computational devices—an average of 22 per U.S. household in 2022—coupled with their contribution to electronic waste, which reached 53.6 million metric tons by 2020, casts a shadow over this vision. My research is positioned at the heart of this conflict, aiming to strike a balance between the proliferation of devices and the maintenance of their versatility, while adhering to sustainable practices. In this chapter, I will explore some of the critical observations and themes that emerge throughout the development of these sustainable devices, as well as the challenges and future directions in this field.

8.1 Life Cycle Assessment

In the context of sustainable development, life cycle assessment (LCA) is a vital methodology and tool for ensuring sustainability by evaluating the environmental impacts of a product, process, or service throughout its entire life cycle, spanning from raw material extraction to end-of-life disposal. LCA’s primary objective is to provide a comprehensive understanding of the environmental burdens associated with a specific system and identify opportunities for improvement, enabling informed decision-making towards more sustainable practices. Typically, an LCA consists of four key steps: (1) goal and scope definition, (2) inventory analysis involving the quantification of material inputs, energy inputs, and environmental discharges across different life cycle phases, (3) impact assessment, which aggregates these flows into various impact categories, and (4) interpretation of the results. By following this systematic approach, LCA enables a holistic assessment of environmen-

tal impacts and facilitates the identification of sustainable pathways.

One challenge with LCA in the context of computing is the availability and quality of inventory data, especially for emerging and ever-changing technologies like computing. Obtaining reliable data can be difficult, such as obtaining accurate information for lab-synthesized silk fibroin substrates compared to standard FR4 PCB boards (materials) or comparing different neural network workloads on alternate hardware. In the near future, I believe partnering with AI experts can significantly enhance the accuracy and scope of Life Cycle Assessment (LCA) in the realm of computing. AI can process and analyze vast amounts of data more efficiently, helping to address the challenges of obtaining reliable inventory data for emerging technologies. By leveraging machine learning algorithms and advanced data analytics, AI can identify patterns and correlations within large datasets, offering deeper insights into environmental impacts.

8.2 Power

Power drives most design choices for any electronic system. However, traditional batteries contain carbon, relatively inert metals (such as aluminum and stainless steel), non-biodegradable polymers (like polypropylene), oxides, and electrolytes that can pose hazards to human health and the environment due to their persistent nature. To address these concerns, I envision to explore more organic or biodegradable "green" battery options. Instead of relying on non-degradable metals, batteries can incorporate material combinations like Mg–Mo or Zn–Cu systems, allowing for fully or partially biodegradable battery designs. It is important to acknowledge that there may be practical challenges associated with these approaches, such as relatively low energy density or location limitations. Nonetheless, our ultimate goal is to develop a completely biodegradable battery system that can serve as an on-board power solution, ensuring independent deployment and achieving high energy density.

Another promising avenue for reducing reliance on batteries is through the utilization of

energy harvested from ambient resources, including body temperature, sunlight, and user interaction inputs. However, a key challenge arises when attempting to directly connect an energy harvester to a microcontroller. The energy harvested from these sources is often intermittent and insufficient to continuously power the device. To overcome this limitation, energy buffering becomes necessary, typically achieved through the use of a capacitor. Once a certain threshold of energy is accumulated, the system activates for a limited duration. The issue of intermittent energy supply has been extensively studied in the context of reliable computer systems. These batteryless energy-harvesting devices have emerged as a promising alternative to their battery-powered counterparts. Battery-powered systems are often costly, pose hazards to the environment, require maintenance, and are prone to failure, leading to shortened lifetimes and limited applications. In contrast, energy-harvesting devices offer advantages such as increased sustainability, reduced environmental impact, and enhanced reliability, expanding their potential range of applications.

8.3 Towards Sustainable And Complex Systems

Most of my completed work described and explored the tiniest class of computers—generally wearable, interactive, ubiquitous, invisible—on the far “edge.” However, the interactions and connections with “big iron”—the data centers and large-scale computing infrastructure, will dramatically affect the total sustainability of the trillion computers of the future. Here, I discussed three crucial components that significantly reduce the embodied carbon of modern computational devices. Reimagining these tiny devices’ lifecycle is the first step. However, we must also reimagine the broader infrastructure around these devices, as well as the decentralized computer operating systems that these devices will run and interact with before we see a positive impact on computing and society as a whole.

Data centers host innumerable applications, including cutting-edge large language models (LLMs), e-commerce websites, video streaming, sensor data fusion and search engines [168]. Regrettably, these data centers contribute to nearly 1% of global carbon emissions

[169] and growing. *A key question is whether the enormous increase of data from a trillion computational devices, will significantly change the calculus of carbon emissions in the operation of a data center.* We expand on open challenges and future works inspired by this question below:

End-of-Life Strategies: Can individual devices within the data center embody the RE-action approach described? Management and disposal strategies are complex for high-performance devices, especially considering the logistical challenges associated with disassembling and recycling. While most devices may not be (for example) biodegradable, potentially they could be repurposed in semi-degradable substrates, and used in new edge applications. In this way, the data center literally moves to the edge over time.

Edge/Cloud Systems Co-Design: Lifecycle based tools explored here could be extended to understand and integrate data movement and data center operation, aware of geographic constraints and cost models. Much like recent calls to make data-center software carbon-aware [170], we explore whether this carbon-awareness can extend to the edge devices and vice-versa. Expanding the design tools of computational materials to include the endpoints (the data center) could assist the programmer/designer in ensuring actual sustainability. For example, RE-action tools that explore placement of applications and compute based on age of infrastructure.

Data Movement and Compute Placement: Finally, a question remains on where computing should happen if, in fact, a trillion new computing devices do enter the world. With a trillion data streams, what level of capacity must be built at the data center, to absorb and effectively coordinate these devices? What actions and tasks should be the locus of the computational material to compute versus transmitting to the data center? Many data centers today are increasingly turning to renewable energy sources like photovoltaic systems to power their operations. This complicates dispatch and workload scheduling [171, 172, 173], but offers interesting flexibility knobs to optimize in terms of computer systems (i.e., scheduling latency insensitive applications for when it is sunny) [174]. A key ques-

tion is: can LCA design tools for computational materials, be "green" data-center aware in how they (as a group) offload and use this centralized resource to achieve high application utility. Would a situation exist, where it would be optimal for every small device on the edge to stream data to the data center for "free" at-scale processing powered by excess renewable energy? This is in conflict with current notions of processing *on-device* to save round trip costs. However, the benefits of a centralized computational powerhouse may be underexplored in this context.

CHAPTER 9

CONCLUSION

I position my research in solving the tension between adding more computational devices in our every day lives and their end of life sustainability. The five research projects completed during my PhD represent significant strides toward integrating IoT devices into daily life in an environmentally responsible manner. These studies collectively emphasize the crucial balance between scalability and sustainability, pioneering techniques that minimize environmental impact while enhancing device functionality and lifespan.

In Chapter 3, Silver Tape project exemplifies innovation in creating versatile and meanwhile repairable circuits that can be attached to a wide range of everyday surfaces through simple fabrication techniques, emphasizing ease of use and material efficiency. This approach not only makes technology more accessible but also more adaptable to various environments. In Chapter 4, Duco further advances this integration by eliminating human intervention in the fabrication of large-scale circuitry, introducing erasable ink to provide flexibility and reduce waste, embodying principles of reusability and adaptability.

Not only sensors, in Chapter 5, PITAS introduces a shape-changing sensing and actuating embedded robotic sheet, which can convey information dynamically across longer distance through physical changes. The inclusion of a renewal process using ethanol allow devices to be reused rather than disposed of, thus extending their lifecycle.

Functional Destruction in Chapter 6 takes a bold step towards sustainability, designing devices to self-destruct after fulfilling their purpose. This project aligns with sustainable practices by reducing long-term waste and environmental footprint. Lastly, in Chapter 7, Recy-ctronics complements this by pushing the boundaries of recyclability in electronics, with the development of fully recyclable circuits that view device end-of-life as a starting point for new creation, rather than an endpoint.

Together, these projects illuminate a path forward in the creation of a pervasive, sustainable, and scalable IoT environment. They demonstrate that the future of computing, as envisioned by Weiser, is not only about the ubiquity of devices but also about their harmonious integration into our ecosystems, embodying principles of sustainability, adaptability, and renewal. This research sets a framework for future developments in the field and underscores the potential of IoT devices to enhance our lives without compromising the health of our planet.

REFERENCES

- [1] M. Weiser, “The computer for the 21 st century,” *Scientific american*, vol. 265, no. 3, pp. 94–105, 1991.
- [2] T. Cheng *et al.*, “Silver tape: Inkjet-printed circuits peeled-and-transferred on versatile substrates,” *Proceedings of the ACM on Interactive, Mobile, Wearable and Ubiquitous Technologies*, vol. 4, no. 1, pp. 1–17, 2020.
- [3] M. Sitti, “Physical intelligence as a new paradigm,” *Extreme Mechanics Letters*, vol. 46, p. 101 340, 2021.
- [4] T. Cheng *et al.*, “Functional destruction: Utilizing sustainable materials’ physical transiency for electronics applications,” in *Proceedings of the 2023 CHI Conference on Human Factors in Computing Systems*, 2023, pp. 1–16.
- [5] C. Dierk, M. J. P. Nicholas, and E. Paulos, “Alterwear: Battery-free wearable displays for opportunistic interactions,” in *Proceedings of the 2018 CHI Conference on Human Factors in Computing Systems*, 2018, pp. 1–11.
- [6] C. Dierk, T. Vega Gálvez, and E. Paulos, “Alternail: Ambient, batteryless, stateful, dynamic displays at your fingertips,” in *Proceedings of the 2017 CHI Conference on Human Factors in Computing Systems*, 2017, pp. 6754–6759.
- [7] L. Kaila, H. Raula, M. Valtonen, and K. Palovuori, “Living wood: A self-hiding calm user interface,” in *Proceeding of the 16th International Academic MindTrek Conference*, 2012, pp. 267–274.
- [8] M. Wessely *et al.*, “Sprayable user interfaces: Prototyping large-scale interactive surfaces with sensors and displays,” in *Proceedings of the 2020 CHI Conference on Human Factors in Computing Systems*, 2020, pp. 1–12.
- [9] T. Cheng *et al.*, “Duco: Autonomous large-scale direct-circuit-writing (dcw) on vertical everyday surfaces using a scalable hanging plotter,” *Proceedings of the ACM on Interactive, Mobile, Wearable and Ubiquitous Technologies*, vol. 5, no. 3, pp. 1–25, 2021.
- [10] Y. Zhang, C. Yang, S. E. Hudson, C. Harrison, and A. Sample, “Wall++ room-scale interactive and context-aware sensing,” in *Proceedings of the 2018 CHI Conference on Human Factors in Computing Systems*, 2018, pp. 1–15.
- [11] S. Muthukumarana, M. A. Messerschmidt, D. J. Matthies, J. Steimle, P. M. Scholl, and S. Nanayakkara, “Clothtiles: A prototyping platform to fabricate customized actuators on clothing using 3d printing and shape-memory alloys,” in *Proceedings*

- of the 2021 CHI Conference on Human Factors in Computing Systems, 2021, pp. 1–12.
- [12] Y. Luo *et al.*, “Digital fabrication of pneumatic actuators with integrated sensing by machine knitting,” in *CHI Conference on Human Factors in Computing Systems*, 2022, pp. 1–13.
- [13] O. Kilic Afsar *et al.*, “Omnifiber: Integrated fluidic fiber actuators for weaving movement based interactions into the ‘fabric of everyday life’,” in *The 34th Annual ACM Symposium on User Interface Software and Technology*, 2021, pp. 1010–1026.
- [14] J. Forman, T. Tabb, Y. Do, M.-H. Yeh, A. Galvin, and L. Yao, “Modifiber: Two-way morphing soft thread actuators for tangible interaction,” in *Proceedings of the 2019 CHI Conference on Human Factors in Computing Systems*, 2019, pp. 1–11.
- [15] B. An *et al.*, “Thermorph: Democratizing 4d printing of self-folding materials and interfaces,” in *Proceedings of the 2018 CHI conference on human factors in computing systems*, 2018, pp. 1–12.
- [16] G. Wang *et al.*, “Printed paper actuator: A low-cost reversible actuation and sensing method for shape changing interfaces,” in *Proceedings of the 2018 CHI Conference on Human Factors in Computing Systems*, 2018, pp. 1–12.
- [17] H. Kaimoto, J. Yamaoka, S. Nakamaru, Y. Kawahara, and Y. Kakehi, “Expandfab: Fabricating objects expanding and changing shape with heat,” in *Proceedings of the Fourteenth International Conference on Tangible, Embedded, and Embodied Interaction*, 2020, pp. 153–164.
- [18] T. Cheng *et al.*, “Pitas: Sensing and actuating embedded robotic sheet for physical information communication,” in *CHI Conference on Human Factors in Computing Systems*, 2022, pp. 1–16.
- [19] S. Swaminathan *et al.*, “Optistruktures: Fabrication of room-scale interactive structures with embedded fiber bragg grating optical sensors and displays,” *Proceedings of the ACM on Interactive, Mobile, Wearable and Ubiquitous Technologies*, vol. 4, no. 2, pp. 1–21, 2020.
- [20] L. Yao, R. Niiyama, J. Ou, S. Follmer, C. Della Silva, and H. Ishii, “Pneui: Pneumatically actuated soft composite materials for shape changing interfaces,” in *Proceedings of the 26th annual ACM symposium on User interface software and Technology*, 2013, pp. 13–22.

- [21] K. Narumi *et al.*, “Self-healing ui: Mechanically and electrically self-healing materials for sensing and actuation interfaces,” in *Proceedings of the 32nd Annual ACM Symposium on User Interface Software and Technology*, 2019, pp. 293–306.
- [22] S. Swaminathan, K. B. Ozutemiz, C. Majidi, and S. E. Hudson, “Fiberwire: Embedding electronic function into 3d printed mechanically strong, lightweight carbon fiber composite objects,” in *Proceedings of the 2019 CHI Conference on Human Factors in Computing Systems*, 2019, pp. 1–11.
- [23] M. Schmitz, M. Khalilbeigi, M. Balwierz, R. Lissermann, M. Mühlhäuser, and J. Steimle, “Capricate: A fabrication pipeline to design and 3d print capacitive touch sensors for interactive objects,” in *Proceedings of the 28th Annual ACM Symposium on User Interface Software & Technology*, 2015, pp. 253–258.
- [24] H.-L. Kao, C. Holz, A. Roseway, A. Calvo, and C. Schmandt, “Duoskin: Rapidly prototyping on-skin user interfaces using skin-friendly materials,” in *Proceedings of the 2016 ACM International Symposium on Wearable Computers*, 2016, pp. 16–23.
- [25] E. Markvicka, G. Wang, Y.-C. Lee, G. Laput, C. Majidi, and L. Yao, “Electrodermis: Fully untethered, stretchable, and highly-customizable electronic bandages,” in *Proceedings of the 2019 CHI Conference on Human Factors in Computing Systems*, 2019, pp. 1–10.
- [26] D. Groeger and J. Steimle, “Lasec: Instant fabrication of stretchable circuits using a laser cutter,” in *Proceedings of the 2019 CHI Conference on Human Factors in Computing Systems*, 2019, pp. 1–14.
- [27] J. Yamaoka *et al.*, “Foldtronics: Creating 3d objects with integrated electronics using foldable honeycomb structures,” in *Proceedings of the 2019 CHI Conference on Human Factors in Computing Systems*, 2019, pp. 1–14.
- [28] M. Nisser, C. Liao, Y. Chai, A. Adhikari, S. Hodges, and S. Mueller, “A laser cutter-based electromechanical assembly and fabrication platform to make functional devices robots,” in *Proceedings of the SIGCHI Conference on Human Factors in Computing Systems*, 2021.
- [29] A. Khan, J. S. Roo, T. Kraus, and J. Steimle, “Soft inkjet circuits: Rapid multi-material fabrication of soft circuits using a commodity inkjet printer,” in *Proceedings of the 32nd Annual ACM Symposium on User Interface Software and Technology*, 2019, pp. 341–354.
- [30] Y. Kawahara, S. Hodges, B. S. Cook, C. Zhang, and G. D. Abowd, “Instant inkjet circuits: Lab-based inkjet printing to support rapid prototyping of ubicomp de-

vices,” in *Proceedings of the 2013 ACM international joint conference on Pervasive and ubiquitous computing*, 2013, pp. 363–372.

- [31] S. Olberding, S. Soto Ortega, K. Hildebrandt, and J. Steimle, “Foldio: Digital fabrication of interactive and shape-changing objects with foldable printed electronics,” in *Proceedings of the 28th Annual ACM Symposium on User Interface Software & Technology*, 2015, pp. 223–232.
- [32] F. Heibeck, B. Tome, C. Della Silva, and H. Ishii, “Unimorph: Fabricating thin film composites for shape-changing interfaces,” in *Proceedings of the 28th Annual ACM Symposium on User Interface Software & Technology*, 2015, pp. 233–242.
- [33] J. Lo, D. J. L. Lee, N. Wong, D. Bui, and E. Paulos, “Skintillates: Designing and creating epidermal interactions,” in *Proceedings of the 2016 ACM Conference on Designing Interactive Systems*, 2016, pp. 853–864.
- [34] M. Weigel, A. S. Nittala, A. Olwal, and J. Steimle, “Skinmarks: Enabling interactions on body landmarks using conformal skin electronics,” in *Proceedings of the 2017 CHI Conference on Human Factors in Computing Systems*, 2017, pp. 3095–3105.
- [35] A. S. Nittala, A. Withana, N. Pourjafarian, and J. Steimle, “Multi-touch skin: A thin and flexible multi-touch sensor for on-skin input,” in *Proceedings of the 2018 CHI Conference on Human Factors in Computing Systems*, 2018, pp. 1–12.
- [36] Y. Zhang and C. Harrison, “Pulp nonfiction: Low-cost touch tracking for paper,” in *Proceedings of the 2018 CHI Conference on Human Factors in Computing Systems*, 2018, pp. 1–11.
- [37] A. Withana, D. Groeger, and J. Steimle, “Tacttoo: A thin and feel-through tattoo for on-skin tactile output,” in *Proceedings of the 31st Annual ACM Symposium on User Interface Software and Technology*, 2018, pp. 365–378.
- [38] M. Weigel, T. Lu, G. Bailly, A. Oulasvirta, C. Majidi, and J. Steimle, “Iskin: Flexible, stretchable and visually customizable on-body touch sensors for mobile computing,” in *Proceedings of the 33rd Annual ACM Conference on Human Factors in Computing Systems*, 2015, pp. 2991–3000.
- [39] S. Nagels, R. Ramakers, K. Luyten, and W. Deferme, “Silicone devices: A scalable diy approach for fabricating self-contained multi-layered soft circuits using microfluidics,” in *Proceedings of the 2018 CHI Conference on Human Factors in Computing Systems*, 2018, pp. 1–13.

- [40] M. Wessely, T. Tsandilas, and W. E. Mackay, “Stretchis: Fabricating highly stretchable user interfaces,” in *Proceedings of the 29th Annual Symposium on User Interface Software and Technology*, 2016, pp. 697–704.
- [41] Y. Zhang, C. (Yang, S. E. Hudson, C. Harrison, and A. Sample, “Wall++: Room-scale interactive and context-aware sensing,” in *Proceedings of the 2018 CHI Conference on Human Factors in Computing Systems*, ser. CHI ’18, Montreal QC, Canada: Association for Computing Machinery, 2018, pp. 1–15, ISBN: 9781450356206.
- [42] J. Qi and L. Buechley, “Electronic popables: Exploring paper-based computing through an interactive pop-up book,” in *Proceedings of the fourth international conference on Tangible, embedded, and embodied interaction*, 2010, pp. 121–128.
- [43] A. Russo, B. Y. Ahn, J. J. Adams, E. B. Duoss, J. T. Bernhard, and J. A. Lewis, “Pen-on-paper flexible electronics,” *Advanced materials*, vol. 23, no. 30, pp. 3426–3430, 2011.
- [44] D. Qin, Y. Xia, and G. M. Whitesides, “Soft lithography for micro-and nanoscale patterning,” *Nature protocols*, vol. 5, no. 3, p. 491, 2010.
- [45] M. Wehner *et al.*, “An integrated design and fabrication strategy for entirely soft, autonomous robots,” *Nature*, vol. 536, no. 7617, pp. 451–455, 2016.
- [46] T. Ranzani, S. Russo, N. W. Bartlett, M. Wehner, and R. J. Wood, “Increasing the dimensionality of soft microstructures through injection-induced self-folding,” *Advanced Materials*, vol. 30, no. 38, p. 1 802 739, 2018.
- [47] C. E. A. 2, 2013.
- [48] G. Pro, 2013.
- [49] H. S. 30M, 2013.
- [50] J. Ou, G. Dublon, C.-Y. Cheng, F. Heibeck, K. Willis, and H. Ishii, “Cillia: 3d printed micro-pillar structures for surface texture, actuation and sensing,” in *Proceedings of the 2016 CHI Conference on Human Factors in Computing Systems*, 2016, pp. 5753–5764.
- [51] M. K. Rasmussen, E. W. Pedersen, M. G. Petersen, and K. Hornbæk, “Shape-changing interfaces: A review of the design space and open research questions,” in *Proceedings of the SIGCHI Conference on Human Factors in Computing Systems*, 2012, pp. 735–744.

- [52] A. A. Stanley, J. C. Gwilliam, and A. M. Okamura, “Haptic jamming: A deformable geometry, variable stiffness tactile display using pneumatics and particle jamming,” in *2013 World Haptics Conference (WHC)*, IEEE, 2013, pp. 25–30.
- [53] S. Follmer, D. Leithinger, A. Olwal, N. Cheng, and H. Ishii, “Jamming user interfaces: Programmable particle stiffness and sensing for malleable and shape-changing devices,” in *Proceedings of the 25th annual ACM symposium on User interface software and technology*, 2012, pp. 519–528.
- [54] J. Ou *et al.*, “Aeromorph-heat-sealing inflatable shape-change materials for interaction design,” in *Proceedings of the 29th Annual Symposium on User Interface Software and Technology*, 2016, pp. 121–132.
- [55] H. Sareen *et al.*, “Printflatables: Printing human-scale, functional and dynamic inflatable objects,” in *Proceedings of the 2017 CHI Conference on Human Factors in Computing Systems*, 2017, pp. 3669–3680.
- [56] I. P. Qamar, R. Groh, D. Holman, and A. Roudaut, “Hci meets material science: A literature review of morphing materials for the design of shape-changing interfaces,” in *Proceedings of the 2018 CHI Conference on Human Factors in Computing Systems*, 2018, pp. 1–23.
- [57] J. Alexander *et al.*, “Grand challenges in shape-changing interface research,” in *Proceedings of the 2018 CHI conference on human factors in computing systems*, 2018, pp. 1–14.
- [58] Y. Tahouni, I. P. Qamar, and S. Mueller, “Nurbsforms: A modular shape-changing interface for prototyping curved surfaces,” in *Proceedings of the Fourteenth International Conference on Tangible, Embedded, and Embodied Interaction*, 2020, pp. 403–409.
- [59] A. Roudaut, A. Karnik, M. Löchtefeld, and S. Subramanian, “Morphees: Toward high” shape resolution” in self-actuated flexible mobile devices,” in *Proceedings of the SIGCHI Conference on Human Factors in Computing Systems*, 2013, pp. 593–602.
- [60] C. Kopic and K. Gohlke, “Inflatibits: A modular soft robotic construction kit for children,” in *Proceedings of the TEI’16: Tenth International Conference on Tangible, Embedded, and Embodied Interaction*, 2016, pp. 723–728.
- [61] J. Qi and L. Buechley, “Animating paper using shape memory alloys,” in *Proceedings of the SIGCHI Conference on Human Factors in Computing Systems*, ser. CHI ’12, Austin, Texas, USA: Association for Computing Machinery, 2012, pp. 749–752, ISBN: 9781450310154.

- [62] Y. Tokuda, D. R. Sahoo, M. Jones, S. Subramanian, and A. Withana, “Flowcuits: Crafting tangible and interactive electrical components with liquid metal circuits,” in *Proceedings of the Fifteenth International Conference on Tangible, Embedded, and Embodied Interaction*, 2021, pp. 1–11.
- [63] N. Pourjafarian, A. Withana, J. A. Paradiso, and J. Steimle, “Multi-touch kit: A do-it-yourself technique for capacitive multi-touch sensing using a commodity microcontroller,” 2019.
- [64] J. Gong, O. Seow, C. Honnet, J. Forman, and S. Mueller, “Metasense: Integrating sensing capabilities into mechanical metamaterial,” in *The 34th Annual ACM Symposium on User Interface Software and Technology*, 2021, pp. 1063–1073.
- [65] C. Honnet *et al.*, “Polysense: Augmenting textiles with electrical functionality using in-situ polymerization,” in *Proceedings of the 2020 CHI Conference on Human Factors in Computing Systems*, 2020, pp. 1–13.
- [66] T. Li *et al.*, “Fast-moving soft electronic fish,” *Science advances*, vol. 3, no. 4, e1602045, 2017.
- [67] T. Cheng *et al.*, “Untethered soft robotic jellyfish,” *Smart Materials and Structures*, vol. 28, no. 1, p. 015 019, 2018.
- [68] C. Laschi and M. Cianchetti, “Soft robotics: New perspectives for robot bodyware and control,” *Frontiers in bioengineering and biotechnology*, vol. 2, p. 3, 2014.
- [69] B. Trimmer, “Soft robots,” *Current Biology*, vol. 23, no. 15, R639–R641, 2013.
- [70] C. Fang, Y. Zhang, M. Dworman, and C. Harrison, “Wireality: Enabling complex tangible geometries in virtual reality with worn multi-string haptics,” in *Proceedings of the 2020 CHI Conference on Human Factors in Computing Systems*, 2020, pp. 1–10.
- [71] S. Jang, L. H. Kim, K. Tanner, H. Ishii, and S. Follmer, “Haptic edge display for mobile tactile interaction,” in *Proceedings of the 2016 CHI Conference on Human Factors in Computing Systems*, 2016, pp. 3706–3716.
- [72] L. He, C. Xu, D. Xu, and R. Brill, “Pneuhaptic: Delivering haptic cues with a pneumatic armband,” in *Proceedings of the 2015 ACM International Symposium on Wearable Computers*, 2015, pp. 47–48.
- [73] A. Delazio, K. Nakagaki, R. L. Klatzky, S. E. Hudson, J. F. Lehman, and A. P. Sample, “Force jacket: Pneumatically-actuated jacket for embodied haptic experiences,” in *Proceedings of the 2018 CHI Conference on Human Factors in Computing Systems*, 2018, pp. 1–12.

- [74] N. A.-h. Hamdan, A. Wagner, S. Voelker, J. Steimle, and J. Borchers, “Springlets: Expressive, flexible and silent on-skin tactile interfaces,” in *Proceedings of the 2019 CHI Conference on Human Factors in Computing Systems*, 2019, pp. 1–14.
- [75] J. C. Mankoff *et al.*, “Environmental sustainability and interaction,” in *CHI’07 extended abstracts on Human factors in computing systems*, 2007, pp. 2121–2124.
- [76] E. S. Lazaro Vasquez, H.-C. Wang, and K. Vega, “Introducing the sustainable prototyping life cycle for digital fabrication to designers,” in *Proceedings of the 2020 ACM Designing Interactive Systems Conference*, 2020, pp. 1301–1312.
- [77] H. Brynjarsdottir, M. Håkansson, J. Pierce, E. Baumer, C. DiSalvo, and P. Sengers, “Sustainably unpersuaded: How persuasion narrows our vision of sustainability,” in *Proceedings of the sigchi conference on human factors in computing systems*, 2012, pp. 947–956.
- [78] C. DiSalvo, P. Sengers, and H. Brynjarsdóttir, “Mapping the landscape of sustainable hci,” in *Proceedings of the SIGCHI conference on human factors in computing systems*, 2010, pp. 1975–1984.
- [79] E. Blevis, “Sustainable interaction design: Invention & disposal, renewal & reuse,” in *Proceedings of the SIGCHI conference on Human factors in computing systems*, 2007, pp. 503–512.
- [80] E. S. L. Vasquez, H.-C. Wang, and K. Vega, “The environmental impact of physical prototyping: A five-year chi review,” in *Self-Sustainable CHI Workshop*, vol. 1, 2020, p. 8.
- [81] K. W. Song and E. Paulos, “Unmaking: Enabling and celebrating the creative material of failure, destruction, decay, and deformation,” in *Proceedings of the 2021 CHI Conference on Human Factors in Computing Systems*, 2021, pp. 1–12.
- [82] K. W. Song, A. Maheshwari, E. M. Gallo, A. Danielescu, and E. Paulos, “Towards decomposable interactive systems: Design of a backyard-degradable wireless heating interface,” in *CHI Conference on Human Factors in Computing Systems*, 2022, pp. 1–12.
- [83] M. Murer, A. Vallgård, M. Jacobsson, and M. Tscheligi, “Un-crafting: Exploring tangible practices for deconstruction in interactive system design,” in *Proceedings of the Ninth International Conference on Tangible, Embedded, and Embodied Interaction*, 2015, pp. 469–472.
- [84] S. Wu and L. Devendorf, “Unfabricate: Designing smart textiles for disassembly,” in *Proceedings of the 2020 CHI Conference on Human Factors in Computing Systems*, 2020, pp. 1–14.

- [85] M. Tavakoli *et al.*, “Egain-assisted room-temperature sintering of silver nanoparticles for stretchable, inkjet-printed, thin-film electronics,” *Advanced Materials*, vol. 30, no. 29, p. 1 801 852, 2018.
- [86] N. Vadgama and J. Steimle, “Flexy: Shape-customizable, single-layer, inkjet printable patterns for 1d and 2d flex sensing,” in *Proceedings of the Eleventh International Conference on Tangible, Embedded, and Embodied Interaction*, 2017, pp. 153–162.
- [87] D. Groeger and J. Steimle, “Objectskin: Augmenting everyday objects with hydroprinted touch sensors and displays,” *Proceedings of the ACM on Interactive, Mobile, Wearable and Ubiquitous Technologies*, vol. 1, no. 4, pp. 1–23, 2018.
- [88] N.-W. Gong *et al.*, “Printsense: A versatile sensing technique to support multimodal flexible surface interaction,” in *Proceedings of the SIGCHI Conference on Human Factors in Computing Systems*, 2014, pp. 1407–1410.
- [89] S. Olberding, M. Wessely, and J. Steimle, “Printscreen: Fabricating highly customizable thin-film touch-displays,” in *Proceedings of the 27th annual ACM symposium on User interface software and technology*, 2014, pp. 281–290.
- [90] D. MATERIALS, 2018.
- [91] N. Products, 1960.
- [92] B. C. E. P. Pen, 2009.
- [93] S. C. Epoxy, 1928.
- [94] Y. Cai, X. Piao, W. Gao, Z. Zhang, E. Nie, and Z. Sun, “Large-scale and facile synthesis of silver nanoparticles via a microwave method for a conductive pen,” *RSC advances*, vol. 7, no. 54, pp. 34 041–34 048, 2017.
- [95] Y.-L. Tai and Z.-G. Yang, “Fabrication of paper-based conductive patterns for flexible electronics by direct-writing,” *Journal of Materials Chemistry*, vol. 21, no. 16, pp. 5938–5943, 2011.
- [96] MOLOTOW, 1959.
- [97] K. Narumi, X. Shi, S. Hodges, Y. Kawahara, S. Shimizu, and T. Asami, “Circuit eraser: A tool for iterative design with conductive ink,” in *Proceedings of the 33rd Annual ACM Conference Extended Abstracts on Human Factors in Computing Systems*, 2015, pp. 2307–2312.

- [98] Y. Wang *et al.*, “Flextouch: Enabling large-scale interaction sensing beyond touchscreens using flexible and conductive materials,” *Proceedings of the ACM on Interactive, Mobile, Wearable and Ubiquitous Technologies*, vol. 3, no. 3, pp. 1–20, 2019.
- [99] E. M. Jung *et al.*, “A wideband, quasi-isotropic, kilometer-range fm energy harvester for perpetual iot,” *IEEE Microwave and Wireless Components Letters*, vol. 30, no. 2, pp. 201–204, 2020.
- [100] FischerAppelt, 2021.
- [101] A. Echasseriau, 2016.
- [102] J. W. Urban Conga Sebastian Coolidge, 2018.
- [103] B. C. T. Board, 2018.
- [104] IFTTT, *Ifttt*, Mar. 2011.
- [105] Smarter, *Smarter coffee maker*, Mar. 2013.
- [106] J. Rekimoto, “Smartskin: An infrastructure for freehand manipulation on interactive surfaces,” in *Proceedings of the SIGCHI conference on Human factors in computing systems*, 2002, pp. 113–120.
- [107] Arduino, 2011.
- [108] SparkFun, 2003.
- [109] LaserPecker, *Laserpecker*, Mar. 2019.
- [110] Polargraph, 2019.
- [111] Y. Hu and G. Hoffman, “Using skin texture change to design emotion expression in social robots,” in *2019 14th ACM/IEEE International Conference on Human-Robot Interaction (HRI)*, IEEE, 2019, pp. 2–10.
- [112] R. Strong, B. Gaver, *et al.*, “Feather, scent and shaker: Supporting simple intimacy,” in *Proceedings of CSCW*, vol. 96, 1996, pp. 29–30.
- [113] A. Miriyev, K. Stack, and H. Lipson, “Soft material for soft actuators,” *Nature communications*, vol. 8, no. 1, pp. 1–8, 2017.

- [114] A. Miriyev, B. Xia, J. C. Joseph, and H. Lipson, “Additive manufacturing of silicone composites for soft actuation,” *3D Printing and Additive Manufacturing*, vol. 6, no. 6, pp. 309–318, 2019.
- [115] K. Nakahara, K. Narumi, R. Niiyama, and Y. Kawahara, “Electric phase-change actuator with inkjet printed flexible circuit for printable and integrated robot prototyping,” in *2017 IEEE International Conference on Robotics and Automation (ICRA)*, IEEE, 2017, pp. 1856–1863.
- [116] T. Noguchi and F. Tsumori, “Soft actuator with large volumetric change using vapor–liquid phase transition,” *Japanese Journal of Applied Physics*, vol. 59, no. SI, SIIL08, 2020.
- [117] S. Hirai, T. Nagatomo, T. Hiraki, H. Ishizuka, Y. Kawahara, and N. Miki, “Micro elastic pouch motors: Elastically deformable and miniaturized soft actuators using liquid-to-gas phase change,” *IEEE Robotics and Automation Letters*, vol. 6, no. 3, pp. 5373–5380, 2021.
- [118] J. Zhu *et al.*, “Curveboards: Integrating breadboards into physical objects to prototype function in the context of form,” in *Proceedings of the 2020 CHI Conference on Human Factors in Computing Systems*, 2020, pp. 1–13.
- [119] S. A. Morin *et al.*, “Using “click-e-bricks” to make 3d elastomeric structures,” *Advanced Materials*, vol. 26, no. 34, pp. 5991–5999, 2014.
- [120] T. D. Ta, T. Umedachi, and Y. Kawahara, “Design of frictional 2d-anisotropy surface for wriggle locomotion of printable soft-bodied robots,” in *2018 IEEE International Conference on Robotics and Automation (ICRA)*, IEEE, 2018, pp. 6779–6785.
- [121] V. T. Textiles, 2006.
- [122] S. A. Materials, 2013.
- [123] Cricut, *Cricut rotary blade*, Mar. 2013.
- [124] E. L. White, M. C. Yuen, J. C. Case, and R. K. Kramer, “Low-cost, facile, and scalable manufacturing of capacitive sensors for soft systems,” *Advanced Materials Technologies*, vol. 2, no. 9, p. 1700072, 2017.
- [125] M. D. Bartlett *et al.*, “High thermal conductivity in soft elastomers with elongated liquid metal inclusions,” *Proceedings of the National Academy of Sciences*, vol. 114, no. 9, pp. 2143–2148, 2017.
- [126] ESPRESSIF, *Esp 32*, Mar. 2008.

- [127] F. Shahmiri *et al.*, “Serpentine: A self-powered reversibly deformable cord sensor for human input,” in *Proceedings of the 2019 CHI Conference on Human Factors in Computing Systems*, 2019, pp. 1–14.
- [128] S. io, *Esp* 32, Mar. 2008.
- [129] R. Rautela, S. Arya, S. Vishwakarma, J. Lee, K.-H. Kim, and S. Kumar, “E-waste management and its effects on the environment and human health,” *Science of the Total Environment*, vol. 773, p. 145 623, 2021.
- [130] S. Sabie *et al.*, “Unmaking@ chi: Concretizing the material and epistemological practices of unmaking in hci,” in *CHI Conference on Human Factors in Computing Systems Extended Abstracts*, 2022, pp. 1–6.
- [131] A. Maheshwari, A. Kumar Aggarwal, and A. Danielescu, “Designing tools and interfaces for ecological restoration: An investigation into the opportunities and constraints for technological interventions,” in *CHI Conference on Human Factors in Computing Systems*, 2022, pp. 1–17.
- [132] S.-W. Hwang *et al.*, “A physically transient form of silicon electronics,” *Science*, vol. 337, no. 6102, pp. 1640–1644, 2012.
- [133] D.-H. Kim *et al.*, “Dissolvable films of silk fibroin for ultrathin conformal bio-integrated electronics,” *Nature materials*, vol. 9, no. 6, pp. 511–517, 2010.
- [134] A. Gumus *et al.*, “Expandable polymer enabled wirelessly destructible high-performance solid state electronics,” *Advanced Materials Technologies*, vol. 2, no. 5, p. 1 600 264, 2017.
- [135] S. H. Jin *et al.*, “Solution-processed single-walled carbon nanotube field effect transistors and bootstrapped inverters for disintegratable, transient electronics,” *Applied Physics Letters*, vol. 105, no. 1, p. 013 506, 2014.
- [136] S.-W. Hwang *et al.*, “High-performance biodegradable/transient electronics on biodegradable polymers,” *Advanced Materials*, vol. 26, no. 23, pp. 3905–3911, 2014.
- [137] H. Film, 2017.
- [138] Q. Dams, 2004.
- [139] J. A. Fan *et al.*, “Fractal design concepts for stretchable electronics,” *Nature communications*, vol. 5, no. 1, p. 3266, 2014.
- [140] M. Nisser, J. Zhu, T. Chen, K. Bulovic, P. Punpongsanon, and S. Mueller, “Sequential support: 3d printing dissolvable support material for time-dependent mecha-

nisms,” in *Proceedings of the Thirteenth International Conference on Tangible, Embedded, and Embodied Interaction*, 2019, pp. 669–676.

- [141] S. M. Won *et al.*, “Natural wax for transient electronics,” *Advanced Functional Materials*, vol. 28, no. 32, p. 1 801 819, 2018.
- [142] K. Zhang, B. Han, and X. Yu, “Electrically conductive carbon nanofiber/paraffin wax composites for electric thermal storage,” *Energy conversion and management*, vol. 64, pp. 62–67, 2012.
- [143] H. W. B. Pellets, 2004.
- [144] G. P. Filler, 1957.
- [145] Y. Wu *et al.*, “Edible and nutritive electronics: Materials, fabrications, components, and applications,” *Advanced Materials Technologies*, vol. 5, no. 10, p. 2 000 100, 2020.
- [146] W. Xu *et al.*, “Food-based edible and nutritive electronics,” *Advanced Materials Technologies*, vol. 2, no. 11, p. 1 700 181, 2017.
- [147] 2. G. E. G. Leaf, 1955.
- [148] N. Segawa, K. Kato, and H. Manabe, “Rapid prototyping of paper electronics using a metal leaf and laser printer,” in *The Adjunct Publication of the 32nd Annual ACM Symposium on User Interface Software and Technology*, 2019, pp. 99–101.
- [149] L. pecker pro L1, 2017.
- [150] A. Vena, E. Perret, and S. Tedjini, “Chipless rfid tag using hybrid coding technique,” *IEEE Transactions on Microwave Theory and Techniques*, vol. 59, no. 12, pp. 3356–3364, 2011.
- [151] R. Want, “An introduction to rfid technology,” *IEEE pervasive computing*, vol. 5, no. 1, pp. 25–33, 2006.
- [152] C. Herrojo, F. Paredes, J. Mata-Contreras, and F. Martín, “Chipless-RFID: A review and recent developments,” *Sensors (Basel)*, vol. 19, no. 15, p. 3385, Aug. 2019.
- [153] O. Rance, R. Siragusa, P. Lemaître-Auger, and E. Perret, “Toward rcs magnitude level coding for chipless rfid,” *IEEE Transactions on Microwave Theory and Techniques*, vol. 64, no. 7, pp. 2315–2325, 2016.

- [154] S. Al-Salem, P. Lettieri, and J. Baeyens, “The valorization of plastic solid waste (psw) by primary to quaternary routes: From re-use to energy and chemicals,” *Progress in Energy and Combustion Science*, vol. 36, no. 1, pp. 103–129, 2010.
- [155] J. A. Chiong, H. Tran, Y. Lin, Y. Zheng, and Z. Bao, “Integrating emerging polymer chemistries for the advancement of recyclable, biodegradable, and biocompatible electronics,” *Advanced Science*, vol. 8, no. 14, p. 2101233, 2021.
- [156] R. Nagarkar and J. Patel, “Polyvinyl alcohol: A comprehensive study,” *Acta Sci. Pharm. Sci.*, vol. 3, no. 4, pp. 34–44, 2019.
- [157] L. Teng, S. Ye, S. Handschuh-Wang, X. Zhou, T. Gan, and X. Zhou, “Liquid metal-based transient circuits for flexible and recyclable electronics,” *Advanced Functional Materials*, vol. 29, no. 11, p. 1808739, 2019.
- [158] H. Li, C. Ye, and A. P. Sample, “Idsense: A human object interaction detection system based on passive uhf rfid,” in *Proceedings of the 33rd Annual ACM Conference on Human Factors in Computing Systems*, 2015, pp. 2555–2564.
- [159] H. Li *et al.*, “Paperid: A technique for drawing functional battery-free wireless interfaces on paper,” in *Proceedings of the 2016 CHI Conference on Human Factors in Computing Systems*, 2016, pp. 5885–5896.
- [160] S. Nakamaru, R. Nakayama, R. Niiyama, and Y. Kakehi, “Foamsense: Design of three dimensional soft sensors with porous materials,” in *Proceedings of the 30th Annual ACM Symposium on User Interface Software and Technology*, 2017, pp. 437–447.
- [161] Y. Luo, K. Wu, T. Palacios, and W. Matusik, “Knitui: Fabricating interactive and sensing textiles with machine knitting,” in *Proceedings of the 2021 CHI Conference on Human Factors in Computing Systems*, 2021, pp. 1–12.
- [162] J. Xu *et al.*, “Printable and recyclable conductive ink based on a liquid metal with excellent surface wettability for flexible electronics,” *ACS applied materials & interfaces*, vol. 13, no. 6, pp. 7443–7452, 2021.
- [163] L. Teng *et al.*, “Fully recyclable liquid-metal-based multi-layer thermally triggered transient electronic devices,” *Advanced Materials Technologies*, vol. 8, no. 4, p. 2201031, 2023.
- [164] Z. Zhang *et al.*, “DeltaLCA: Comparative Life-Cycle Assessment for Electronics Design,” *Proceedings of the ACM on Interactive, Mobile, Wearable and Ubiquitous Technologies*, vol. 8, no. 1, 29:1–29:29, Mar. 2024.

- [165] M. N. Nassajfar, I. Deviatkin, V. Leminen, and M. Horttanainen, “Alternative Materials for Printed Circuit Board Production: An Environmental Perspective,” *Sustainability*, vol. 13, no. 21, p. 12 126, Jan. 2021, Number: 21 Publisher: Multidisciplinary Digital Publishing Institute.
- [166] Z. Zhang *et al.*, “Recyclable vitrimer-based printed circuit board for circular electronics,” *arXiv preprint arXiv:2308.12496*, 2023.
- [167] Y. Xian, Y. Tao, F. Ma, and Y. Zhou, “Recovery of metals from heat-treated printed circuit boards via an enhanced gravity concentrator and high-gradient magnetic separator,” *Materials*, vol. 14, no. 16, p. 4566, 2021.
- [168] E. M. Bender, T. Gebru, A. McMillan-Major, and S. Shmitchell, “On the dangers of stochastic parrots: Can language models be too big?” In *Proceedings of the 2021 ACM conference on fairness, accountability, and transparency*, 2021, pp. 610–623.
- [169] D. Centres and D. T. Networks, 2022.
- [170] T. Anderson, A. Belay, M. Chowdhury, A. Cidon, and I. Zhang, “Treehouse: A case for carbon-aware datacenter software,” in *1st Workshop on Sustainable Computer Systems Design and Implementation*, ser. HotCarbon ’22, 2022.
- [171] L. Lin and A. A. Chien, “Adapting datacenter capacity for greener datacenters and grid,” in *Proceedings of the 14th ACM International Conference on Future Energy Systems*, ser. e-Energy ’23, Orlando, FL, USA: Association for Computing Machinery, 2023, pp. 200–213, ISBN: 9798400700323.
- [172] A. A. Chien, R. Wolski, and F. Yang, “The zero-carbon cloud: High-value, dispatchable demand for renewable power generators,” *The Electricity Journal*, vol. 28, no. 8, pp. 110–118, 2015.
- [173] A. A. Chien, C. Zhang, L. Lin, and V. Rao, “Beyond pue: Flexible datacenters empowering the cloud to decarbonize,” in *1st Workshop on Sustainable Computer Systems Design and Implementation*, ser. HotCarbon ’22, 2022.
- [174] B. Acun *et al.*, “Carbon dependencies in datacenter design and management,” in *1st Workshop on Sustainable Computer Systems Design and Implementation*, ser. HotCarbon ’22, 2022.